Towards luminescent lanthanide-containing coordination polymers

Dissertation submitted in fulfilment of the requirements

for the degree of Doctor of Science: Chemistry

By

Roel Decadt

Department of Inorganic and Physical Chemistry

Faculty of Sciences

Ghent University

2015

Promoter: Prof. dr. R. Van Deun

Composition of the reading and examination commission

Prof. Dr. Klaartje De Buysser, Ghent University, Chairman
Prof. Dr. Rik Van Deun, Ghent University, Promoter
Prof. Dr. Kristof Van Hecke, Ghent University, Reading commission
Prof. Dr. Matthias D'hooghe, Ghent University, Reading commission
Dr. Valentina Utochnikova, Lomonosov Moscow State University, Moscow, Russia, Reading commission
Prof. Dr. Peter Nockemann, Queen's University, Belfast, UK, Examination Commission


UNIVERSITEIT
GENT
Luminescent
Lanthanide
Lab
f-element coordination chemistry

Preface

The research in this work involves incorporating lanthanides in coordination polymers. If this last term is somewhat obscure, consider that the extremely hot topic of Metal-Organic-Frameworks is a subclass of these materials.

Very soon though, during the course of the work, it became apparent that the field definitely has some hurdles and bottlenecks that need to be overcome in order to achieve positive results (i.e. new materials). Presented here are as many positive results as were possibly obtained and an attempt to rationalize why certain concepts would not work.

It has not given me instantaneous joy or satisfaction, but it was a valuable lesson nonetheless, one whose full value will be revealed to me later. The chance to be able to work with high-end analysis equipment and rare earths has definitely been an added value.

Acknowledgements

I would like to thank the people who were involved in one way or another with this work. Some of them I want to name specifically.

First, my promoter, Prof. Rik Van Deun, for the trust, the help, the ideas and the opportunity to work in the research group.

The members of the reading commission, for their efforts into making this document better.

The members of the L^3 group, specifically Anna, for being a friend and a source of inspiration.

Prof. dr. Kristof Van Hecke, for help and encouragement.

The staff of the Department of Inorganic and Physical Chemistry, for the pleasant atmosphere during my time there.

My fellow students and friends: Fabienne, Liesje, Duchan, Stijn, Matthias, Bo, Sofie, for being wonderful, all of you.

My parents and family, for caring.

My amazing wife Eva, for everything and more, now and beyond. My two beautiful daughters Lyra and Rhune, for steering my life in the direction it needed to go.

Table of Contents

1 Outline, definitions and general concepts

1.1 Outline of the work

This thesis consists out of 6 chapters. In this first chapter, the concept of lanthanide coordination polymers is given, along with the necessary background on the topic.

In the next chapter, the structure and luminescence of several new 1,4-benzenedicarboxylate-based lanthanide coordination polymers is discussed, as a means to better grasp the synthesis methods and hurdles in this class of compounds.

The third chapter also presents structure and luminescence of some new 2,5-pyridine-dicarboxylate-based compounds of the same class, as a step into more advanced coordination modes and new structures.

The fourth chapter details the luminescence of some similar compounds that were synthesized by a fellow research group, as an attempt to correlate luminescence to structure.

The fifth chapter is perhaps the most important of this work. In it, we attempt to make the idea of β-diketonate-based lanthanide coordination polymers work.

In the sixth chapter, a conclusion is made. The seventh chapter summarizes the technical details of synthesis and characterization.

1.2 Introduction

The goal of the research conducted in this study was the synthesis of new materials in the class of ordered lanthanide coordination polymers. Of particular interest were the

luminescent properties and the crystal structure of some newly synthesized compounds. The reason for this is threefold.

1. Whenever a material contains lanthanide ions, it is possible that it will exhibit luminescent properties. The emission of characteristic lanthanide luminescence is well known, but to obtain new compounds that emit an appreciable amount of light is still a challenge.
2. Already, a significant number of coordination polymer structures containing lanthanide ions has been synthesized and structurally characterized. However, in-depth analysis of luminescence is usually omitted. There is no empirical, let alone theoretical, guideline in order to create lanthanide coordination polymers with the purpose of intensely emitting characteristic light.
3. The electronic properties of lanthanide ions give rise to unpredictable coordination geometries, which in turn lead to unexpected yet highly ordered coordination polymers. If these crystal structures can somehow be correlated to luminescent activity, new pathways arise to optimize the intensity of emitted light.

In this project we sought to expand our knowledge and delve deeper into a subject that is constrained in scope but infinite in depth. The many different combinations one could devise with the fundamental constituents of the desired chemical compounds is vast. A thorough examination of each of these constituents will therefore be called for.

The area of this scientific topic can be divided into a multitude of different aspects:

- the synthesis of metal-organic frameworks or coordination polymers;
- the coordination chemistry of lanthanide ions involved in said compounds;
- the crystal structures of the resulting materials;
- the luminescent properties;
- the correlation between all of the above.

To better grasp the concepts outlined above and detailed further below, a brief introduction into the theories surrounding them is in place.

1.3 Lanthanides

1.3.1 Definitions and key concepts

Within the 90 naturally occurring elements of the periodic table, the lanthanide series is more often than not overlooked. Indeed, in regular periodic tables, their location is cut away from the main body and pasted below. This is regretful, because their properties are fascinating in their own regard.[1]

The lanthanides are a group of elements with atomic number ranging from 57 to 71. Within this series, the defining feature is the gradual filling of the 4f-atomic orbitals with electrons.

Table 1-1: Symbols, names and electronic structures of rare earths

Symbol	Name	e^- config. metal	e^- config. trivalent ion
Sc	Scandium	$[Ar]3d^14s^2$	[Ar]
Y	Yttrium	$[Kr]4d^15s^2$	[Kr]
La	Lanthanum	$[Xe]5d^16s^2$	[Xe]
Ce	Cerium	$[Xe]4f^15d^16s^2$	$[Xe]4f^1$
Pr	Praseodymium	$[Xe]4f^35d^06s^2$	$[Xe]4f^2$
Nd	Neodymium	$[Xe]4f^45d^06s^2$	$[Xe]4f^3$
Pm	Prometheum	$[Xe]4f^55d^06s^2$	$[Xe]4f^4$
Sm	Samarium	$[Xe]4f^65d^06s^2$	$[Xe]4f^5$
Eu	Europium	$[Xe]4f^75d^06s^2$	$[Xe]4f^6$
Gd	Gadolinium	$[Xe]4f^75d^16s^2$	$[Xe]4f^7$
Tb	Terbium	$[Xe]4f^95d^06s^2$	$[Xe]4f^8$
Dy	Dysprosium	$[Xe]4f^{10}5d^06s^2$	$[Xe]4f^9$
Ho	Holmium	$[Xe]4f^{11}5d^06s^2$	$[Xe]4f^{10}$
Er	Erbium	$[Xe]4f^{12}5d^06s^2$	$[Xe]4f^{11}$
Tm	Thulium	$[Xe]4f^{13}5d^06s^2$	$[Xe]4f^{12}$
Yb	Ytterbium	$[Xe]4f^{14}5d^06s^2$	$[Xe]4f^{13}$
Lu	Lutetium	$[Xe]4f^{14}5d^16s^2$	$[Xe]4f^{14}$

Oftentimes, the elements from the third group (Sc, Y) are included and the common denominator for this extended collection is the “rare earth elements”. The rarity of these elements is questionable. When looking at the abundances of the elemental constituents of the earth’s crust, one can spot the lanthanides close together, since they are only found within the same minerals.[2] The odd-even periodicity in abundance is due to the added stability from paired protons in the core. More importantly, the abundance of the rarest lanthanide, Tm, is still higher than that of some very well-known and widely-used elements such as the noble metals silver, gold and platinum.

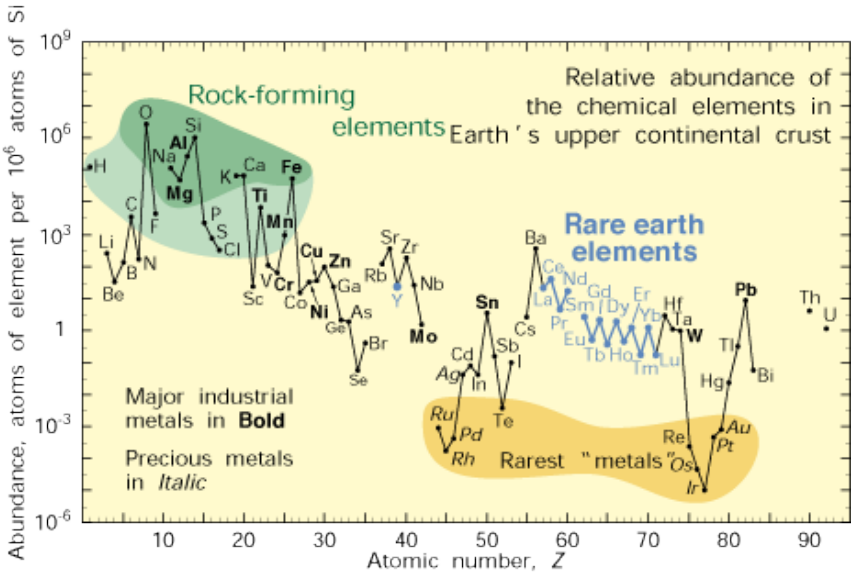

Figure 1-1: Abundance of elements in the earth's crust, taken from ref. 2

The problem with exploitation, therefore, does not lie with the rarity of the elements themselves. The limiting factors are the facts that the few minerals in which lanthanides are present are not found globally, and that in those minerals the percentage of lanthanides is quite low. Furthermore, because of similar properties, separating the ions from one another is not an easy task and subject to closely guarded expertise.

Excluding organometallic chemistry, for most fields of chemical research pertaining lanthanides the ionic form is needed as to make bonding possible. Most of the lanthanides favour an oxidation number of +III mostly due to the ionization potentials, solvation energies and lattice energies. Some exceptions arise because of a stabilized electron configuration.

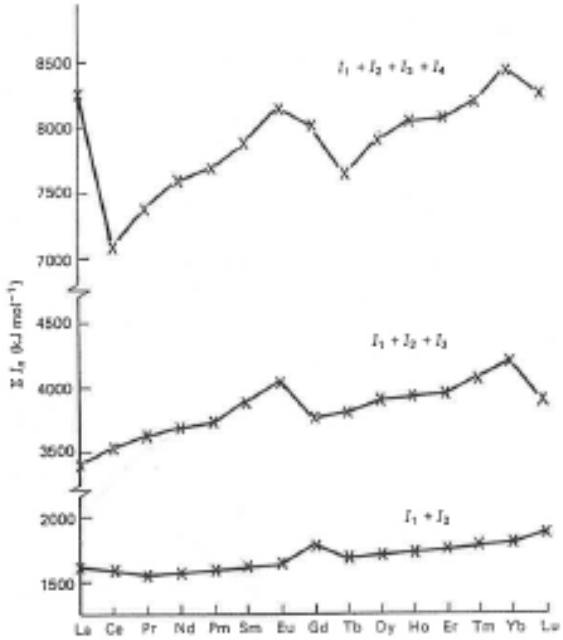

Figure 1-2: Ionization potentials of the lanthanides

The 4f electrons determine most, if not all of the features and phenomena linked to lanthanide ions. The radial density maximum of these electrons is found at a lower extension than that of the 5s and 5p electrons. This means that the actual valence electrons penetrate the Xe electronic core and are shielded away from the environment. Even in their ionic forms, this shielding is present.

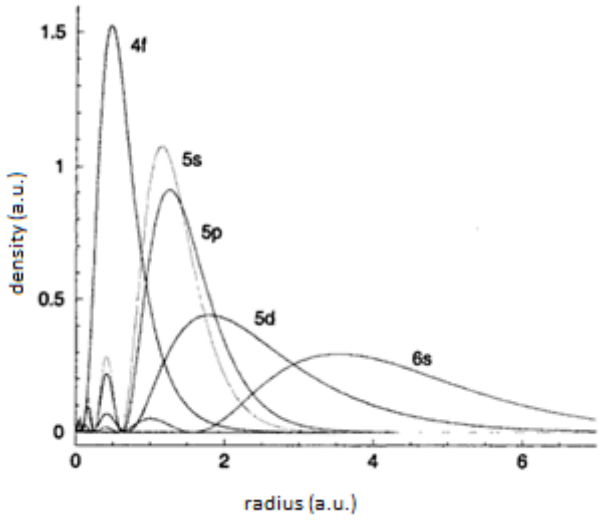

Figure 1-3: Radial density of lanthanide valence orbitals

This feature is the most important item to remember when dealing with lanthanides. Many chemical properties and interactions are governed by this. One of the most striking, however, is to be found in the radii of atoms and ions alike.

Because of the increasing nuclear charge and the ineffective shielding ability of the 4f valence electrons, the outermost electrons of both the atoms and the ions (listed in Table 1-1) are attracted more closely to the lanthanide nucleus as the series progresses into higher atomic numbers.

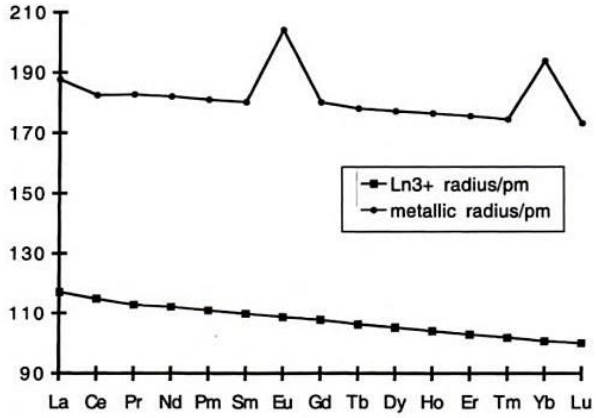

Figure 1-4: Radius of the electron cloud of lanthanides

This decrease is often called the "lanthanide contraction", as the heavier lanthanides are also the smaller ones. It offers subtle differences within any structural series.

1.3.2 Lanthanide coordination chemistry

The shielding of the 4f orbitals and therefore of the 4f electrons severely limits their interaction with the immediate environment. Depicted below is one of the most common representations, the so-called cubic set.

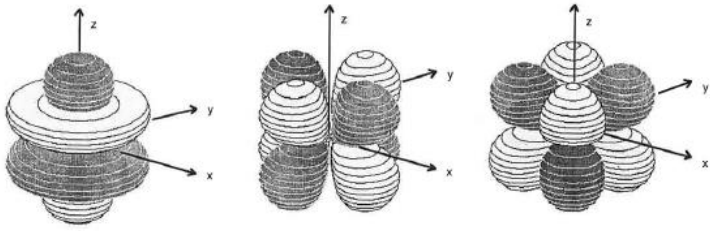

Figure 1-5: The cubic set of 4f orbitals. left: f_z^3 (=$f_{z(2z^2-3x^2-3y^2)}$), similar to the f_x^3 and f_y^3, middle: $f_{z(x^2-y^2)}$, similar to $f_{x(y^2-z^2)}$ and $f_{y(z^2-x^2)}$, right: f_{xyz}

The consequence of the shielding is that coordinative binding receives a negligible contribution from orbital effects. The coordination of organic ligands to positive

lanthanide ions is mainly governed by electrostatic interactions. This means that suitable ligands are usually negatively charged, conforming to "hard" bases as described by Pearson's HSAB theory.[3] Also, since the orbitals cannot dictate a predetermined regular coordination geometry, the first coordination sphere does not take on the classical symmetries found in transition metal chemistry.

In order to rationalize the observed coordination numbers, two interacting effects can be distinguished. The first order effect pertains to the coordination of small ligands to the lanthanide ion. In this case, the coordination number is related to the packing of the ligands around the ion and determined by the repulsion of ligands among themselves. A second order effects is noticed when bulky ligands are attached to the ligand. Steric hindrance will determine the amount and location of donor atoms. For the larger lanthanides, this may give rise to coordination numbers ranging from 6 to as high as 12, resulting in "crowded" first coordination spheres.

1.3.3 Lanthanide luminescence

The electron configuration of any isolated lanthanide ion is degenerated. This degeneracy or multiplicity may be calculated when the amount of f-electrons (n) and the azimuthal quantum number (ℓ) are known.[4]

$$multiplicity = \frac{(4\ell + 2)!}{n!(4\ell + 2 - n)!}$$

Equation 1-1: Combinatorial formula to calculate the degeneracy of electronic configurations

Several perturbations will lift this degeneracy. The first is the electron repulsion, a paired repulsion among electrons. The result is a partial decrease in degeneracy in so-called electron repulsion levels or $^{2S+1}$L-terms, which are typically separated by around 20000 cm^{-1}.

The second perturbation is the spin-orbit coupling, caused by the interaction of the magnetic spin momentum of an electron with the magnetic momentum that is created by the motion of the electron around the nucleus. The magnitude of this splitting is usually around 1000 cm^{-1}.

The resulting energy levels within lanthanides are denominated with term symbols originated from Russell-Saunders spin-orbit coupling. This is an approximation, however. The Russell-Saunders coupling is the one extreme, where spin-orbit coupling happens between the total orbital angular momentum and the total spin angular momentum to form a total angular momentum. On the other side is the j-j-coupling, where every single spin couples with an orbital momentum. The sum of these then creates the total angular momentum.

In truth, the actual coupling that will determine the electronic structure in lanthanides is a mixed form of both approximations, but for simplicity the Russell-Saunders scheme and notation is used.

To denote an electronic state, one assigns the magnetic quantum numbers ℓ from highest to lowest to the 4f-orbitals, meaning that each orbital corresponds to an integer ranging from +3 to -3. Additionally, one assigns the spin quantum number s = +/- 1/2 to electrons with spin up or spin down, respectively.

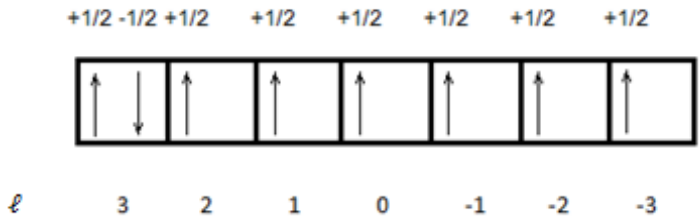

Figure 1-6: Orbital box notation of the Tb^{3+} ground state with the spin quantum numbers above each electron and the magnetic quantum number below each orbital

Adding together all of the spin quantum numbers of all present electrons generates the total spin angular momentum S (and subsequently the spin multiplicity 2S+1). Adding the magnetic quantum numbers of each electron yields the total orbital angular momentum L and the corresponding state symbol.

Table 1-2: Total orbital angular momenta and corresponding term symbols

L	0	1	2	3	4
	S	P	D	F	G

The total angular momentum J is then derived from vectorial addition of L and S, meaning that the highest possible value for J can be (L+S) and the lowest possible (L-S), divided by increments of 1.

Ground states are derived following Hund's Rules:

1. the spin multiplicity is maximized,
2. the total orbital angular momentum is maximized,
3. depending on the amount of electrons, the ground state has a minimized (6 or less electrons) or maximized (more than 7 electrons) J.

As an example, the ground state of the Tb^{3+} ion is derived as follows (Figure 1-6, Equation 1-2)

.

Equation 1-2: Calculation of J for the Tb^{3+} ground state

$$L = \sum_{1}^{n} l = 3 \Rightarrow F$$

$$S = \sum_{1}^{n} s = 6 \times \left(+1/2\right) + 1 \times \left(-1/2\right) = 3 \Rightarrow 2S + 1 = 7$$

$$J = \left|L \pm S\right| = 6,5,4,3,2,1,0$$

According to the above rules and calculations, the ground state for Tb^{3+} is the $^7F_6$ level.

Finally, the energy levels are split even further into sublevels by the presence of ligands. A coulombic interaction between electrons from the metal ion and electrons from the ligands will perturb the spheric symmetry of the electron cloud. There is a theoretical 2J+1 degeneracy that is lifted due to the ligand field interaction, but it will only be visible in very ordered systems at low temperature. Due to the shielding of the 4f electrons, this splitting is typically very small (no larger than 10-100 cm^{-1}). At higher temperatures and in less ordered systems, the fine structure will blend together to show the broad bands corresponding to transition between spin-orbit coupling levels.

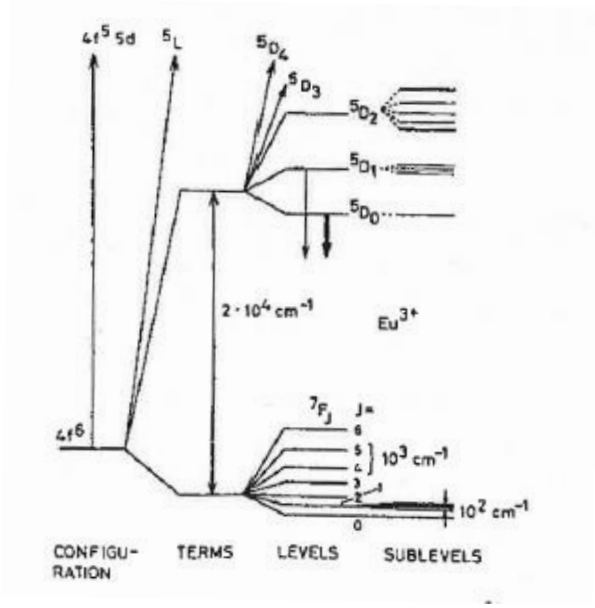

Figure 1-7: Energy level splitting of the Eu^{3+} ion

Electronic transitions from an excited state to a lower level are synonymous for a release in energy. This may be radiationless, but in lanthanide ions, the possibilities for radiative luminescent decay are more interesting than in any other metal ion.

Because of the shielding of the 4f-shell, the transitions within the lanthanide ion energy states are comparable to transitions that occur in the gas phase, meaning that the emitted energy is nearly monoenergetic. In lanthanide ions, the energy differences between emissive states and the ground state are often of a magnitude that will cause emission in the visible region and infrared regions of the spectrum. Since the transitions are unaltered by the environment, sharp emissions are to be expected with colour-pure spectra.

Depending on the identity of the used lanthanide, distinct characteristic emissions are known for every separate ion, excluding lanthanum and lutetium because the 4f-shell is empty and filled, respectively.

Table 1-3: Characteristic luminescence in lanthanides

	Excited state	*Terminal state*	*J range*	*Wavelength (nm)*	*Colour*
Pr	$^1G_4$	^3H_J	4-6	1300	NIR
	$^1D_2$	^3F_J	2-4	890, 1060	NIR
	$^3P_0$	^3H_J	4-6	525-680	Orange
Nd	$^4F_{3/2}$	^4I_J	9/2-15/2	900, 1050, 1300	NIR
Sm	$^4G_{5/2}$	^6H_J	5/2-15/2	590	Orange
Eu	$^5D_0$	^7F_J	0-6	620	Red
Gd	$^6P_{7/2}$	$^8S_{7/2}$		312	UV
Tb	$^5D_4$	^7F_J	6-0	550	Green
Dy	$^4F_{9/2}$	^6H_J	15/2-5/2	570	Yellow-orange
Ho	$^5F_5$	^5I_J	8-4	970, 1450	NIR
	$^5S_2$	^5I_J	8-4	540	Green
Er	$^4S_{3/2}$	^4I_J	15/2-9/2	1530	NIR
Tm	$^1G_4$	^3H_J	6-4	450	Blue
Yb	$^2F_{5/2}$	$^2F_{7/2}$		980	NIR

Some remarks accompany this table: for Ce^{3+}, the actual luminescence is usually a 5d -> 4f transition. Promethium luminescence has not been studied thoroughly because of the radioactive nature of the element. The Gd^{3+} emissive state is very high in energy and would give rise to UV emission. The list of energy states in lanthanide ions is visualized in a Dieke diagram.[5] In a more detailed collection of data, the energies associated with these states are calculated in several papers by Carnall.[6]

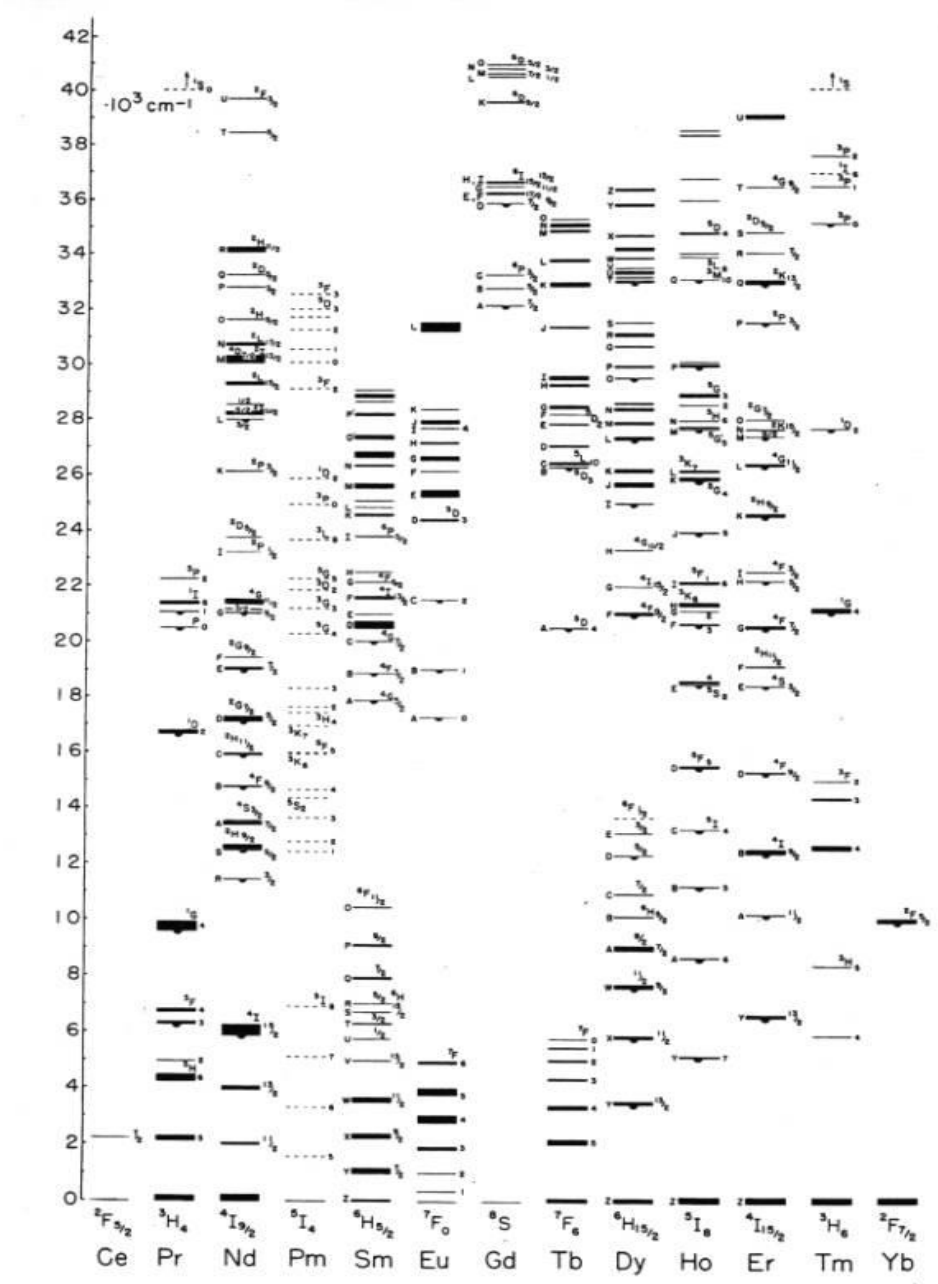

Figure 1-8: Dieke diagram of lanthanide energy levels

In order to get these visible, colour-pure transitions to occur, one needs to excite the lanthanide ion. This is not always straightforward due to the very low molar absorptivities of the ions. Absorption of light can be seen as a coupling of the wave with the lanthanide, transferring energy and pushing an electron to an orbital with higher energy. Three operators promote this absorption: the electric dipole, magnetic dipole and electric quadrupole operators. These are linked to the nature of light. However, one needs to take the Laporte parity selection rules into account. Electronic dipole transitions are parity forbidden but non-centrosymmetric interaction will partially relax this rule. As a consequence the induced electric dipole transitions are weak in intensity. Magnetic dipole transitions are allowed but weak in intensity. For 4f-4f transitions, induced electric dipole and magnetic dipole transitions have comparable intensities. Electric quadrupole transitions are so weak that they are generally not observed, even though they are allowed.

These absorptivity values ε, then, are in the range of less than 10 $L \cdot mol^{-1} \cdot cm^{-1}$. For organic molecules such as benzene for comparison, ε approaches 10000 $L \cdot mol^{-1} \cdot cm^{-1}$ at 178 nm. For transition metals, the value for d-d transitions in aquo complexes is still two orders of magnitude larger than those of f-f transitions within lanthanide ions. The origin for this low absorptivity is that the transitions within the 4f-orbitals are parity forbidden by the Laporte selection rules. This means that regular light sources will have difficulties to properly excite lanthanide ions. It is therefore interesting to find alternative pathways in order to get the required energy transfer.

Combining lanthanide ions with a suitable matrix is easily rationalized when luminescence is the goal. If the matrix is somehow capable of absorbing energy and transferring it to the lanthanide ion, one can circumvent the low absorptivity of the ions themselves. This is commonly referred to as the antenna effect; a light harvesting entity is able to absorb the necessary energy and transfer it to a nearby lanthanide ion, thereby exciting it indirectly.[7]

This matrix can be inorganic, such as a salt crystal, nanoparticle or glass. In this context however, one wants to look at organic groups, i.e. ligands that coordinate the lanthanide ion. The pathway for this specific transfer of energy was theorized by Weissman *et al*.[8] In its most rudimentary form, the singlet ground state of the ligand is excited by light of the appropriate wavelength. This excited singlet state reverts to a long-lived excited triplet state. Normally, this transition is forbidden, but the spin-orbit coupling from paramagnetic atoms with high atomic number mixes the ligand singlet and triplet states, permitting the transition. This is called the "heavy atom effect". If the intersystem crossing does not occur, the excitation is undone by ligand-based fluorescence. The triplet state may also lose its energy in ligand-based phosphorescence, however, the energy transfer from this triplet level to an excited lanthanide ion state is ultimately what makes the antenna effect feasible.

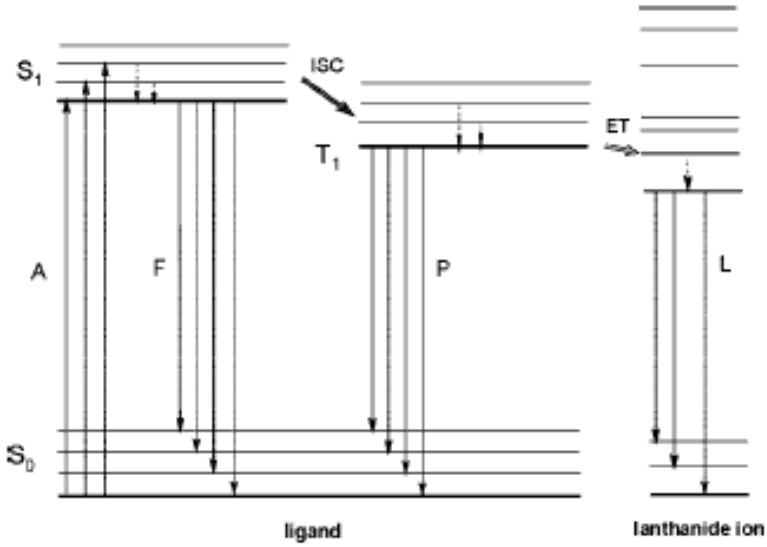

Figure 1-9: Representation of the antenna effect, taken from ref 7. S_0: singlet ground state, S_1: excited singlet state, T_1: excited triplet state, A: absorption, F: fluorescence, ISC: intersystem crossing, P: phosphorescence, ET: energy transfer, L: lanthanide luminescence

Some key remarks need to be made here. To account for the conservation of energy, the energy level of the excited triplet state naturally needs to be higher than the emissive excited state within the lanthanide. This is the main reason gadolinium ions are extremely difficult to excite via the antenna effect, since the triplet energy levels of most organic ligands are simply too low. Compare the energy of the excited $^6P_{7/2}$ level of the Gd^{3+} ion (312 nm) with the triplet state energies of common ligands such as dibenzoylmethane (dbm, 492 nm)[9] or the condensate of salicylaldehyde and ethylenediamine (salen, 490 nm).

In order for this energy transfer to be efficient certain boundaries for the separation of the relevant energy levels need to be respected. If the levels differ too slightly, there is a chance of energy back transfer from the lanthanide ion to the ligand (not depicted in

Figure 1-9, it would be the reverse of the ET arrow). If the difference is too great, the transfer is less efficient (here the ET arrow in Figure 1-9 would be crossed out).

When the difference is too small and back transfer occurs, there is also a chance for radiationless deactivation of the excited triplet state by coupling with local vibrations. This results in a smaller population of the excited state and therefore lower luminescence intensity and longevity.

Finally, the excited state of the lanthanide, too, may couple with local small modes of vibration such as C-H, O-H and N-H stretch vibrations.

This last radiationless deactivation or quenching is unfavourable but can be reduced in several ways. Three of these strategies are directly relevant to this research. The first is to shield the ion from water solvent molecules by using bulky, multidentate ligands. This way, the water molecules are expelled from the first coordination sphere of the ions.

More intuitive is to simply not use materials that sport these deactivating vibrations. Since lanthanide salts often need to be dissolved in water, methanol or ethanol, this is actually far less straightforward.

Another possibility is to incorporate lanthanide ions in solid-state matrices, where the overall rigidity reduces this unfavourable coupling. Reducing the movement of the carriers of the O-H vibrations reduces the amount of collisions these molecules can have with excited lanthanide centres, which will in turn reduce the amount of quenching these compounds have to undergo.

1.4 Coordination polymers

1.4.1 General concept

Metal-organic frameworks (MOFs) are a subclass of materials that received a lot of attention and dedicated research during the last two decades. They are fascinating from every viewpoint.

MOFs can be crudely defined as a subclass of three-dimensional coordination polymers, possessing ordered structure and high internal surface. Coordination polymers themselves can also be two-dimensional (sheet-like) and one-dimensional (chain-like). All MOFs are coordination polymers but not all coordination polymers are MOFs, the criterion for a MOF is the readily available internal surface. Therefore we will only use the coordination polymer name, even though obtaining a high-internal surface MOF is usually more interesting towards applications.

This class of compounds incorporates many different aspects of materials chemistry. Here follows how they are built up. Metal ions or metal clusters are coordinated by donor atoms originating from organic ligands. These ligands are attached to a spacing group, which in turn contains a new set of donor atoms. These new donor atoms coordinate another metal in order to create a separate coordination environment. In this process of multiple coordinative bindings, order and regularity will make these structures accessible for analysis techniques. Regular geometry within the coordination spheres and ordering of the organic ligands will, in tandem, produce an ordered structure, capable of being analysed by single crystal methods.

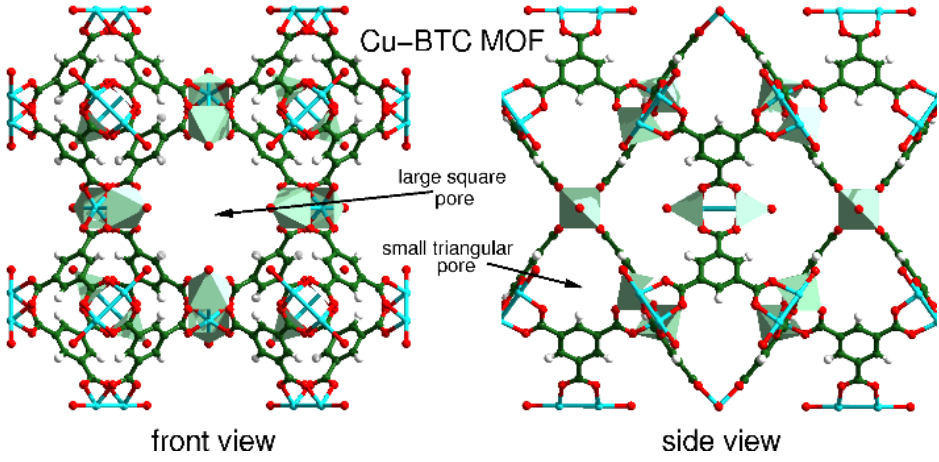

Figure 1-10: Coordination polymer constructed from Cu^{2+} ions and 1,3,5-benzenetricarboxylic acid (BTC), taken from ref. 10

One can therefore view coordination polymers as constructed from two types of building blocks. On the one hand there is the central metal ion, in Figure 1-10 this is a Cu^{2+} ion. The manifold of coordinative binding to this metal, with respect to geometry, and magnitude of coordination number are the causes of variation within the first type of building block. This variation is actually twofold:

1. One can change the chemical identity of the metal.
2. For the same metal, different coordination polyhedra are also possible.[11]

For example, Er^{3+} can adopt a square antiprismatic coordination environment in which each Er^{3+} ion is octacoordinated and bridged to a second Er^{3+} ion.[12] This unit can be seen as a hexagon in which each vertex point may be connected to six other similar units (points of extension). However, the polyhedra can be bridged differently.[13] In another example, four Er^{3+} ions are placed on the vertices of a tetrahedron. Each Er^{3+} adopts a square antiprismatic octacoordinated coordination geometry. Here, the secondary

building unit also has six points of extension but functions as an octahedron. Barring a different amount of end-capped water, Yb^{3+} and Nd^{3+} can adopt the same SBU as well.

.

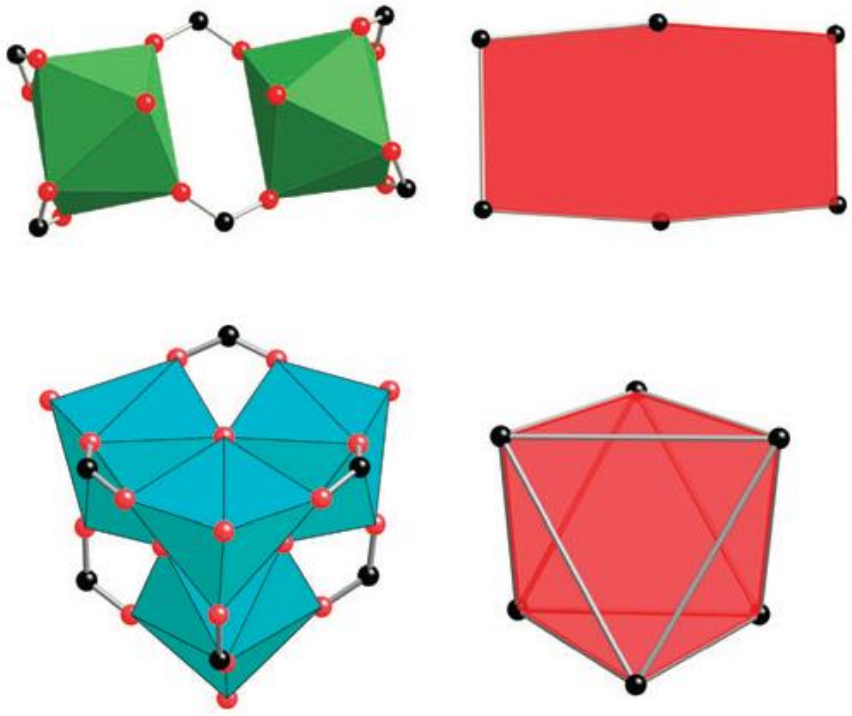

Figure 1-11: Coordination polyhedra forming a secondary building unit, taken from ref. 11. Top left: Er^{3+} square antiprism dimer. Top right: reduction of this unit to a hexagon. Bottom left: Er^{3+}, Yb^{3+} and Nd^{3+} tetragonal antiprism tetramer. Bottom right: reduction of this unit to an octahedron.

On the other hand, the organic "linking" groups that connect the metal nodes can be virtually endlessly varied. In Figure 1-10 for example, 1,3,5-benzenetricarboxylic acid serves as the linker.

Not only is there a great deal of suitable donor atoms, but they can also be present in different functional groups with more or less affinity for the metal ion. For more on this, refer to the introduction to chapter 5.

The coordinating groups can be placed at different distances from one another, or at different angles relative to each other. Each successful combination of building blocks yields a new structure in its own right.

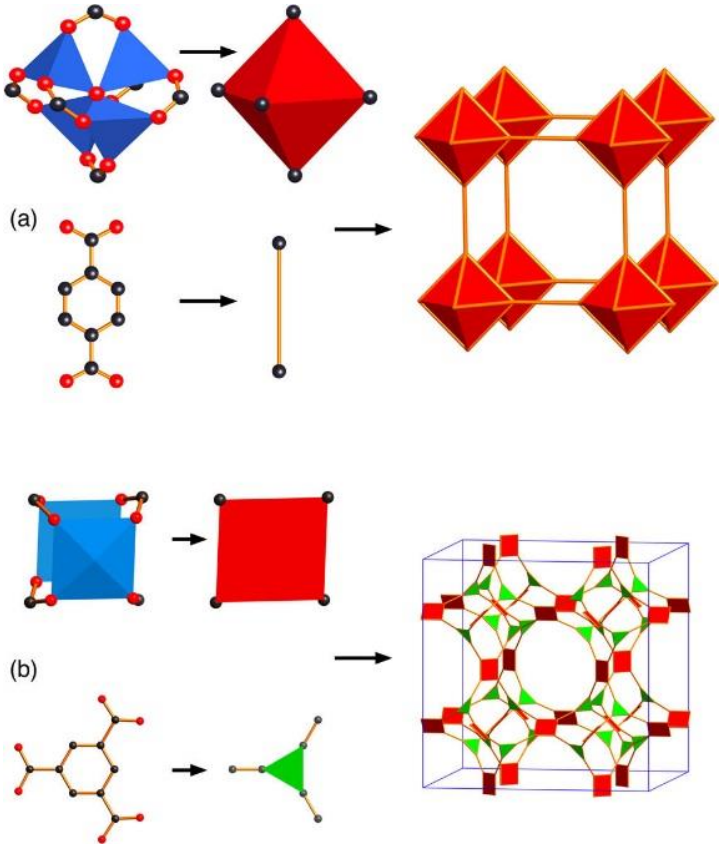

Figure 1-12: Combination of building blocks leads to new structures.

For example, consider the structures of both MOF-5 (Figure 1-12, top, right) and HKUST-1 or Cu-BTC (Figure 1-12, bottom, right). In MOF-5, the Zn_4O-$(CO_2)_8$ clusters are abstracted as octahedral nodes and the terephthalic acid molecules as rod-like building blocks. In Cu-BTC, the Cu_2-$(CO_2)_4$ paddle-wheel clusters are abstracted as squares and the BTC linker as a triangle.

Furthermore, secondary functionalization will alter not only the identity of the ligand, but also the properties of the entire macrostructure (Figure 1-13), making it fit for specific applications such as catalysis, sensing, gas storage, chemical separations and ion exchange.[14,15]

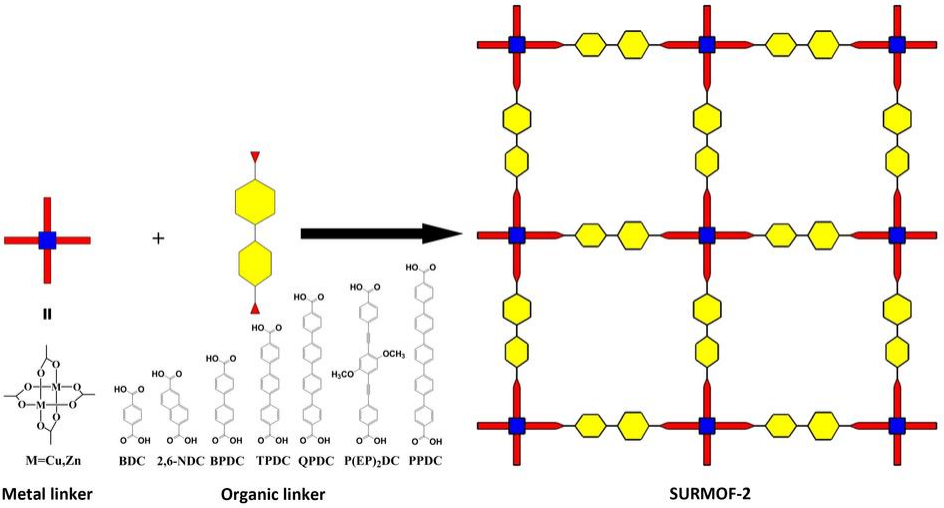

Figure 1-13: A series of isoreticular MOFS: changing the organic linker does not change the network topology, only the size of the unit cell increases.[16]

The term metal-organic framework is used when the material is porous. Many of these porous structures exist; in fact, it has been one of the prime reasons to research these materials. Indeed, when observing a most basic three dimensional network comprised of terephthalic acid as the organic linker and zinc ion clusters as the metal nodes (Figure 1-14), there is no electron density in the centre of the formed cages, causing an internal surface that is among the highest in materials chemistry.[17] In the same figure below, the yellow sphere represents void space.

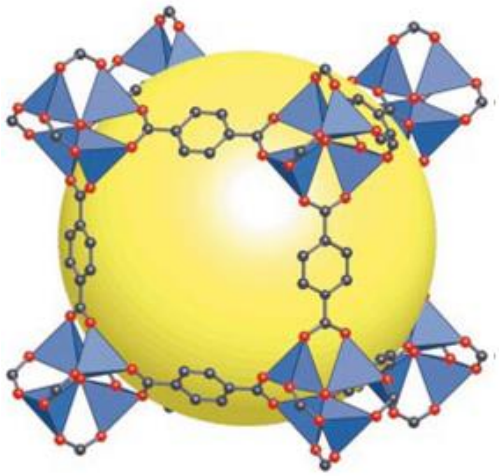

Figure 1-14: The iconic MOF-5, a metal-organic framework constructed from Zn clusters (blue polyhedra) and terephthalic acid (balls and sticks).

1.4.2 Lanthanide coordination polymers

When creating coordination polymers with lanthanide ions, some relatively unique properties will arise. As mentioned before, the shielding of geometry-inducing valence orbitals allows for higher coordination numbers. This ensures that the first coordination sphere is filled with donor atoms, and the central metal nodes can connect multiple ligands, usually more than for transition metals. Predicting the crystal structure is extremely difficult because of this.

Additionally, the close proximity of many linker molecules is prone to lead to dense structures with lower internal surface, making them less suitable for applications such as gas storage.

Lastly, coordinated solvent molecules are often essential in stabilizing the coordination environment of the lanthanide ion. These molecules take up a lot of space within the porous structure and “block” the pores. Still, porous lanthanide MOFs do exist; what is

interesting is how the luminescence may change when different species are brought into the pores.

The actual reasoning for incorporating lanthanide ions into coordination polymers is owed to the rigidity of ordered structures. With fewer vibrations that can couple to the excited state of a lanthanide ion, non-radiative deactivation is less of an issue. Secondly, since it is possible to employ different organic linking groups, each with their own triplet level, the search for optimal emitters can continue. Third, it is possible to maintain this structure even when coordinated solvent molecules are removed, which in turn may lead to variations in luminescence intensity when the structure “senses” different guest molecules.

In a large part of this work, extensive luminescent studies are performed upon synthesized compounds. Afterwards, the aim is to incorporate different, nonconventional linker molecules into new compounds that should have the many interesting features of lanthanide coordination chemistry.

1.5 References

[1] Lanthanide and actinide chemistry, S. Cotton, ISBN: 978-0-470-01005-1, **2006**

[2] Rare Earth Elements—Critical Resources for High Technology, G. B. Haxel, J. B. Hedrick, and G. J. Orris, U.S. Geological Survey Fact Sheet 087-02, **2002**

[3] Hard and Soft Acids and Bases, R. G. Pearson, J. Am. Chem. Soc., **1963**, Vol. 85, p. 3533

[4] Basics of Lanthanide Photophysics, J.C. Bünzli, S.V. Eliseeva, a chapter in Lanthanide Luminescence: Photophysical, Analytical and Biological Aspects, P. Häninnen, H. Härmä (eds.), **2010**, Springer Ser Fluoresc, Springer-Verlag Berlin Heidelberg, DOI 10.1007/4243_2010_3

[5] The spectra of the Doubly and Triply Ionized Rare Earths, G.H. Dieke, H. Crosswhite, Applied Optics, **1963**, Vol. 2, No. 7, p. 675

[6] Electronic Energy Levels in the Trivalent Lanthanide Aquo Ions, W.T. Carnall, P.R. Fields, K. Rajnak, J. Chem. Phys., **1968**, Vol. 49, p. 4424 (several articles)

[7] Lanthanide-Based Luminescent Hybrid Materials, K. Binnemans, Chem. Rev., **2009**, Vol. 109, No. 9

[8] Intramolecular Energy Transfer: The Fluorescence of Complexes of Europium, S.I. Weissmann, J. Chem. Phys., **1942**, Vol. 10, p. 214

[9] Substituent Effects on Intramolecular Energy Transfer. 1. Absorption and Phosphorescence Spectra of rare Earth β-Diketone Chelates, W.F. Sager, N. Filipescu, F.A. Serafin, J. Phys. Chem., **1965,** Vol. 69, p. 1092

[10] A Chemically Functionalizable Nanoporous Material $Cu_3(TMA)_2(H_2O)_3]_n$, S.S.Y. Chui, S.M.F. Lo, J.P.H. Charmant, A. Guy Orpen, I.D. Williams, Science, **1999**, Vol. 283, no 5405, p. 1148

[11] Secondary building units, nets and bonding in the chemistry of metal-organic frameworks, D.J. Tranchemontagne, J.L. Mendoza-Cortès, M. O'Keeffe, O.M. Yaghi, Chem. Soc. Rev., **2009**, Vol. 38, p. 1257

[12] Synthesis and Structural Diversity of Rare Earth anithralate complexes, G.B. Deacon, M. Forsyth, P.C. Junk, S.G. Leary, G.J. Moxey, Polyhedron, **2006**, vol. 25, p. 379

[13] Lanthanide Coordination with r-Amino Acids under Near Physiological pH Conditions:

Polymetallic Complexes Containing the Cubane-Like $[Ln_4(\mu_3\text{-}OH)_4]^{8+}$ Cluster Core, R. Wang, H. Liu, M.D. Carducci, T. Jin, C. Zheng, Z. Zheng, Inorg. Chem. **2001**, Vol. 40, p. 2743

[14] Metal-organic frameworks-prospective industrial applications, U. Müller, M. Schubert, F. Teich, H. Puetter, K. Schierle-Arndt, J. Pastré, J.Mater. Chem., **2006**, Vol. 16, p. 626

[15] Industrial application of metal-organic frameworks, A.U. Czaja, N. Trukhan, U. Müller, Chem. Soc. Rev., **2009**, Vol. 38, p. 1284

[16] A novel series of isoreticular metal organic frameworks: realizing metastable structures by liquid phase epitaxy, J. Liu, B. Lukose, O. Shekhah, H. Kemal Arslan, P. Weidler, H. Gliemann, S. Bräse, S. Grosjean, A. Godt, X. Feng, K. Müllen, I.-B. Magdau, T. Heine, C. Wöll, Scientific Reports, **2012,** Vol. 2, article no. 921

[17] Reticular synthesis and the design of new materials, O.M. Yaghi, M. O'Keeffe, N.W. Ockwig, H.K. Chae, M. Eddaoudi, J. Kim, Nature, **2003**, Vol. 423, p. 705

2 Coordination polymers based on lanthanide ions and terephthalic acid

2.1 Outline and goals

In this first part of the work, we wanted to achieve a basic understanding of the materials class. Synthesis of lanthanide coordination polymers was a new field in the department and no prior experience was present, save for the COMOC group who deals with ordered structures such as transition metal MOFs.

This understanding was initially grown by scoping out literature sources in order to see if, at first sight, any trends arise in synthesis methods and resulting structural properties. With this done, we elected a simple system that is extensively studied in order to ensure a high chance of success, hoping to find new materials.

It is of course challenging to find these unpublished new materials in a field that is widely studied. After viewing relevant publications, we argued that oftentimes a handful of analogous structures are synthesized featuring identical organic parts and identical synthesis methods while varying the identity of the lanthanide ion. It is not unreasonable that the same synthesis method could yield results for other members of the lanthanide series as well. If, indeed, results are obtained, we have new structures fit for publication. If not, we know that the conditions that allow these materials to form and grow need to be very well defined.

The challenge for this part of the work was to find if mimicking or slightly modifying known synthesis methods could indeed yield new structures and to find what qualities

these materials needed to have to be fit for structural analysis. Investigating the luminescence properties is a second objective here.

2.2 Introduction

To start exploring the field of lanthanide-based coordination polymers, the terephthalic acid molecule (1,4-benzenedicarboxylic acid, from here on abbreviated as H_2BDC, BDC^{2-} for the twice deprotonated ligand, in formulas this will be noted as BDC) was elected to serve as the organic linker molecule.

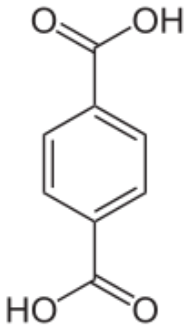

Figure 2-1: Terephthalic acid

The reasons for this are listed hereunder:

a. the carboxylato anionic ligands show good affinity for the hard Pearson-acidic lanthanide ions,
b. the orientation of the coordinating groups are at 180°, giving rise to rod-like building blocks,
c. the chemical and thermal stabilities are high,
d. there are strong secondary structuring effects present:
    1. the aromatic pi-system,
    2. hydrogen-bonding accepting and donating atoms (depending on the degree

of deprotonation),

3. high symmetry within the molecule.

e. the ligand is not toxic

f. it is commercially available and cheap

Carboxylato ligands in lanthanide coordination polymers have been reported to exhibit five different modes of coordination, as seen in Figure 2-2:.

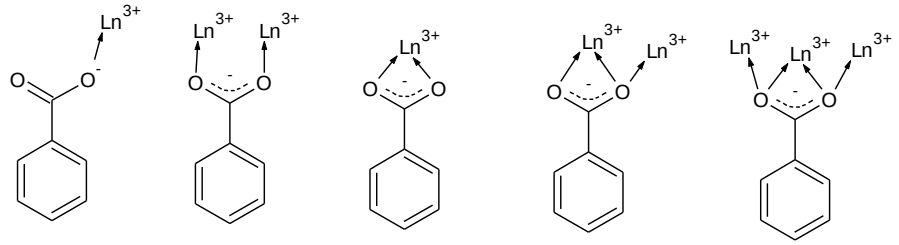

Figure 2-2: Coordination modes of the benzenecarboxylate motif. From left to right: monodentate, bis-monodentate, bidentate/chelating, chelating-bridging bidentate and chelating-bridging tridentate

2.3 Reported relevant research

2.3.1 Combining lanthanides with BDC

One of the earliest characterized compounds sporting a lanthanide ion as central ion and BDC^{2-} was reported by Reineke *et al.* in 1999.[1] In that project, combining the appropriate hydrated lanthanide nitrate salt with H_2BDC and triethylamine in water yielded small crystals after hydrothermal treatment. Tb^{3+} or Eu^{3+} ions are coordinated by the oxygen atoms from the carboxylate moieties, giving rise to a structure with general formula $Ln_2(BDC)_3{\cdot}(H_2O)_4$, where Ln = Eu^{3+} and Tb^{3+}. Figure 2-3 shows the asymmetric unit of this material. The lanthanides are eight-coordinate, with six donor

atoms originating from monodentate coordination from the BDC^{2-} ligands and two oxygens from water molecules. Each BDC^{2-} ligand bridges 4 lanthanide ions.

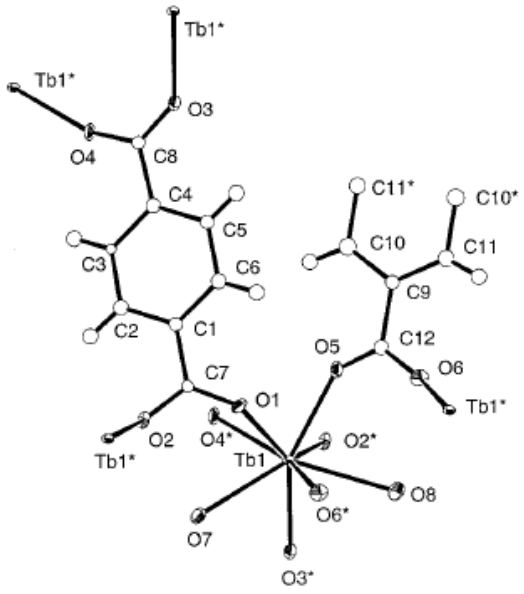

Figure 2-3: Asymmetric unit of $Tb_2BDC_3 \cdot (H_2O)_4$ taken from ref. 1

In the same year, the same group published their results on a very similar compound with formula $Ln(BDC)(NO_3) \cdot 2DMF$ with Ln = Eu^{3+} or Tb^{3+} and DMF = N,N'-dimethylformamide.[2] This time, the synthesis proceeded via a mild method; in a mixture of methanol and DMF containing H_2BDC and the corresponding lanthanide nitrate salt, pyridine vapours were allowed to diffuse. Figure 2-4 shows the resulting compound. The terbium(III) ions are coordinated by four oxygen atoms from four different carboxylate groups, two oxygen atoms from a bidentate nitrate anion and two oxygen atoms from two DMF ligands.

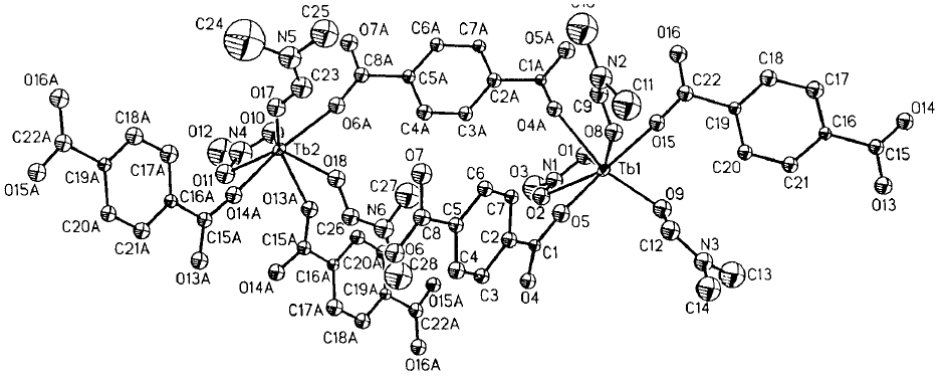

Figure 2-4: Crystal structure of $Tb(BDC^{2-})(NO_3)\cdot DMF$ taken from ref. 2

Upon heating, both of these materials revert to a solvent-free framework with slightly degraded crystallinity, $Ln_2(BDC)_3$ and $Ln(BDC)(NO_3)$, respectively. Of the former, the unevacuated material may be regenerated by exposure to water vapour, or transformed into the compound with formula $Ln_2(BDC)_3\cdot(NH_3)_4$ by reacting the dehydrated material with anhydrous ammonia gas. The $Ln(BDC)(NO_3)$ compound can be immersed in water to yield $Ln_2(BDC)_3\cdot(H_2O)_4$. Luminescence lifetime studies show that the hydrated network quenches the luminescence more than the one with ammonia inside, which in turn quenches more than the evacuated material, showing that O-H oscillators are stronger quenchers than N-H oscillators.

In 2001, a similar compound was reported by Pan *et al.* with trivalent erbium as central metal ion, obtained after solvothermal treatment in an H_2O/ethanol mixture.[3] The general formula is found to be $Er_4(BDC)_6\cdot(H_2O)_6$ and depicted in Figure 2-5. There are four independent erbium(III) sites in the structure, and the BDC^{2-} ligands bridge either four or three Er^{3+} ions. Here, too, dehydration into $Er_4(BDC)_6$ is possible, rehydration however yields $Er_2(BDC)_3\cdot(H_2O)_4$, an isostructural compound when compared to the aforementioned examples. Upon dehydration, the contraction of the structure,

combined with the creation of unsaturated ion sites and unstable coordination geometries, force an irreversible rearrangement of the structure. No luminescence was reported.

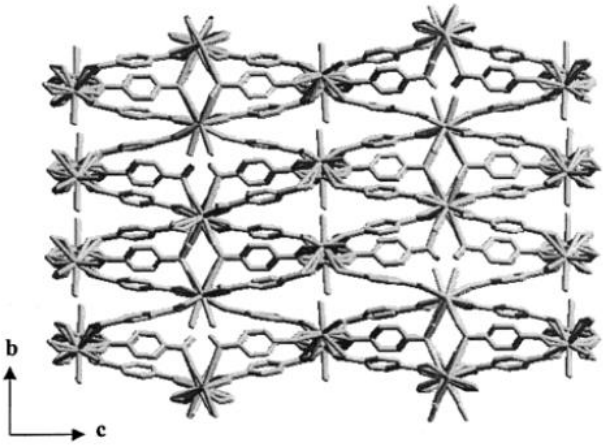

Figure 2-5: The $Er_4(BDC)_6{\cdot}(H_2O)_6$ network taken from ref. 3

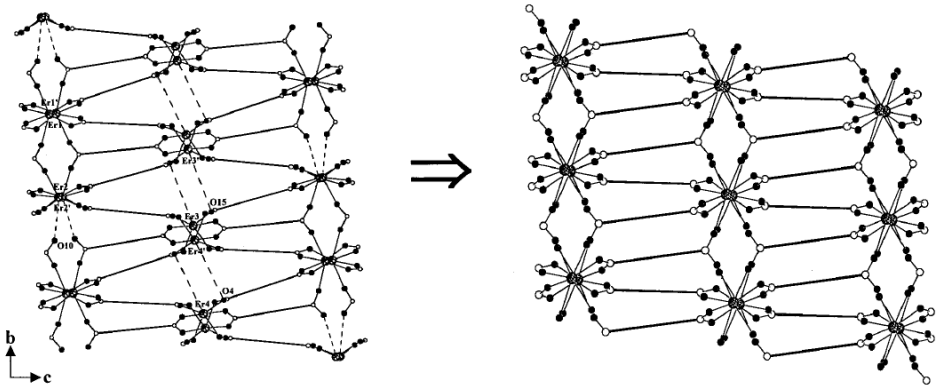

Figure 2-6: Rearrangement from $Er_4(BDC)_6{\cdot}6H_2O$ into $Er_2(BDC)_3{\cdot}4H_2O$

The Er^{3+}-BDC^{2-} combination has been repeated in gel media by Daiguebonne *et al.* in 2003 and in 2006, yielding multiple compounds with slightly differently numbers of crystallized water, all dependent on the type of gel and the gel density.[4,5]

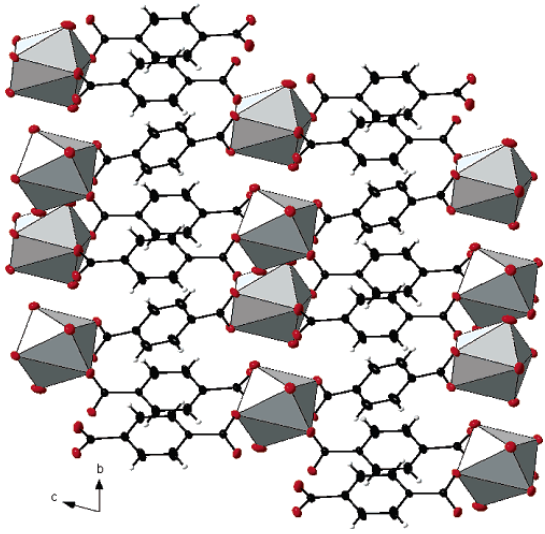

Figure 2-7: The $Er_2(BDC)_3(H_2O)$ network taken from ref. 5

Serre *et al.* made and named three coordination polymers containing europium: MIL-51^{LT} and MIL-51^{HT}, shown in Figure 2-8 contain the trivalent europium(III) cation while MIL-52 is constructed with the divalent Eu^{2+} ion.[6] The formula for MIL-51^{LT} is $Eu_2(OH)_4(H_2O)_4(BDC)$, for MIL-51^{HT} it is $Eu_2(OH)_4(BDC)$ and for MIL-52 it is $(Eu^{II})_2(BDC)_2$. Crystals of MIL-51^{LT} suitable for single crystal X-ray diffraction analysis were not obtained but instead the structure was determined through Rietveld refinement. In that article, no luminescence studies were performed.

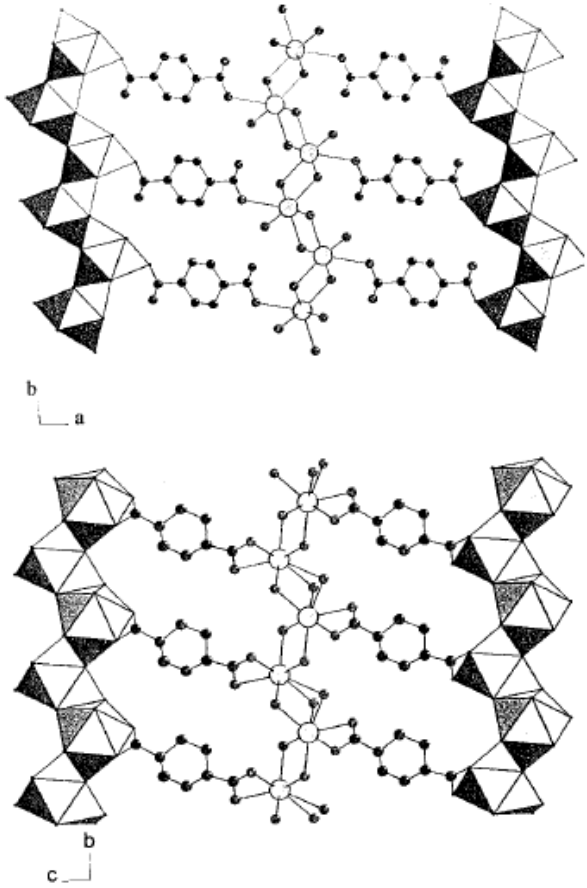

Figure 2-8: Top: MIL-51^{LT}, Bottom: MIL-51^{HT}, as taken from ref. 6

In 2006, Guo *et al.* reported four compounds obtained by the mild reaction of H_2BDC with hydrated lanthanide nitrate salts in a solvent mixture containing DMF, water and ethanol.[7] After careful adjustment of the pH with a polyamine and hydrochloric acid, the mixture is placed in the oven at 50°C. The resulting crystalline networks contain Tb^{3+}, Dy^{3+}, Ho^{3+} and Er^{3+} ions and are isostructural. The typical Tb^{3+} emission is observed besides ligand-to-metal charge transfer emission (LMCT) and BDC^{2-} fluorescence, for the other three networks no characteristic lanthanide emission is reported. They contain coordinated water and DMF ligands as well as crystallized free water and/or ethanol and

DMF molecules present in the voids in the network. The formulae for these networks are reported as $Tb_3(BDC)_{4.5}(DMF)_2(H_2O)_3\cdot(DMF)(H_2O)$, which is shown in Figure 2-9 below and $Ln_3(BDC)_{4.5}(DMF)_2(H_2O)_3\cdot(DMF)(EtOH)_{0.5}(H_2O)_{0.5}$ with Ln = Dy^{3+}, Ho^{3+}, Er^{3+}.

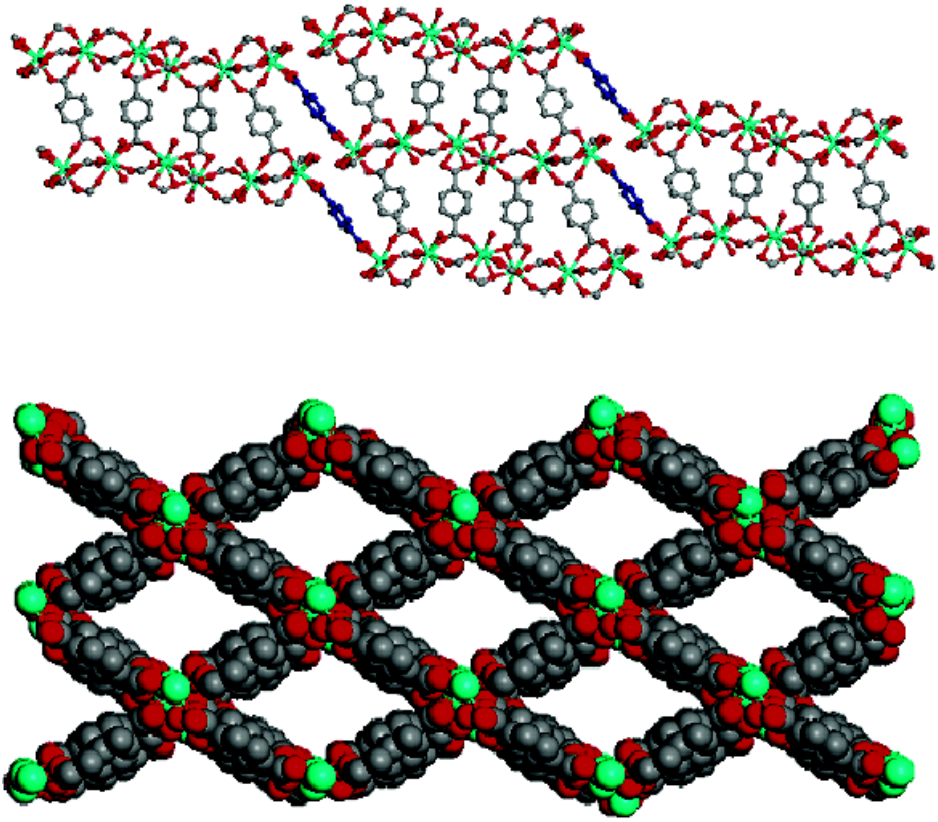

Figure 2-9: The $Tb_3(BDC)_{4.5}(DMF)_2(H_2O)_3\cdot(DMF)(H_2O)$ network as taken from ref. 7

Another analogue of the previous structure was reported in 2009 by Na *et al.*[8] Slight variations of the solvent system and the used base gave the compound with formula $Yb_3(BDC)_{4.5}(DMF)_2(H_2O)_3\cdot(DMF)_2$. No Yb^{3+}-characteristic emission is observed but again, LMCT emission and fluorescence are assigned to specific emission bands.

For a brief comparison, the structure of $[Sc_2(BDC)_3]$ presented by Perles *et al.* in 2005 is included in this overview.[9] Although not part of the lanthanide group, the contrast of

this rare earth-based network with lanthanide-containing compounds is immediately visible from the coordination numbers; no water or other solvent molecules are present. Also the coordination polyhedron is described as an octahedron, which gives more symmetry to the network, as seen in Figure 2-10.

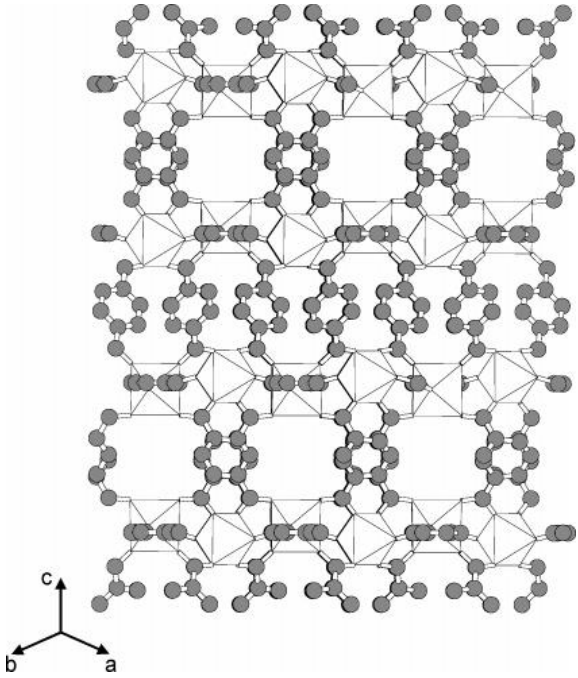

Figure 2-10: The [Sc_2BDC_3] network, as taken from ref. 9

The oxidative properties of solvothermal reaction conditions led to the compound with formula $Eu_2(BDC)_3(DMF)_2(H_2O)_2$. Zhang reported this structure in 2006; it was found after reacting europium(III) nitrate with 1,3,5-triazine-2,4,6-tri(4-benzenecarboxylate) in a mixture of DMF and water at 115°C for 5 days, during which the organic molecule underwent hydrolysis.[10] Analogues of this interpenetrating network were reported by another Zhang (2006, Gd^{3+}), by using the exact same synthesis route as the Guo paper from the same year, and by solvothermal methods by He *et al.* for Er^{3+} and Tm^{3+}

analogues in 2010.[11] The main interest here was gas storage, so no photoluminescence was reported. A third Zhang published the structure with formula $Er_2(BDC)_3(DMF)_2$ in 2007, and even though the bruto formulae are very much alike, the resulting compound is not an analogue since it possesses an entirely different crystal structure.[12] The characteristic IR-emission from Er^{3+} was recorded for this compound.

Another alternative method for synthesizing coordination polymers with BDC^{2-} and lanthanide ions was developed by Yang *et al.* in 2007.[13] Here, the reagents are refluxed in methanol in the presence of an acetonitrile solution of triethylamine. Depending on the precipitation method (either slow evaporation or slow vapour diffusion of diethylether into the mixture) or the counterion (either chloride or nitrate) in the lanthanide salt, the composition of the product changes. Six compounds were obtained: $[Eu_2(BDC)_3(MeOH)_4]\cdot 8MeOH$, $[Ln(BDC)NO_3(MeOH)_2]\cdot MeCN\cdot H_2O$ with Ln = Eu^{3+} or Gd^{3+} (Figure 2-11) and $[Ln(BDC)(MeOH)_4]\cdot Cl\cdot MeOH\cdot 0.25H_2O$ with Ln = Eu^{3+}, Tb^{3+} or Gd^{3+}. Of these, the typical Eu^{3+} and Tb^{3+} visible emissions were recorded in DMF solution.

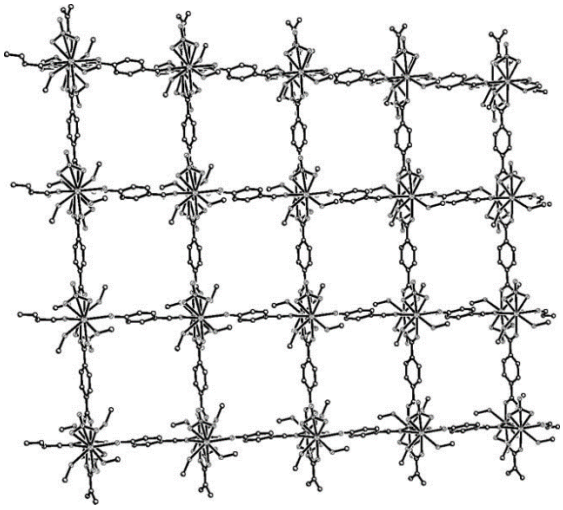

Figure 2-11: The $[Gd(BDC)NO_3(MeOH)_2]\cdot MeCN\cdot H_2O$ network as taken from ref. 13

Aiming to achieve upconversion, Weng *et al.* reported three compounds in 2006 with formula $[Ln_3(BDC)_{3.5}(OH)_2(H_2O)_2]\cdot H_2O$ with Ln = Y^{3+}, Er^{3+} or Yb^{3+} after hydrothermal synthesis.[14] They codoped the obtained compounds by using a mixture of the aforementioned ions with predetermined molar composition, giving rise to an isomorphous series of compounds, of which the Y analogue is given. (see Figure 2-12). Again, Y is not a lanthanide but this structure shows that it is possible to expect similar results when working with this non-lanthanide rare earth. The visible upconversion emission spectrum is recorded for the Y:Er-Yb codoped coordination polymer upon excitation at 980 nm.

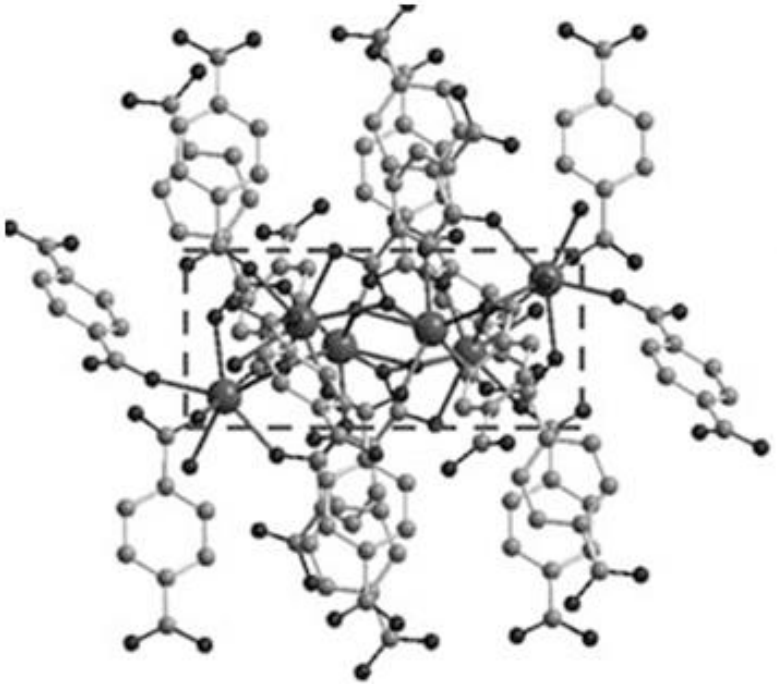

Figure 2-12: The $[Y_3(BDC)_{3.5}(OH)_2(H_2O)_2]\cdot H_2O$ network as taken from ref. 14

A potential contrasting agent containing Gd^{3+} was obtained by Rieter *et al.*[15] The compound has the same stoichiometry as the Reineke compound, but the synthesis employs the use of a water-in-oil micro-emulsion through the addition of cetyltrimethylammonium bromide (CTAB), a surfactant, to a mixture of isooctane, 1-hexanol and water.

Solvothermal synthesis with diethylformamide (DEF) as the solvent yielded three isostructural compounds for Yu *et al.* in 2007, using tetraethylammonium hydroxide as a pH-adjusting reagent.[16] They are $Ln(BDC)_{1.5}(DEF)$ with Ln = La^{3+}, Ce^{3+} and Nd^{3+} and are depicted in Figure 2-13. Emission spectra are recorded and again show LMCT and BDC fluorescence emission.

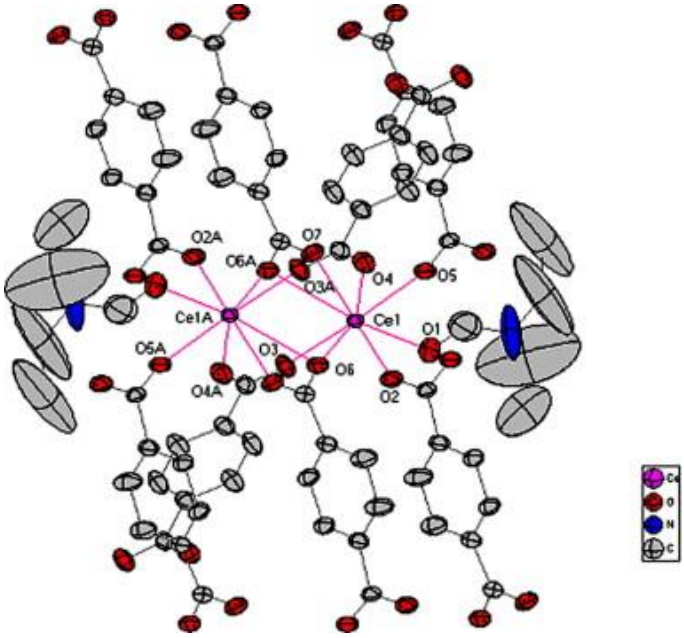

Figure 2-13: Crystal structure of $Ce(BDC)_{1.5}(DEF)$ as taken from ref. 16

Han *et al.* reported a number of compounds with formulae $Ln_6(BDC)_9(DMF)_6(H_2O)_3{\cdot}2DMF$ with Ln = La^{3+}, Ce^{3+} and Nd^{3+} and $Ln_2(BDC)_3(DMF)_2(H_2O)_2$

with Ln = Y^{3+}, Dy^{3+} and Eu^{3+}.[17] Of this last compound, the characteristic Eu^{3+} emission was recorded. The synthesis proceeded through a slow diffusion of two solutions into each other.

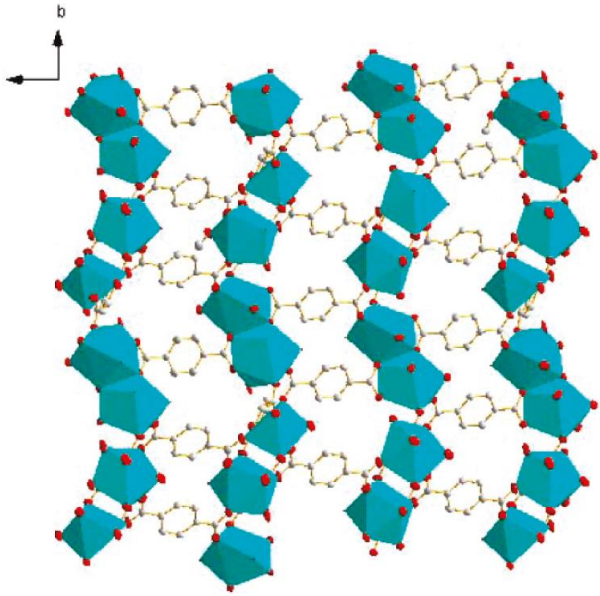

Figure 2-14: The $La_6(BDC)_9(DMF)_6(H_2O)_3 \cdot DMF$ network as taken from ref. 17

A large series of coordination polymers containing BDC^{2-} and lanthanide ions was reported in 2008 by Daiguebonne *et al.*[18] Three of them were suitable for single crystal X-ray diffraction analysis and found to be isostructural with $Tb_2(BDC)_3(H_2O)_4$, the only difference is the lanthanide ion used (La^{3+}, Ce^{3+} and Er^{3+}, respectively. See Figure 2-15). Microcrystalline powders were also obtained for Ln = Y, La-Tm except Pm; they were found to be isostructural with the aforementioned compound based on their X-ray powder diffraction patterns. The synthesis of these compounds was carried out in gel media. For Eu^{3+}, Tb^{3+} and Er^{3+}, nanosized particles of the same structure were obtained by encapsulating the reagents with an insoluble polymer. The same group also

controlled the size by restraining the growth of the compound by using poly(vinylpyrrolidone), an organic porous polymer. This is interesting because the biological application of coordination polymers is severely limited by their insolubility; however, reducing the size to nanoparticles, they may yet be useful in this regard. Detailed luminescence studies were performed on the Eu^{3+}, Tb^{3+} and Dy^{3+}-containing compounds.

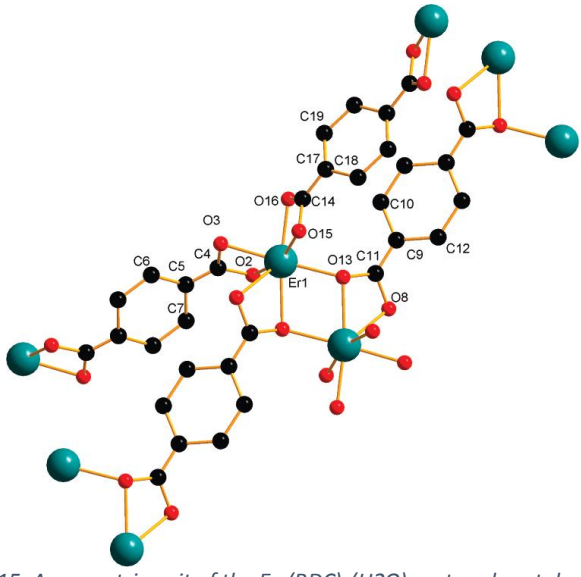

Figure 2-15: Asymmetric unit of the $Er_2(BDC)_3(H2O)_4$ network as taken from ref. 18

One year later, the same group published an article describing how one lanthanide may be substituted for another in the very same $Tb_2(BDC)_3(H_2O)_4$ structure without impacting the structure significantly, but allowing for efficient tuning of the luminescent output of the compounds.[19] The reported formulae are $La_{2-x}Y_x(BDC)_3(H_2O)_4$ with $0 \leq x \leq 2$ (to prove the random distribution of dopants), $Eu_{2-x}Tb_x(BDC)_3(H_2O)_4$ with $0 \leq x \leq 2$ (to show the difference between a mixed-metal heterodinuclear coordination polymer and a corresponding mixture of two mononuclear networks), $[\sum^{13}Ln_{2/13}(BDC)_3(H_2O)_4]$ with $0 \leq$

$x \leq 2$ (to show that incorporating all the lanthanides except Pm and including Y in equal proportions does not change the monophasic structure) and finally the ternary system $Ce_{2-x-y}Eu_xTb_y(BDC)_3(H_2O)_4$ with $x + y \leq 2$ (to obtain a wide variety of emitted colours, including white light, as shown in Figure 2-16).

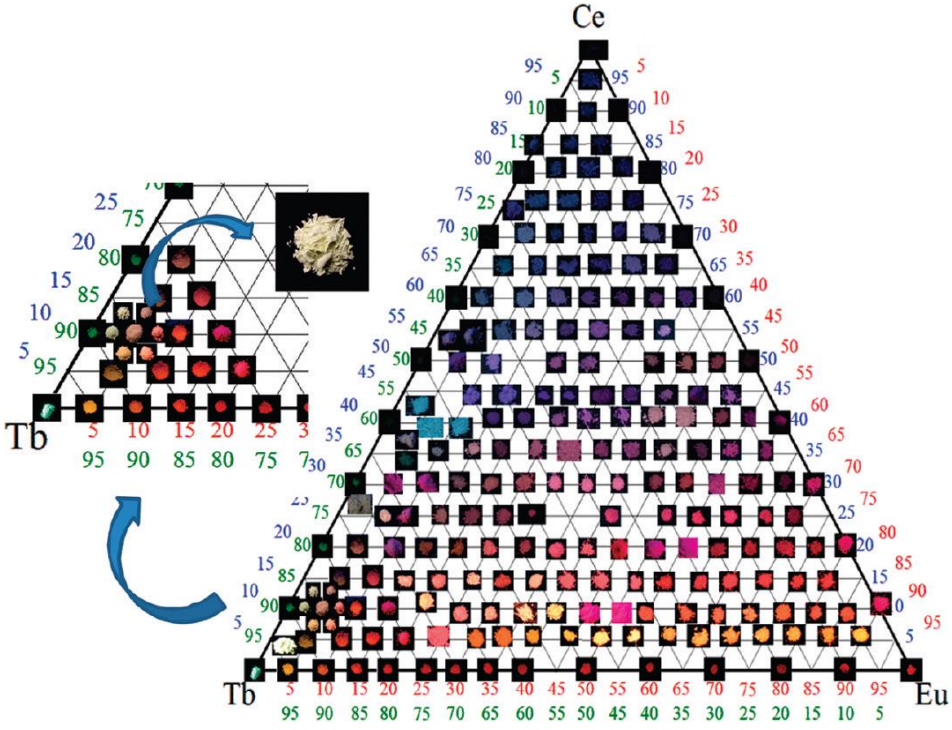

Figure 2-16: Photographs of the luminescent $Ce_{2-x-y}Eu_xTb_y(BDC)_3(H_2O)_4$ family under UV irradiation, as taken from ref. 19

A more in-depth investigation of the luminescent properties of the $Tb_2(BDC)_3(H_2O)_4$ structure was published in 2013.[20] The same group demonstrated how both colour and brightness can be tuned.

That the luminescence of lanthanide coordination polymers would prove to be useful for sensing was already confirmed by Xu *et al.* in 2011.[21] Thanks to a synthesis similar to that of Rieter, an isostructural Eu^{3+} compound was obtained and used as a

straightforward, highly sensitive sensor of nitroaromatic explosive compounds in an ethanol solution.

2.3.2 Mixing ligands

Purposefully mixing ligands provides new molecular architectures. In 2003, Wan *et al.* synthesized in hydrothermal fashion two coordination polymers with Eu^{3+} and with Yb^{3+}, using 1,10-phenanthroline to support the supramolecular structure as seen in Figure 2-17.[22] The formulae are $Eu(BDC)_{1.5}(phen)(H_2O)$ and $Yb_2(BDC)_3(phen)_2(H_2O)$, respectively. In the same work, they also obtained compounds with the 1,2- and 1,3-isomers of benzenedicarboxylate. Only of the 1,2-type was an Eu^{3+}-emission spectrum recorded.

In a work described above, He *et al.* obtained through a mild synthesis the compound $Er_2(BDC)_3(phen)_2 \cdot 3H_2O$

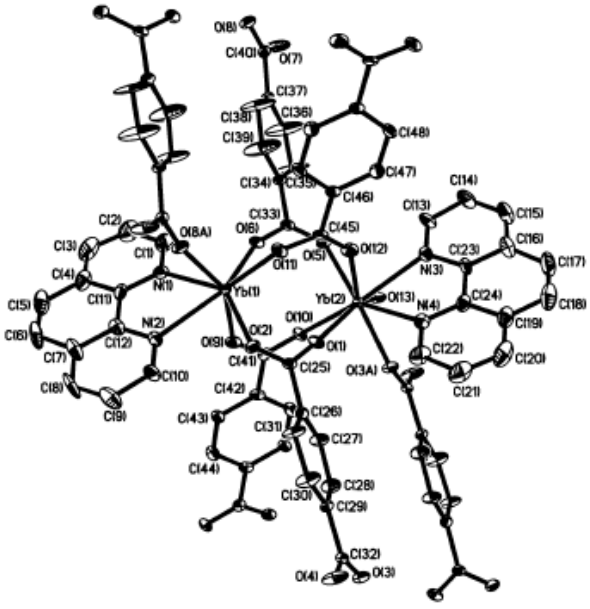

Figure 2-17: Asymmetric unit of the $Yb_2(BDC)_3(phen)_2(H_2O)$ network, as taken from ref. 22

Thirumurugan and Natarajan reported in 2004 that they had obtained mixed-ligand coordination polymers by the combination of terephthalic acid and 1,2-dicyanobenzene.[23] The latter oxidizes to 1,2-benzenedicarboxylate (the dianion is named phthalate; abbreviated as 1,2-BDC) during the hydrothermal synthesis. The compounds are of general formula $[Ln_2(H_2O)_4(1,2\text{-}BDC)_2(1,4\text{-}BDC)]$ with Ln = La^{3+}, Pr^{3+}, Gd^{3+}, Dy^{3+} and Y^{3+}. Two different structure classes are distinguished, based on the network connectivity and the coordination sphere around the lanthanide ions. The first type contains the lighter and larger lanthanide ions La^{3+} and Pr^{3+} (Figure 2-18, left), the smaller ions Gd^{3+}, Dy^{3+} and Y^{3+} (Figure 2-18, right) give rise to a different structure. Of these last three, photoluminescence spectra are recorded (although I am not sure how the Gd, Dy and Y spectra in this reference can show "the expected $^5D_4 \rightarrow {}^7F_n$ transitions").

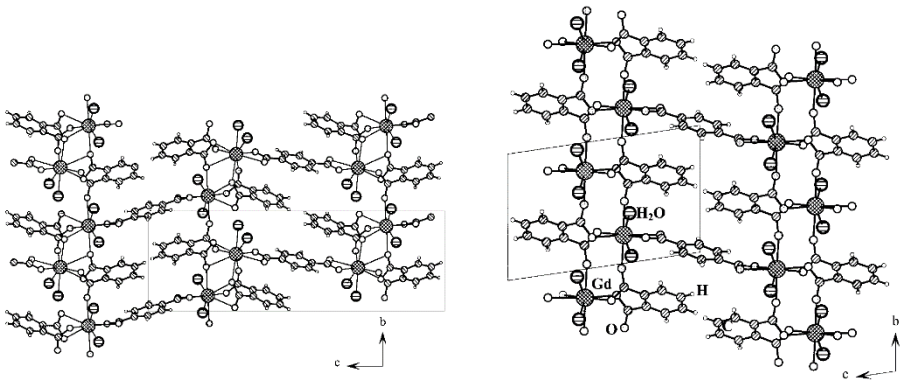

Figure 2-18: Two types of different networks with 1,4-BDC and 1,2-BDC as taken from ref. 23

In 2009, Wang *et al.* were able to obtain five compounds with formulae $[Ln(SUC)_{0.5}(BDC)]$ with Ln = Eu^{3+}, Sm^{3+}, Tb^{3+}, Pr^{3+}, Ho^{3+} and H_2SUC = succinic acid, a flexible non-aromatic dicarboxylic acid.[24] Both from the formula and the crystal structure in Figure 2-19 it can be seen that no water is present in the first coordination sphere. For the Eu^{3+} and Tb^{3+}

analogues the steady-state emission spectrum is recorded and the characteristic peaks assigned to transitions.

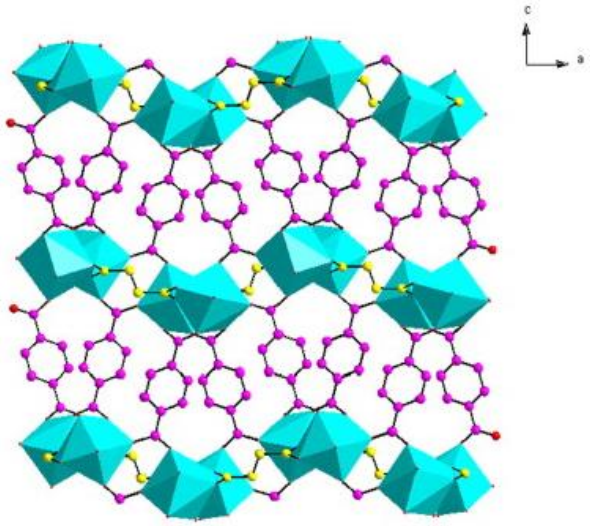

Figure 2-19: The $Ln(SUC)_{0.5}(BDC)$ network with SUC^{2-} carbon atoms in yellow and BDC^{2-} carbon atoms in pink, as taken from ref. 24

The same group published another mixed-ligand structure in 2012, this time with 1,2,4,5-benzenetetracarboxylic acid (H_4BTEC).[25] Using diisopropylamine to control the pH, after hydrothermal reaction three structures were obtained with formula $[Ln(BDC)_{0.5}(BTEC)_{0.5}(H_2O)]$ with Ln = Eu^{3+}, Gd^{3+} (Figure 2-20, left) and Tb^{3+} (Figure 2-20, right), where the Tb^{3+} compound shares the same formula but is a different structure due to different coordination modi. The Eu^{3+} and Tb^{3+} emission is briefly discussed.

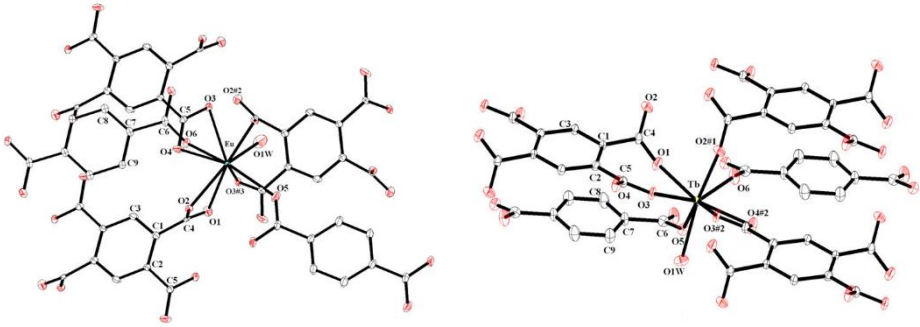

Figure 2-20: Two different $Ln(BDC)_{0.5}(BTEC)_{0.5}(H_2O)$ structures as taken from ref. 25, left: Ln = Eu^{3+}, Gd^{3+}, right: Ln = Tb^{3+}

2.3.3 State of the art

The most recent relevant pieces of research are briefly noted here in order to sketch what is happening right now in the field.

Recently, two articles were published in 2014 highlighting yet different research on Ln-BDC^{2-}-based coordination polymers. The first was written by Zhao *et al.* and uses CTAB again, as in the Rieter article.[26] The obtained compounds have the formula $Tb_{2-x}Eu_x(BDC)_3(H2O)_n$ with $0 \leq x \leq 2$, remarkably reminiscent of the Kerbellec work. The resulting materials were used for aldehyde sensing.

Another synthesis method recently published employed the use of the ionic liquid 1-ethyl-3-methylimidazolium bromide (EMIM-Br).[27] Three networks were obtained by Cao *et al.*: $\{(EMIM)_2[Sm_2(BDC)_3(H_2BDC)Cl_2]\}$ and $\{(EMIM)[Ln_2(Cl)(BDC)_3]\}$ with Ln = Eu^{3+} and Tb^{3+}. In all cases, the $EMIM^+$ cation acts as a charge-balancing species.

Finally, Utochnikova *et al.* reported in detail on the luminescence of $Eu_2(BDC)_3(H_2O)_4$ upon substituting a fraction of the Eu^{3+} ions with either Gd^{3+}, Y^{3+}, La^{3+} or Lu^{3+} to eliminate concentration quenching or with Tb^{3+} to achieve an alternative excitation pathway (from the BDC molecule via Tb^{3+} to Eu^{3+}).[28] It is shown that diluting the Eu^{3+} content does not

change the lifetime of quantum yields of the luminescence, and that the Tb → Eu energy transfer is quite efficient.

2.4 This work

2.4.1 On analysis techniques

We present here the synthesis and characterization of some compounds that have not yet before been reported.

In the research pertaining the formation of new, ordered coordination polymers, characterization becomes nigh impossible when no crystalline materials, suitable for single-crystal X-ray diffraction analysis, are formed. Since these compounds are also insoluble, nucleation and crystal growth proceed very differently when compared to small molecules. Small molecule single crystal growth can be seen as the gradual ordering within a lattice so that the molecules adopt the same orientation and molecular geometry. This contrasts with the synthesis of a crystalline coordination polymer, which is essentially the ordered formation of coordinative bonds. Rearrangements during this growth are possible and sometimes even necessary to correct faults in the crystal structure, but where rearrangements in small molecule single crystals involve simple translations and rotations around bonds, these rearrangements in coordination polymers are only possible when coordinative bonds break and reform, which is more demanding in energy. Recrystallization by dissolving is impossible because there are no intermolecular attraction forces to break, only coordination bonds. Purification by recrystallization, therefore, is excluded from the possibilities as well. If the goal is to prove the formation of a new product, then the synthesis must yield crystals of decent phase purity or it can be considered failed.

When obtaining nano- or microcrystalline materials that do not yield suitable single crystals but are suspected or known analogues of existing compounds, X-ray powder diffraction analysis can be useful. It can be used for either on-sight confirmation of the desired product if the diffraction peaks are at the same location and relative intensities. If small deviations occur, Rietveld refinement starting from a known structures powder diffraction pattern into a refined structure is also a possibility. However, for lanthanide coordination polymers with a high number of atoms in the unit cell, where the metal ions possess a significantly higher electron count, the patterns to refine are much more complicated than those of simpler crystals such as inorganic salts. Powder diffraction is also useful to determine whether the obtained structures have phase purity or if other side products have been co-crystallized, for example into the large voids within frameworks.

Other commonly applied characterization techniques that complement the main diffraction methods are:

a. thermogravimetric analysis to investigate the thermal stability of the compounds and to check for leftover unreacted ligands trapped but not participating to the structure of the network,
b. infrared spectroscopy to confirm the unchanged nature of organic molecules and specific functional groups,
c. elemental analysis to confirm the percentages of elements present
d. determination of the internal surface and porosity by nitrogen sorption is “optional”; with dense structures like these containing solvent molecules and high coordination numbers, there is not much void space in the network.

2.4.2 On synthesis methods

The crystallization bottleneck is why many of the reported synthesis methods in literature describe a hydrothermal or solvothermal route. Reaching temperatures higher than the normal boiling point under atmospheric pressure allows for atypical behaviour. Many insoluble materials become soluble. Through this solvation the organic molecules are able to come into contact with lanthanide salts. Sometimes the solubility is still quite minimal, this can be used to control the amount of reagents that come into contact with one another and therefore the growth rate. In these conditions, viscosity decreases, so the transport of molecules within solution becomes more efficient. Usually, solvothermal synthesis methods employing autoclaves or sealed tubes feature a warmer and colder area with respective sub- and supersaturation as far as reagents are concerned, giving rise to directed transfer and growing.

A very different method can be described as a somewhat more “mild” route and has been mentioned in the above literature summary: in a homogeneous mixture of solvents containing the reagents that is kept at slightly elevated temperature, the desired crystal will grow over a longer period of time. The elevated temperature is needed to allow the various components to react and arrange themselves in a product that is thermodynamically as stable as possible. It is this method that has proven to be of use to us in this work.

2.4.3 The compounds

In particular, lanthanide nitrate salts (Ln = Pr^{3+}, Nd^{3+}, Sm^{3+}, Eu^{3+} and Lu^{3+}) and terephthalic acid were dissolved in a mixture of DMF, water and/or ethanol. Complete

desolvation occurred after some time. A small amount of an amine base was added to deprotonate the carboxylic acid groups. Upon addition of this amine, the solution became non-transparent. Diluted nitric acid was added to this to solution until it became clear. Afterwards, this clear solution was kept at 60°C for one week, after which the compounds precipitated.

The europium-based compound yielded suitable crystals. The others yielded crystalline materials but no single crystals could be harvested. Subjecting the material to single crystal X-ray diffraction, collecting, interpreting and integrating the intensity data, solving and refining the structure showed us that a previously unreported material had crystallized.

Several remarks need to be made here. The reaction procedure was a modification of an existing one. Guo *et al.* and Na *et al.* both had similar methods. The temperature was increased with respect to Guo *et al.* (from 55°C to 60°C), as well as the quantities used (triple all the values). We changed the composition of the solvent mixture when compared to Na *et al.* (DMF:H_2O:EtOH in a 5:1:1 volume ratio instead of DMF:EtOH in a 5:1 ratio), and the amine base was not methylamine but triethylenetetramine. The greatest difference however was the fact that we used four larger, lighter lanthanide ions compared to Guo (Tb^{3+}, Dy^{3+}, Ho^{3+}, Er^{3+}) or Na (Yb^{3+}). Although different lanthanides often have similar chemistries, subtle differences can occur when traversing the series. These variations are usually encountered in comparisons between the respective first and second halves of the lanthanide series. As a testament to that, using the described procedures without modifications did not yield the necessary crystals. Therefore we can assume that temperature, quantity and chemical properties of the reagents play an

important part, but the metal ion has a more prominent role than the exact reaction conditions. The proof for this assumption is found in the resulting crystal structures, which are significantly different from the previously published ones. It is not straightforward to correlate synthesis conditions or lanthanide ion identity with structure. The way the synthesis method was chosen was an educated guess, based on literature procedures. Without high-throughput equipment, simple modification of existing recipes might be the most reliable way to get positive results. Therefore we consider the fact that crystals decided to form fortuitous. This goes for the next structure and the one in the following chapter as well, and extends to the results from chapter 5 as well.

The fifth structure was obtained with the Lu^{3+} ion and proved to be an entirely different structure. Slightly varying the synthesis method by using triethylamine instead of triethylenetetramine and omitting the EtOH solvent in the synthesis, proved to yield crystals, other attempts were unsuccessful. This shows again that a portion of trial and error is involved when searching for new crystals.

Using lutetium in these networks is rarely done. There is no possibility for 4f transition-based luminescence since the 4f orbitals are completely filled. This makes the element fit for use as a matrix in which luminescent ions can be doped. Specifically the heavier lanthanides can be expected to be good substitutions since the difference this would impart on the lattice is smaller.

2.4.4 The crystal structures

2.4.4.1 Eu-BDC and analogues

2.4.4.1.1 Discussion of the crystal structures

The obtained material crystallizes in the triclinic space group P-1, this means that there is an inversion centre present. It has the formula $Eu_2(BDC)_3(DMF)_2(H_2O)\cdot DMF$. As this molecular formula suggests, there are two distinct Eu(III) centres, three BDC^{2-} ligands, two coordinating DMF molecules, one coordinating water molecule and one DMF solvent "guest" molecule that is ordered but does not take part in bonds.

The first trivalent europium ion, coded Eu1, has a coordination number of eight. Six oxygen atoms from six different BDC^{2-}-ligands bond to the metal ion. The BDC^{2-} carboxylato ligands are bis-monodentate. The remaining oxygen atoms come from one coordinating DMF molecule (O14) and one aqua ligand (O15). This is presented in Figure 2-21.

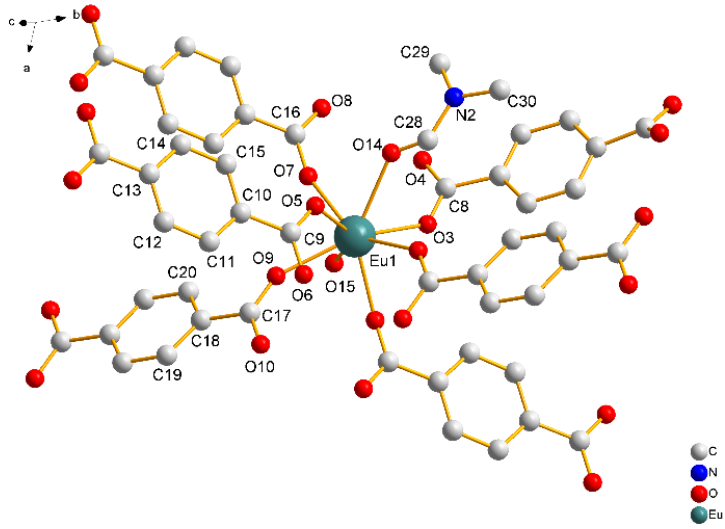

Figure 2-21: Coordination of Eu1

The second Eu(III) center, coded Eu2, is also octacoordinated (see Figure 2-22). This time there are seven oxygen atoms from BDC^{2-} ligands; these come from five bis-monodentately coordinating groups and one bidentately chelating (O1 and O2) carboxylate groups. The eighth oxygen is again from a coordinating DMF molecule (O18).

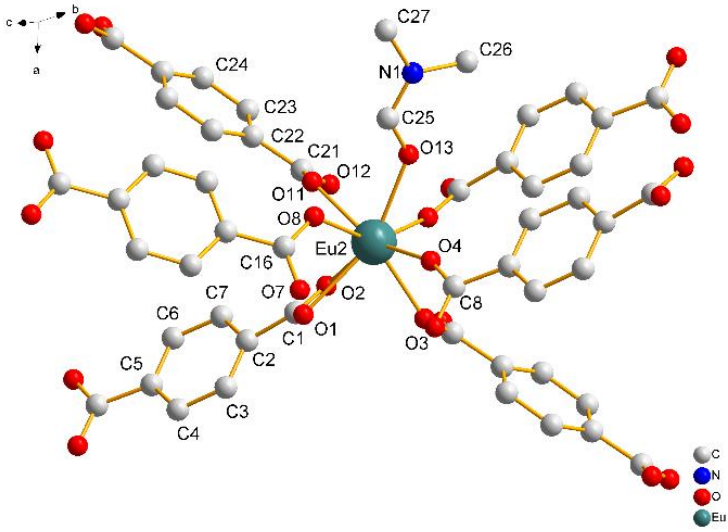

Figure 2-22: Coordination of Eu2

Both coordination environments can be described as distorted square antiprisms. In fact, finding ideal regular or even semiregular polyhedra as a coordination sphere for lanthanide ions is rather rare.

The antiprisms are connected to each other to create infinite chains. These chains are crosslinked with each other, forming a threedimensional network. Here follows how the chains are built up: Eu1 is connected to its inversion counterpart Eu1' by four bis-monodentately coordinating carboxylate groups. Eu2 and Eu2' are connected by two bridging chelating and two bis-monodentately coordinating ligands, forming an edge-sharing dimer.

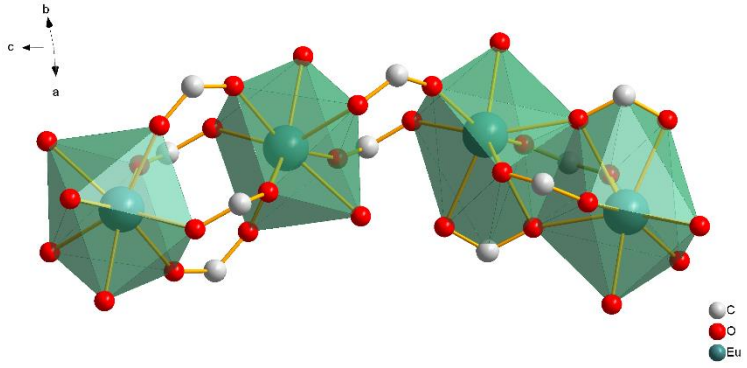

Figure 2-23: Secondary building unit construct of a tetranuclear cluster

The Eu1-Eu1' and Eu2-Eu2' dimers are in turn connected by two bis-monodentately coordinating carboxylate groups. This leads to a building unit consisting out of four metal ions. These secondary building units (SBU's) are further assembled into infinite chains once the packing is applied.

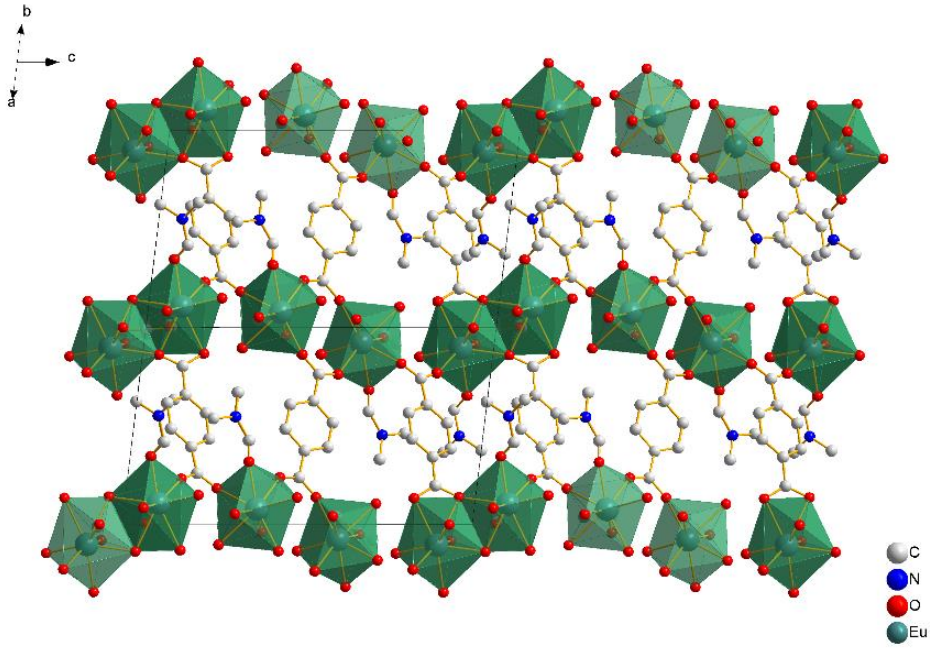

Figure 2-24: Packing of the Eu compound

Table 2-1: Crystallographic data for $Eu_2(BDC)_3(DMF)_2(H_2O)\cdot DMF$

molecular formula	$C_{33}H_{33}Eu_2N_3O_{16}$
fw (g mol^{-1})	1031.56
cryst dimensions (mm^3)	0.21 × 0.14 × 0.11
cryst syst	triclinic
space group	$P\bar{1}$ (No. 2)
a (Å)	11.0552(7)
b (Å)	11.0713(6)
c (Å)	17.6488(10)
α (deg)	93.084(5)
β (deg)	104.429(5)
γ (deg)	119.032(6)
V ($Å^3$)	1789.8(2)
Z	2
ρcalcd (g cm_{-3})	1.914
2θmax (deg)	50.7
T (K)	100(2)
F(000)	1012
measured reflns	11 627
unique reflns	9981
obsd reflns (I > 2σ(I))	7985
params refined	494
R1	0.0672
wR2	0.1891
R1 (all data)	0.0842
wR2 (all data)	0.2094
GOF	1.092
μ (mm^{-1})	3.551
CCDC entry	CCDC-891471

The results of both the measurement and structure refinement are summarized in Table 2-1.

This crystal structure differs from any existing compound. When comparing, we have looked to all coordination polymers that contain the fully deprotonated BDC^{2-} ligand, DMF as a coordinating ligand, and any lanthanide in general but europium in particular. The isostructural compounds presented by Guo *et al.* and Na *et al.* were the first to have the comparison made since the synthesis would suggest a structural similarity. However, there, instead of infinite chains, pseudochains are formed by the combination of three crystallographically distinct ions, not two.

Our result is also unlike the structures reported by Han *et al.* that have six different Ln ions with three different coordination numbers.

Lastly, the structure that was accidentally obtained by Zhang *et al.* where an organic molecule hydrolysed during the solvothermal reaction also contains the BDC ligand, DMF and trivalent europium. It forms a 3D- network but with a different topology: the europium centres again form dimers but are nona- instead of octacoordinated by three chelating bridging coordinating and one chelating carboxylate, one DMF and one H_2O. It forms an interpenetrating network, this means that the space in between is taken up by a parallel (in some cases antiparallel) coordination polymer instead of solvent molecules. In this network, the first coordination environment is described as a distorted tricapped trigonal prism.

The other three syntheses were carried out with different lanthanide ions, namely Pr^{3+}, Nd^{3+} and Sm^{3+}. Although crystalline materials were obtained, none were found to be

single crystals. We recorded the XRPD patterns and at first glance suspected that they were isostructural to the Eu compound.

To confirm this, one can apply Rietveld refinement to the Eu structure to see how the crystal parameters need to change in order to correspond to the experimentally obtained powder patterns of the unidentified structures. Assuming that the structures are similar allows for retrieval of the lattice parameters. However, for a unit cell that contains a large amount of atoms both light and heavy, the powder patterns are very rich in diffraction peaks. This makes the Rietveld analysis increasingly complicated as there are much more parameters to be refined. We sought to facilitate this problem by omitting the lighter atoms (H, C, N and O) from the unit cell. The assumption is validated by the resulting theoretical powder pattern: the position and intensities of the diffraction peaks do not change. Compare the top and second from top patterns in Figure 2-26. This leads us to the conclusion that here, only the heaviest elements (i.e. the lanthanide ions) determine the powder pattern. Refining the position of these heavy lanthanides should therefore yield the three unknown structures.

Seeing as how the lanthanide ions are positioned on chains in primary lattice planes (Figure 2-25), and these planes show diffraction at lower angles according to the Bragg law (Figure 2-26, top), we can limit ourselves to refining a small range of angles (2θ = 8 to 11).

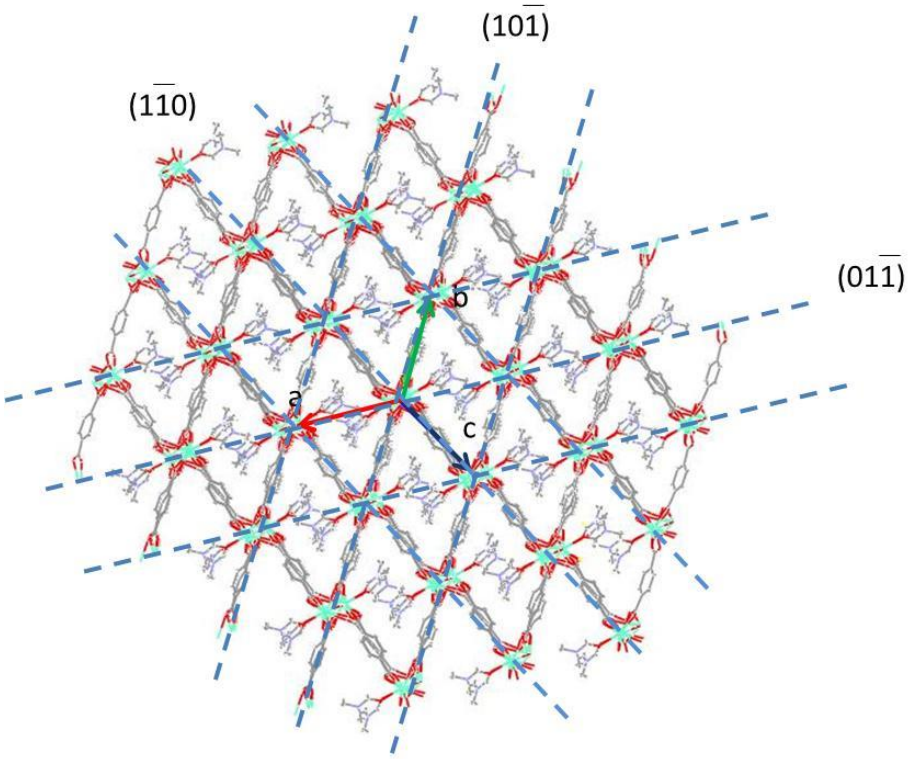

Figure 2-25: Scheme of primary lattice planes containing the lanthanide ions

The Rietveld refinement is an analysis technique that is based on simulating (by iteration) an experimental powder pattern by making small, controlled changes in an existing crystal structure, which produces small, controlled changes in the powder pattern of that structure.

To this end, we have used the MAUD (Materials Analysis Using Diffraction) software package, available as freeware online.[29] To start using the MAUD software, there are two things that one needs: a crystallographic information file (.cif extension) from a structure that closely resembles the hypothetical target structure, and a data file containing a diffractogram with intensity I in counts s^{-1} as a function of 2θ.

In a stepwise refinement, we first refined the background and scale factors while keeping the other parameters fixed. Afterwards, the cell parameters a, b, c and α, β, and γ were refined and lastly the atomic coordinates. This proved to be the most controlled method to get the adjusted structure approach the experimental diffractogram without producing illogical results, because only a few parameters at a time are released, while the previously refined ones are already in place. Upon completion, we achieved a near perfect agreement between fits and experimental curves of the powder patterns (Figure 2-26, bottom four patterns).

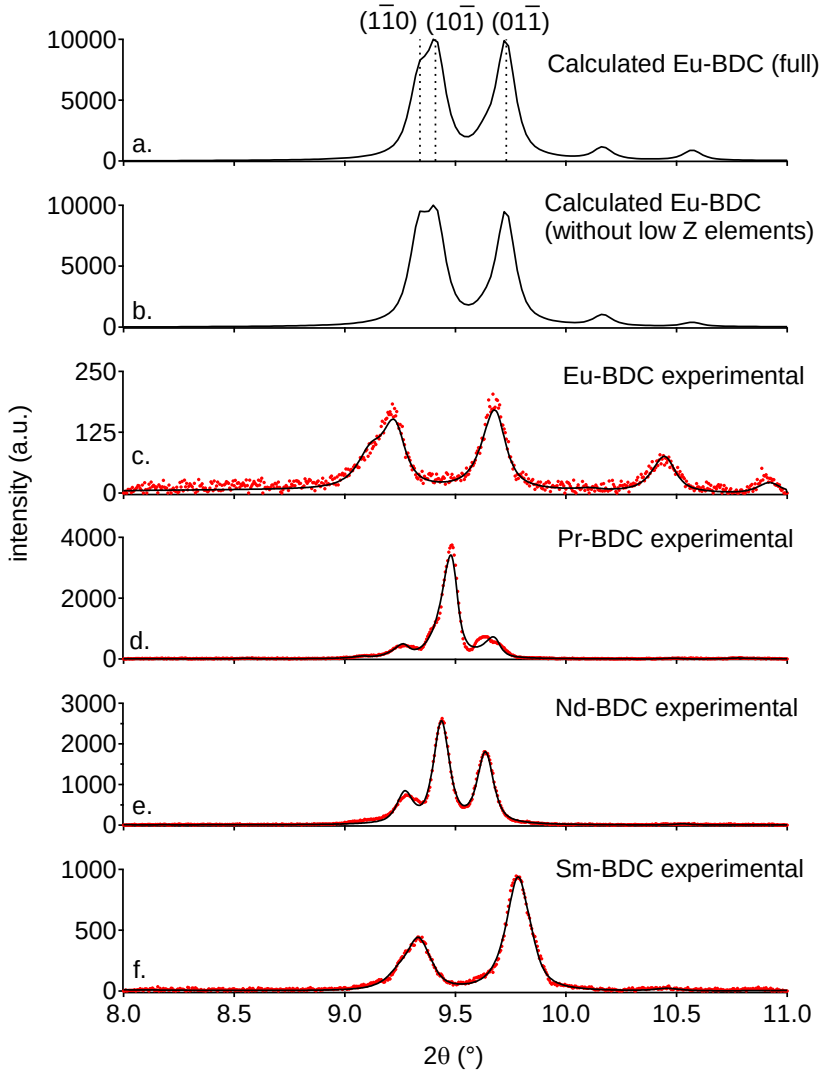

Figure 2-26: Scheme of the Rietveld refinement results.
From top to bottom: the powder pattern calculated from the crystallographic data;
the same pattern but with only Eu1 and Eu2;
results of the fitting procedure; red dots: the powder pattern as recorded, black line: the powder pattern calculated after the refinement (the "fit")

The experimental powder pattern peaks are somewhat shifted compared to the calculated ones, which is unsurprising since calculated patterns are based on ideal infinite crystals without any mosaicity and low thermal vibrations. The observed 2θ-

range is also greatly limited; viewing the complete powder patterns from 5 to 50° shows that the differences are indeed minimal. Furthermore, the calculated pattern is based on a crystal measured at cryogenic temperature (100 K), whereas the experimental pattern was recorded at room temperature. Based upon seeing that the cell parameters did not change drastically and remained almost identical in this short range, we can see that there is a highly isostructural relationship between the four compounds.

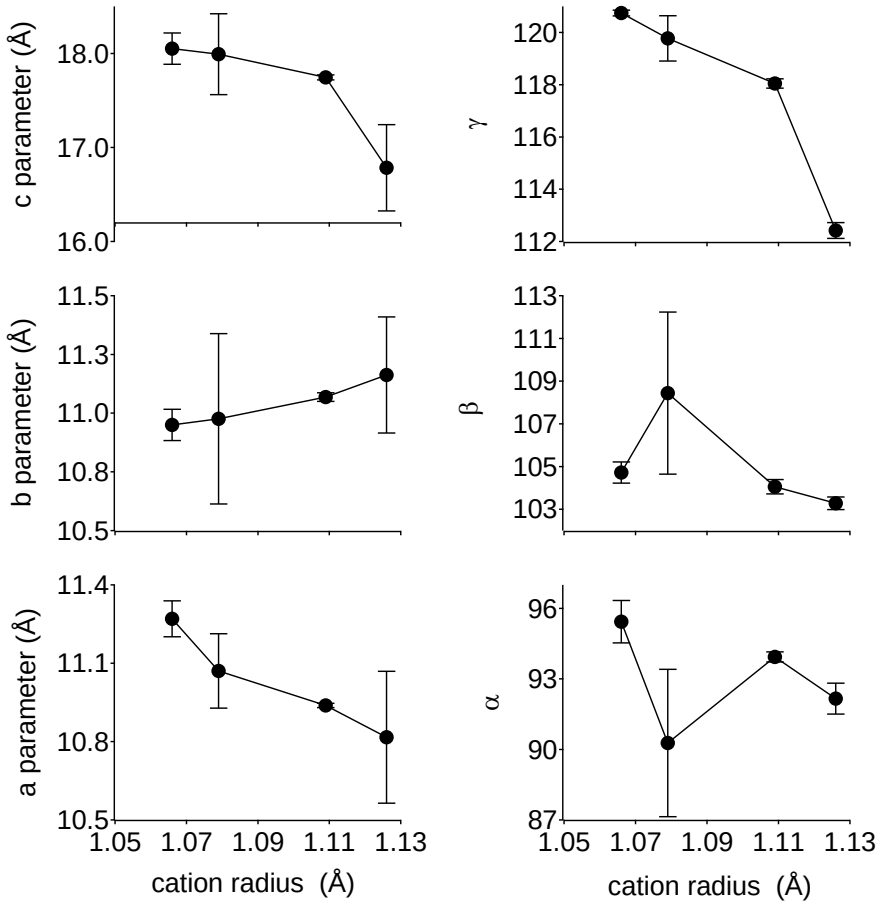

Figure 2-27: Compilation of lattice parameters after Rietveld refining. The y-axis has been expanded to fit the data.

Further characterization was performed with infrared spectroscopy. At 3061 cm^{-1} the aromatic C-H stretch is visible. The aromatic benzene skeleton vibration is found at 1512 cm^{-1}, and a peak at 828 cm^{-1} is attributed to the 1,4-substitution pattern on benzene. The characteristic symmetric and asymmetric stretching vibrations from the deprotonated carboxylic acids can be assigned and are located at 1313 and 1580 cm^{-1}, respectively. Around 1700 cm^{-1} the carbonyl bands from DMF are visible. Finally, the peak at 3500 cm^{-1} is attributed to O-H stretching from coordinated water All four compounds show an analogous IR spectrum.

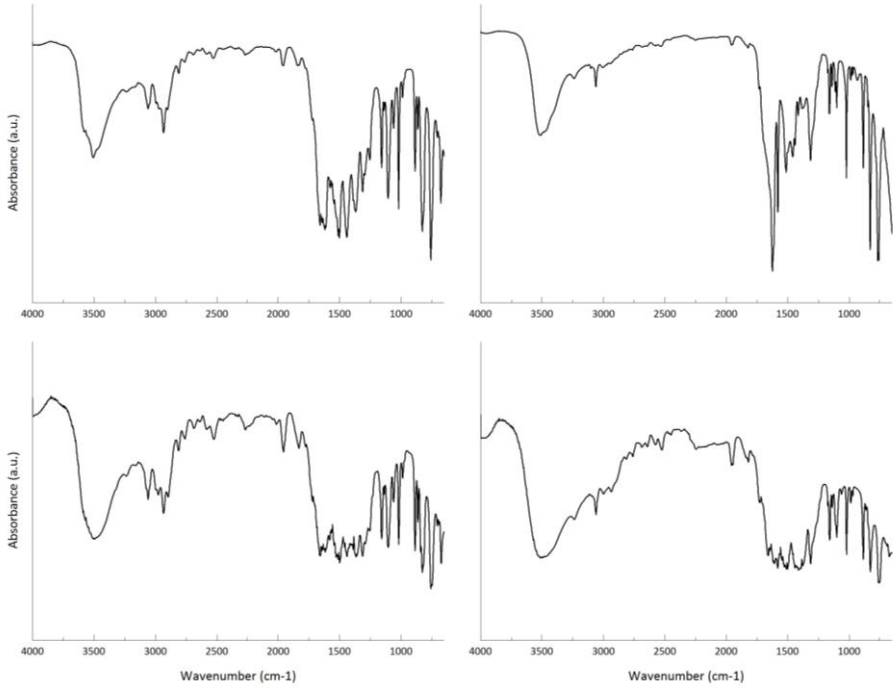

Figure 2-28: IR absorbance spectra of the BDC compounds: Sm, top left; Eu, top right; Pr, bottom left; Nd, bottom right

The thermal stability of the coordination polymers was checked with thermogravimetric analysis (TGA, Figure 2-29). The first weight loss of 6.2% occurs between 80 and 120°C

and corresponds to the loss of a guest DMF molecule (calculated at 7.08%). A second weight loss of 8.9% is attributed to the removal of a coordinated DMF and a water molecule between 190 and 240°C (calculated at 8.83%). Beyond 390°C the compounds decomposes leaving only the europium oxide Eu_2O_3 at 34.6% of the initial weight remaining (calculated at 31.2%). It has to be noted that the coordinated DMF molecules were not removed by high temperature treatment.

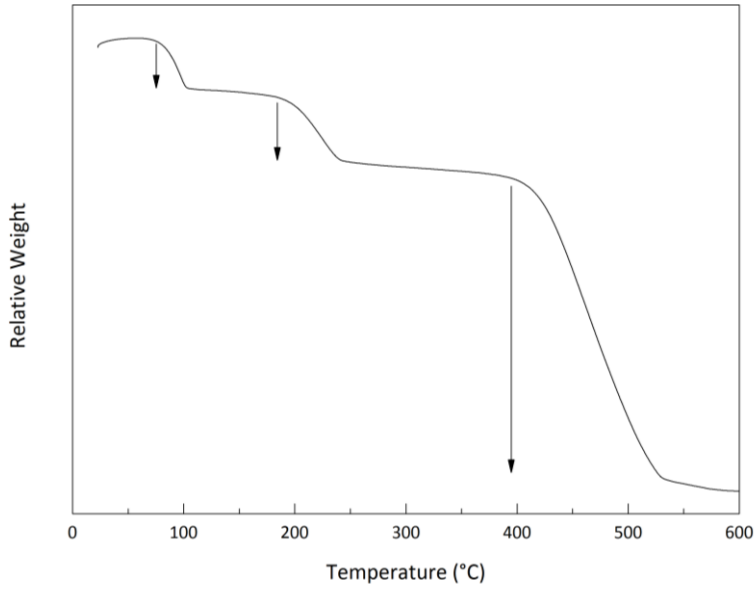

Figure 2-29: Thermogravimetric analysis of $Eu_2(BDC)_3(DMF)_2(H_2O)\cdot DMF$ (downward arrows correspond to weight losses)

To check the internal surface and porosity of the compounds, we performed BET analysis on them and found surfaces of 3.4138 m²/g, 5.1376 m²/g, 2.6876 m²/g and 2.9818 m²/g for the Pr, Nd, Sm and Eu compounds, respectively. These surfaces are low, in essence they are the surface of the outer area of the particles. This indicates that the compounds are not porous, which is unsurprising, in fact, seeing as how the coordinated and guest

molecules take up all the space inside the crystal structure and fill the voids (see Figure 2-30).

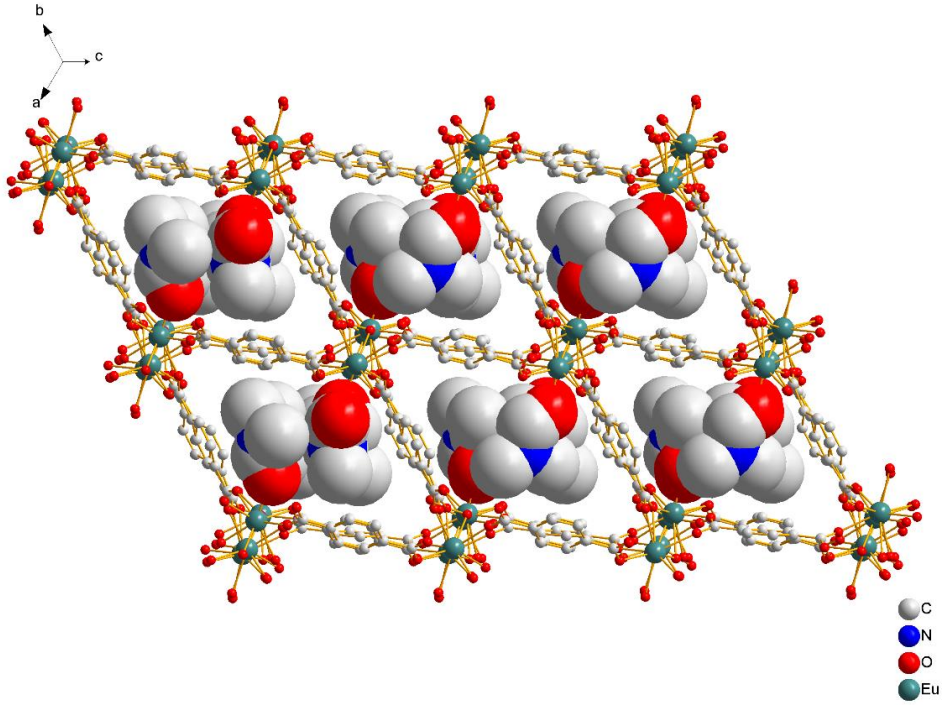

Figure 2-30: The network with Eu^{3+} and BDC^{2-} in ball-and-stick mode and the DMF in space-fill mode

The DMF guest molecules are hard to remove due to their high boiling point; this is even more so for DMF coordinated to Ln(III) ions. Even though we are able to calculate the hypothetical internal surface by removing the guest and coordinated solvent molecules in the crystal structure, this does not mean that this feature is readily accessible.

2.4.4.1.2 Steady-state photoluminescence

By containing lanthanides, the compounds are expected to show some luminescence activity. Even though the carboxylato ligands may not be the most suitable moieties for sensitization through the antenna effect, a number of promising results have been published already. Although weak for some, all four compounds show the typical lanthanide-based luminescence with sharp peaks. The 4f-4f transitions are obviously present and can be assigned.

Praseodymium-based luminescence is less frequently reported than Eu-luminescence, which is actually the most studied ion of the lanthanide series. In fact, only one other carboxylate-based Pr-containing coordination polymer has been found to emit its characteristic light. There are two emitting levels in Pr(III) which makes the assignment of the peaks more difficult. However, we have made an attempt to assign the correct transitions (see Table 2-2).

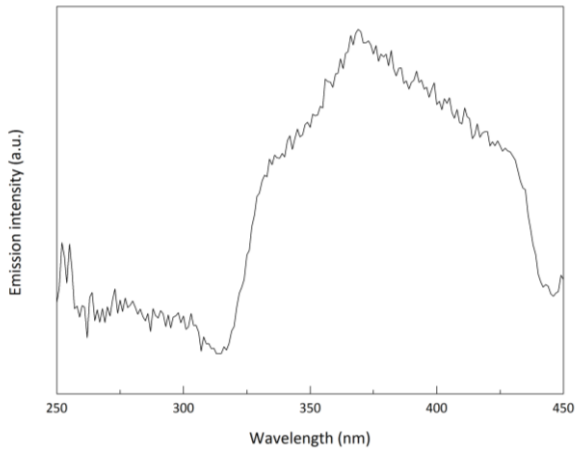

Figure 2-31: Excitation spectrum of $Pr_2(BDC)_3(DMF)_2(H_2O)\cdot DMF$ monitoring the 643.5 nm emission intensity

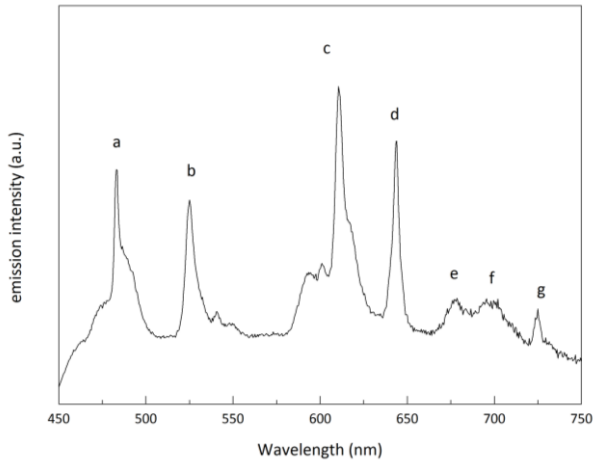

Figure 2-32: Emission spectrum of $Pr_2(BDC)_3(DMF)_2(H_2O)\cdot DMF$ upon excitation at 300 nm

Table 2-2: Assignment of the peaks in Figure 2-32

label	λ (nm)	ῡ (cm^{-1})	transition
a	483.3	20690	$^3P_0 \rightarrow {}^3H_4$
b	525.1	19045	$^3P_0 \rightarrow {}^3H_5$
c	610.6	16375	$^3P_0 \rightarrow {}^3H_6$
d	643.6	15535	$^3P_0 \rightarrow {}^3F_2$
e	677.8	14755	$^1D_2 \rightarrow {}^3H_5$
f	697.2	14345	$^3P_0 \rightarrow {}^3F_3$
g	724.9	13795	$^3P_0 \rightarrow {}^3F_4$

For the Nd^{3+} and Sm^{3+} analogues, the emission is rather weak but the peaks can be easily assigned. The characteristic Nd infrared emission is well known; the peak at 1064 nm is used primarily in Nd:YAG lasers.

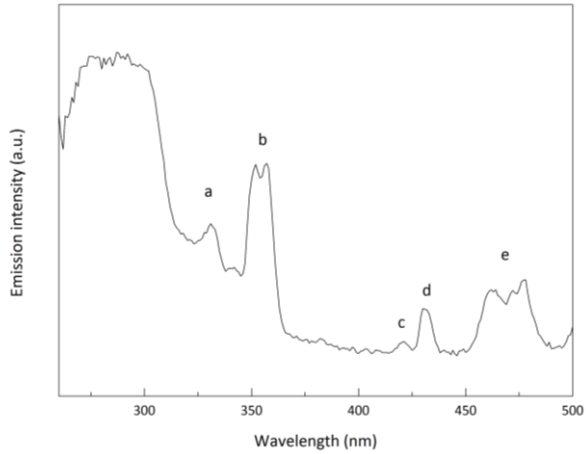

Figure 2-33: Excitation spectrum of $Nd_2(BDC)_3(DMF)_2(H_2O)\cdot DMF$ monitoring the 1066 nm emission

Table 2-3: Assignment of the peaks in Figure 2-33

label	λ (nm)	ῡ (cm^{-1})	transition
a	330.8	30230	$^2L_{15/2}$, $^4D_{7/2}$, $^2I_{13/2} \leftarrow {}^4I_{9/2}$
b	354.4	28220	$^4D_{3/2}$, $^4D_{5/2}$, $^2I_{11/2}$, $^4D_{1/2} \leftarrow {}^4I_{9/2}$
c	420.8	23760	$^2D_{5/2} \leftarrow {}^4I_{9/2}$
d	430.9	23210	$^2P_{1/2} \leftarrow {}^4I_{9/2}$
e	469.1	21320	$^4G_{11/2}$, $^2D_{3/2}$, $^2P_{3/2}$, $^2G_{9/2}$, $^2K_{15/2} \leftarrow {}^4I_{9/2}$

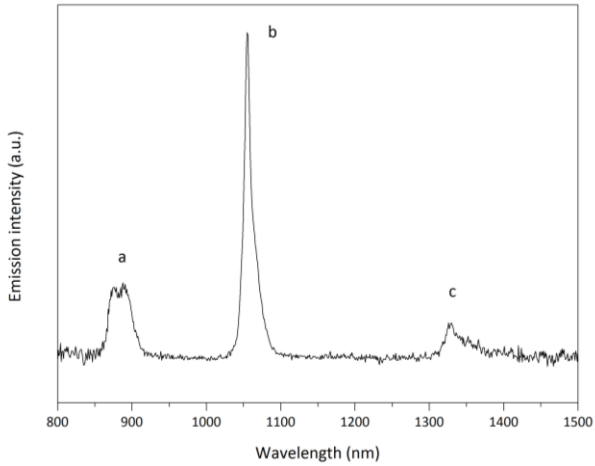

Figure 2-34: Emission spectrum of $Nd_2(BDC)_3(DMF)_2(H_2O)\cdot DMF$ upon excitation at 298 nm

Table 2-4: Assignment of the peaks in Figure 2-34

label	λ (nm)	ῡ (cm^{-1})	transition
a	884.0	11310	$^4F_{3/2} \rightarrow {}^4I_{9/2}$
b	1055.9	9470	$^4F_{3/2} \rightarrow {}^4I_{11/2}$
c	1330.8	7515	$^4F_{3/2} \rightarrow {}^4I_{13/2}$

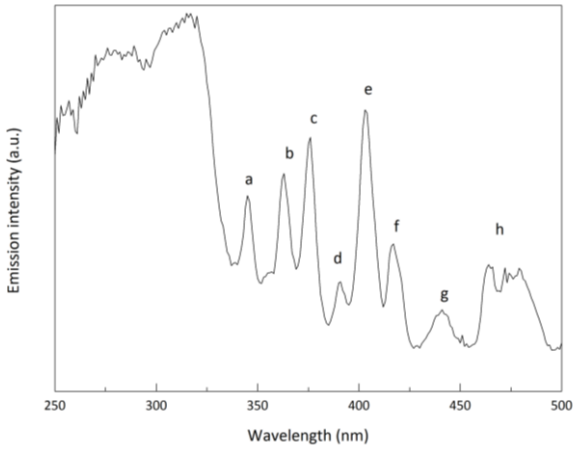

Figure 2-35: Excitation spectrum of $Sm_2(BDC)_3(DMF)_2(H_2O)\cdot DMF$ monitoring the 598 nm emission

Table 2-5: Assignment of the peaks in Figure 2-35

label	λ (nm)	ῡ (cm^{-1})	transition
a	344.8	29000	$^4D_{7/2} \leftarrow {}^6H_{5/2}$
b	362.8	27560	$^4D_{3/2}$, $^4D_{5/2}$, $^6P_{5/2} \leftarrow {}^6H_{5/2}$
c	376.0	26595	$^6P_{7/2} \leftarrow {}^6H_{5/2}$
d	390.7	25600	$^4L_{15/2} \leftarrow {}^6H_{5/2}$
e	403.2	24805	$^6P_{3/2} \leftarrow {}^6H_{5/2}$
f	416.8	23995	$^6P_{5/2}$, $^4P_{5/2} \leftarrow {}^6H_{5/2}$
g	441.2	22665	$^4G_{9/2}$, $^4M_{17/2} \leftarrow {}^6H_{5/2}$
h	472.0	21185	$^4I_{13/2}$, $^4I_{11/2,}$ $^4M_{15/2} \leftarrow {}^6H_{5/2}$

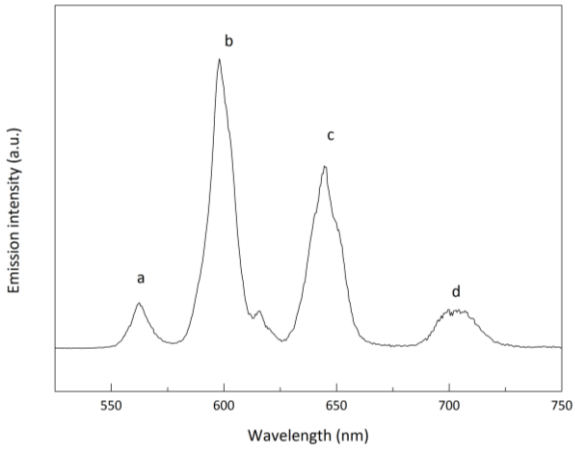

Figure 2-36: Emission spectrum of $Sm_2(BDC)_3(DMF)_2(H_2O)\cdot DMF$ upon excitation at 290 nm

Table 2-6: Assignment of the peaks in Figure 2-36

label	λ (nm)	ῡ (cm^{-1})	transition
a	562.6	17775	$^4G_{5/2} \rightarrow {}^6H_{5/2}$
b	598.1	16720	$^4G_{5/2} \rightarrow {}^6H_{7/2}$
c	645.0	15505	$^4G_{5/2} \rightarrow {}^6H_{9/2}$
d	702.9	14225	$^4G_{5/2} \rightarrow {}^6H_{11/2}$

The same relative weakness in signal goes for the Eu compound, even though this is by far the brightest of the four. As an added level of complexity in this spectrum however, we can see in Figure 2-37 there are three different ways in which the europium is excited. The broad band around 300 nm corresponds to the excitation of the ligand followed by sensitization through the antenna effect, as described in Figure 1-9. The narrow transitions come from both the $^7F_0$ ground state excitation as well as excitation of the first excited state $^7F_1$.

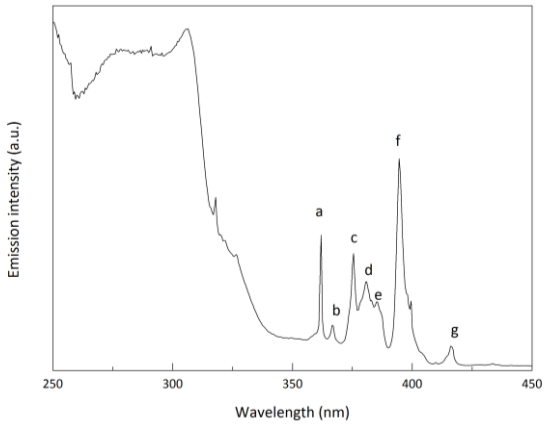

Figure 2-37: Excitation spectrum of $Eu_2(BDC)_3(DMF)_2(H_2O)\cdot DMF$ monitoring the 616 nm emission

Table 2-7: Assignment of the peaks in Figure 2-37

label	λ (nm)	ῡ (cm^{-1})	transition
a	362.1	27620	$^5D_4 \leftarrow {}^7F_0$
b	367.0	27250	$^5D_4 \leftarrow {}^7F_1$
c	375.4	26640	$^5G_4 \leftarrow {}^7F_0$
d	380.6	26275	$^5G_2 \leftarrow {}^7F_0$
e	385.4	25950	$^5G_2 \leftarrow {}^7F_1$
f	394.4	25355	$^5L_6 \leftarrow {}^7F_0$
g	416.4	24015	$^5D_3 \leftarrow {}^7F_1$

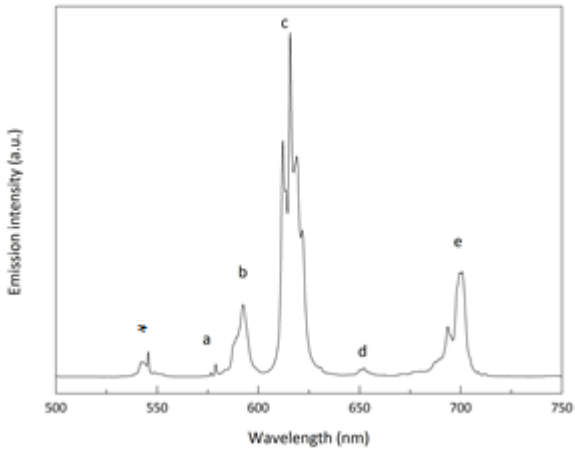

Figure 2-38: Emission spectrum of $Eu_2(BDC)_3(DMF)_2(H_2O)\cdot DMF$ upon excitation at 298 nm

Table 2-8: Assignment of the peaks in Figure 2-38

label	λ (nm)	ῡ (cm^{-1})	transition
The transition labelled with an * is attributed to a Tb transition, originating in cuvette contamination.			
a	579.0	17270	$^5D_0 \rightarrow {}^7F_0$
b	592.5	16880	$^5D_0 \rightarrow {}^7F_1$
c	616.0	16235	$^5D_0 \rightarrow {}^7F_2$
d	652.3	15330	$^5D_0 \rightarrow {}^7F_3$
e	700.0	14285	$^5D_0 \rightarrow {}^7F_4$

When we add the low overall intensity of the spectra to these findings, we can theorize that the BDC^{2-} ligand is, for these ions, a suboptimal choice.

That the dianionic terephthalate ion is a relatively poor sensitizer can be explained by looking at the energy levels of the ligand. We found the relevant data in literature[30], Hilder *et al.* determined the triplet level of BDC at 23256 cm^{-1}. For energy transfer to be efficient, the triplet level of the ligand needs to be in close proximity of the emitting lanthanide energy level.

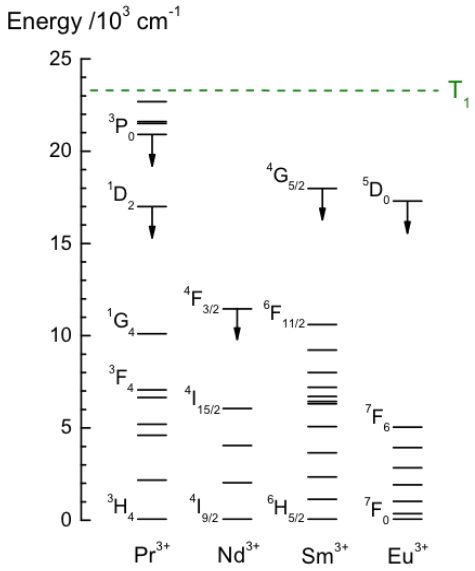

Figure 2-39:Solid lines: energy levels of selected lanthanide ions, green dashed line: BDC triplet level

This is not the case for the Nd, Sm and Eu compounds; the difference is too large and there are too many radiationless deactivation pathways that make it possible to avoid luminescent decay. For the Pr analogue, however, the triplet energy is too close to the emitting level. This opens the possibility for energy back transfer from the metal to the ligand, making ligand phosphorescence more plausible. This is indeed visible in the emission spectrum of the compound, where the characteristic Pr lines are superimposed on a broad organic emission band.

2.4.4.1.3 Luminescent decay

The luminescent decay rates of the four compounds were measured and compared to literature values of relevant compounds.

Table 2-9: Luminescent decay times of the BDC compounds

Ln	Decay time τ (µs)
Pr	11
Nd	0.43
Sm	11
Eu	475

There was only one report found of a luminescent Pr^{3+}-containing coordination polymer[31], but it does not contain an excitation spectrum or time-resolved measurements, so it is not possible to make a decent comparison. For a comparison with other luminescent Nd^{3+}, Sm^{3+} and Eu^{3+} coordination polymers, we turned to a compiled list in an excellent review by Cui *et al.* and the many references it contains.[32] No luminescent decay times were reported for Nd^{3+}- and Sm^{3+}–containing materials though. For Eu^{3+}, many are present, and the decay rates range from 0.344 to 2 ms. Narrowing this number down is possible by excluding all non-terephthalate networks. The range then becomes 0.344 to 0.47 ms for hydrated and 0.94 ms for anhydrous compounds, meaning that our Eu^{3+} sample compares well.

One could compare other compounds with ours. For example, Voloshin *et al.* could not measure the decay time of Pr β-diketonate and carboxylate chelates since it was shorter than the 4 µs detection limit of their setup.[33] In a crystal with composition $Gd_3Ga_5O_{12}:Pr^{3+}$, Mahlik *et al.* reported lifetimes from 23 to 6.5 µs, depending on

pressure.[34] Our value of 11 µs for the Pr compound holds up well. For Nd^{3+} and Sm^{3+}, Bassett *et al.* reported lifetimes of Nd^{3+} and Sm^{3+} homologues of β-diketonate complexes of 1.5 µs and 13 µs, which are well within the order of magnitude of our compounds.

2.4.4.2 Lu-BDC

2.4.4.2.1 Discussion of the crystal structure

Since lutetium is on the other end of the lanthanide series, it is not unreasonable to expect a different structure when the synthesis method is repeated but with substituting the lanthanide element for lutetium. The main condition, of course, is that a product that can be characterized is actually obtained, but this has a high chance of occurring since the Tb^{3+}, Dy^{3+}, Ho^{3+}, Er^{3+} and, in another instance, Yb^{3+} analogues were successfully synthesized. However, these structures are all isostructural, so only results can confirm whether the series is isostructurally continued or a newer architecture is obtained.

This product, then, crystallizes in the C2/c space group. In the asymmetric unit there is one lutetium(III) cation, 1.5 BDC^{2-} linkers, one DMF molecule and one water molecule. This means that we can write the formula of this compound as $Lu_2(BDC)_3(DMF)_3(H_2O)_2$. It was found to be isostructural with the Er^{3+} analogue published by Zhang *et al.* in 2008.

The asymmetric unit is presented in Figure 2-40. One BDC^{2-} dianion is fully included, the other is only obtained after performing the symmetry operations on this cell, again confirming the somewhat higher amount of symmetry within the structure.

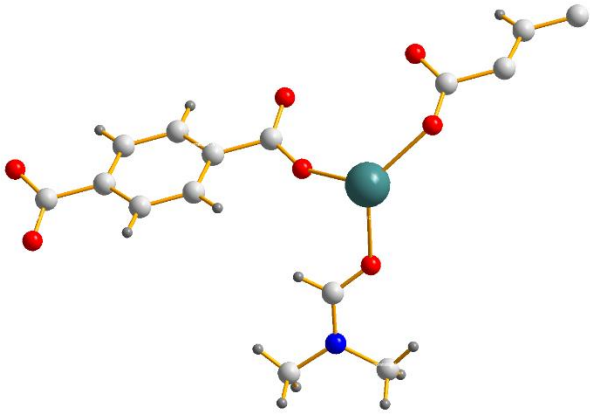

Figure 2-40: Asymmetric unit of $Lu_2(BDC)_3(DMF)_3(H_2O)_2$

Every Lu^{3+} ion is heptacoordinated by seven oxygen atoms. Six of these originate from the terephthalic acid carboxylate groups. The seventh oxygen is from the DMF molecule, and the water molecules are present as guest solvent. The coordination polyhedron of Lu^{3+} can be seen as a monocapped trigonal prism.

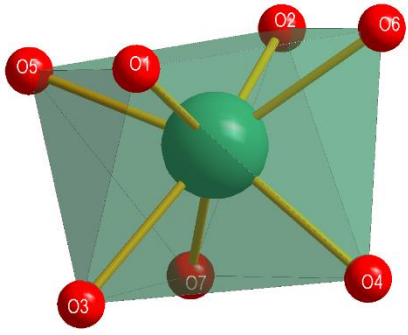

Figure 2-41: Coordination polyhedron of the Lu(III) ion

The BDC linkers show only one mode of coordination, all carboxylate groups coordinate in bis-monodentate fashion. This allows for a highly symmetrical network.

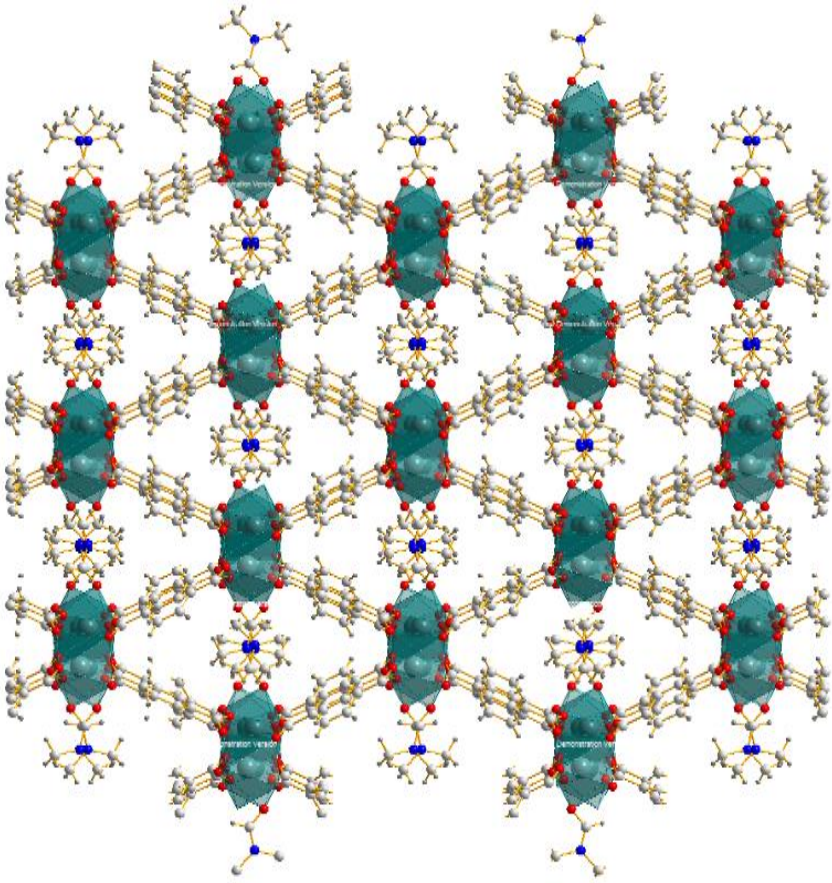

Figure 2-42: Packing of the Lu-BDC compound

It is somewhat striking that in relatively similar systems the two smaller lanthanides (Er^{3+}, Lu^{3+}) that have lower coordination numbers yield structures with more inherent symmetry.

Table 2-10: Crystallographic data for $Lu_2(BDC)_3(DMF)_3(H_2O)_2$

molecular formula	$C_{15}H_{13}NLuO_7$
fw (g mol^{-1})	502.83
cryst dimensions (mm^3)	0.1511 x 0.1009 x 0.058
cryst syst	monoclinic
space group	C2/c (No. 15)
a (Å)	18.2964(5)
b (Å)	10.8429(3)
c (Å)	17.3889(4)
α (deg)	90
β (deg)	101.489(3)
γ (deg)	90
V ($Å^3$)	3380.59(16)
Z	8
ρ_{calcd} (g cm^{-3})	1.976
2θmax (deg)	52.74
T (K)	100(2)
F(000)	1930
measured reflns	17968
unique reflns	3463
obsd reflns (I > 2σ(I))	2635
params refined	229
R1	0.0377
wR2	0.0581
R1 (all data)	0.0661
wR2 (all data)	0.0664
GOF	1.045
μ (mm^{-1})	5.879
CCDC entry	CCDC-999885

2.5 Conclusion and outlook

We have successfully synthesized five new lanthanide terephthalate coordination polymers. Two of these, with formula $Eu_2(BDC)_3(DMF)_2(H_2O)\cdot DMF$ and $Lu_2(BDC)_3(DMF)_3(H_2O)_2$ yielded single crystals. Their structures were elucidated, and out of the Eu^{3+} compound three more analogous compounds were found after Rietveld refinement. They were found to be not porous. The luminescence was measured for these compounds except for $Lu_2(BDC)_3(DMF)_3(H_2O)_2$.

This could prove to be quite interesting for the near future; if one can obtain a lutetium-based coordination polymer it should be possible to dope this with small amounts of other lanthanides in order to achieve spectrometrically interesting properties such as upconversion.

2.6 References

[1] From Condensed Lanthanide Coordination Solids to Microporous Frameworks Having Accessible Metal Sites, T.M. Reineke, M. Eddaoudi, M. Fehr, D. Kelley, O.M. Yaghi, J. Am. Chem. Soc., **1999**, Vol. 121, Issue 8, p. 1651

[2] A Microporous Lanthanide-Organic Framework, T.M. Reineke, M. Eddaoudi, M. O'Keeffe, O.M. Yaghi, Angew. Chem. Int. Ed., **1999**, Vol. 38, Issue 17, p. 2590

[3] Synthesis, Characterization and Structural Transformation of A Condensed Rare Earth Metal Coordination Polymer, L. Pan, N. Zheng, Y. Wu, S. Han, R. Yang, X. Huang, J. Li, Inorg. Chem., **2001**, Vol. 40, p. 828

[4] Interplane Distances Modulation in Lanthanide-Based Coordination Polymers, A. Deluzet, W. Maudez, C. Daiguebonne, O. Guillou, Cryst. Growth Des., **2003**; Vol. 3, No.4, p. 475

[5] Synthesis, Crystal Structure, and Porosity Estimation of Hydrated Erbium Terephthalate Coordination Polymers, C. Daiguebonne, N. Kerbellec, K. Bernot, Y. Gérault, A. Deluzet, O. Guillou, *Inorg. Chem.*, **2006**, Vol. 45, Issue 14, p. 5399

[6] Hydrothermal Synthesis, Structure Determination, and Thermal Behavior of New Three-Dimensional Europium Terephthalates: MIL-$51_{LT,HT}$ and MIL-52 or $Eu_2^n(OH)_x(H_2O)_y(O_2C{-}C_6H_4{-}CO_2)_z$ (n = III, III, II; x = 4, 0, 0; y = 2, 0, 0; z = 1, 1, 2), C. Serre, F. Millange, J. Marrot, G. Férey, Chem. Mater., **2002**, Vol. 14, Issue 2, p. 2409

[7] Synthesis, Structure, and Luminescent Properties of Microporous Lanthanide Metal–Organic Frameworks with Inorganic Rod-Shaped Building Units, X. Guo, G. Zhu, F. Sun, Z. Li, X. Zhao, X. Li, H. Wang, S. Qiu, Inorg. Chem., **2006**, Vol. 45, Issue 6, p. 2581

[8] Synthesis, Structure and Luminescent Property of a Novel Lanthanide Metal-Organic Coordination Polymer $Yb_3(BDC)_{4.5}(DMF)_2(H_2O)_3{\cdot}(DMF)_2$, L. Na, R. Hua, L. Zhang, G. Ning, J. Chem. Cryst., **2009**, Vol. 39, Issue 9, p. 688

[9] Metal-Organic Scandium Framework: Useful Material for Hydrogen Storage and Catalysis, J. Perles, M. Iglesias, M.-A. Martin-Luengo, M.A. Monge, C. Ruiz-Valero, N. Snejko, Chem. Mater., **2005**, Vol. 17, p. 5837

[10] Synthesis and Crystal Structure of Two Lanthanide Complexes with Benzenecarboxylic Derivatives, Z.-H. Zhang, S.-Y. Wan, T. Okamura, W.-Y. Sun, N. Ueyama, Z. Anorg. Allg. Chem., **2006**, Vol. 632, Issue 4, p. 679

[11] Control over Interpenetration in Lanthanide-Organic Frameworks: Synthetic Strategy and Gas-Adsorption Properties, H. He, D. Yuan, H. Ma, D. Sun, G. Zhang, H.-C. Zhou, Inorg. Chem., **2010**, Vol. 49, 7605

[12] Synthesis, structures and photoluminescence of two Er(III) coordination polymers, Y. Zhang, J. Yang, G.-D. Li, F. Zhang, J.-S. Chen, J. Coord. Chem., **2008**, Vol. 61, Issue 6, p. 945

[13] Syntheses, structures and luminescent properties of new lanthanide-based coordination polymers based on 1,4-benzenedicarboxylate (bdc), X.-P. Yang, R.A. Jones, J.H. Rivers, R. Pen-jen Lai, Dalton Trans., **2007**, Issue 35, p. 3936

[14] Assembly and Upconversion Properties of Lanthanide Coordination Polymers Based on Hexanuclear Building Blocks with (μ_3-OH) Bridges, D. Weng, X. Zheng, L. Jin, Eur. J. Inorg. Chem, **2006**, Issue 20, p. 4184

[15] Nanoscale Metal-Organic Frameworks as Potential Multimodal Contrast Enhancing Agents, W.J. Rieter, K.M.L. Taylor, H. An, W. Lin, W. Lin, J. Am. Chem. Soc., **2006**, Vol. 128, Issue 28, p. 9024

[16] Syntheses, structures and properties of novel 3D lanthanide metal-organic frameworks with paddle-wheel building blocks, L.-Q. Yu, R.-D. Huang, Y.-Q. Xu, T.-F. Liu, W. Chu, C.-W. Hu, Inorg. Chim. Acta, **2008**, Vol. 361, Issue 7, p. 2115

[17] Structures and Properties of Porous Coordination Polymers Based on Lanthanide Carboxylate Building Units, Y. Han, X. Li, L. Li, C. Ma, Z. Shen, Y. Song, X. You, Inorg. Chem., **2010**, Vol. 49, Issue 23, p. 10781

[18] Structural and Luminescent Properties of Micro- and Nanosized Particles of Lanthanide Terephthalate Coordination Polymers, C. Daiguebonne, N; Kerbellec, O. Guillou, J.-C. Bünzli, F. Gumy, L. Catala, T. Mallah, N. Audebrand, Y. Gérault, K. Bernot, G. Calvez, Inorg. Chem., **2008**, Vol. 47, Issue 9, p. 3700

[19] An Unprecedented Family of Lanthanide-Containing Coordination Polymers with Highly Tunable Emission Properties, N. Kerbellec, D. Kustaryono, V. Haquin, M. Etienne, C. Daiguebonne, O. Guillou, Inorg. Chem., **2009**, Vol. 48, Issue 7, p. 2837

[20] Color and Brightness Tuning in Heteronuclear Lanthanide Terephthalate Coordination Polymers, V. Haquin, M. Etienne, C. Daiguebonne, S. Freslon, G. Calvez, K. Bernot, L. Le Pollès, S.E. Ashbrook, M.R. Mitchell, J.-C. Bünzli, S.V. Eliseeva, O. Guillou, Eur. J. Inorg. Chem., **2013**, Issue 20, p. 3464

[21] A luminescent nanoscale metal–organic framework for sensing of nitroaromatic explosives , H. Xu, F. Liu, Y. Cui, B. Chen, G. Qian, Chem. Commun., **2011**, Vol. 47, Issue 11, 3153

[22] High-Dimensional Architectures from the Self-Assembly of Lanthanide Ions with Benzenedicarboxylates and 1,10-Phenanthroline, Y. Wan, L. Zhang, L. Jin, S. Gao, S. Lu, Inorg. Chem., **2003,** Vol. 43, p. 4985

[23] Inorganic–Organic Hybrid Compounds: Synthesis and Structures of New Metal Organic Polymers Synthesized in the Presence of Mixed Dicarboxylates, A. Thirumurugan, S. Natarajan, Eur. J. Inorg. Chem., **2004**, Issue 4, p. 762

[24] Synthesis, crystal structures and properties of a series of three-dimensional lanthanide coordination polymers with the rigid and flexible mixed dicarboxylate ligands of 1,4-benzene dicarboxylic acid and succinic acid, C.-G. Wang, Y.-H. Xing, Z.-P. Li, J. Li, X.-Q. Zeng, M.-F. Ge, S.-Y. Niu, J. Molec. Struc., **2009**, Vol. 921, Issues 1-3, p. 126

[25] Hydrothermal synthesis, crystal structure, and photoluminescence of novel lanthanide metal organic frameworks constructed from 1,4-benzene-dicarboxylic acid and 1,2,4,5-benzenetetracarboxylic acid as ligands, J.-L.Wang, K.-L. Hou, F.-Y. Bai, Y.-H. Xing, Z. Shi, Struct. Chem., **2012**, Vol. 23, Issue 1, p. 275

[26] Metal–organic coordination polymers of $Tb_{2-x}Eu_x(BDC)_3(H_2O)_n$ with tunable fluorescence and smart response toward aldehydes ($0 \le x \le 2$, BDC = 1,4-benzenedicarboxylate), X.J. Zhao, J.H. Yang, Y. Liu, P.F. Gao, Y.F. Li, RSC Adv., **2014**, Vol. 4, Issue 5, p. 2554

[27] Ionothermal syntheses, crystal structures and luminescence of three three-dimensional lanthanide-1,4-benzenedicarboxylate frameworks, H.-Y. Cao, Q.-Y. Liu, M.-Y. Gao, Y.-L. Wang, L.-L. Chen, Y. Liu, Inorg. Chim. Acta, **2014,** Vol. 414, p. 226

[28] Unusual Luminescence Properties of Heterometallic REE Terephthalates, A.Y. Grishko, V.V. Utochnikova, A.A. Averin, A.V. Mironov, N.P. Kuzmina, Eur. J. Inorg. Chem., **2015**, Issue 10, p. 1660

[29] Dowloaded from http://www.ing.unitn.it/~maud/index.html as found january **2010**

[30] Spectroscopic properties of lanthanoid benzene carboxylates in the solid state: Part 1, M. Hilder, P.C. Junk, U.H. Kynast, M.M. Lezhnina, J. Photochem. Photobiol. A: Chemistry, Vol. 202, Issue 1, p. 10

[31] A novel praseodymium coordination polymer with Pcu topology: Crystal structure, thermal decomposition, luminescence and magnetic properties, X. Feng, Y.F. Wang, Z.Q. Shi, J.J. Shang, L.Y. Wang, Inorg. Chem. Commun., **2012,** Vol. 22, p. 131

[32] Luminescent Functional Metal-Organic Frameworks, Y.L. Cui, Y. F. Yue, G. D. Qian, B. L. Chen, Chem. Rev, **2012**, Vol 112, p. 1126 and all references therein

[33] Luminescence of praseodymium (III) chelates from two excited states ($^3P_0$ and $^1D_2$) and its dependence on ligand triplet state energy, A.I. Voloshin, N.M. Shavaleev, V.P. Kazakov, J. Lumin., **2001**, Vol. 93, p. 199

[34] High pressure and time resolved luminescence spectra of $Gd_3Ga_5O_{12}:Pr^{3+}$ crystal, S. Mahlik, M. Malinowksi, M. Grinberg, Opt. Mater., **2011**, Vol. 33, p. 1529

3 Coordination polymers based on 2,5-pyridinedicarboxylic acid

3.1 Outline and goals

A second part in the research was trying to find out what happens to crystal architecture and luminescence activity when the organic linker is varied. One of the easiest and cheapest variations possible is the incorporation of a heteroatom in the aromatic ring, which will make the coordination slightly more complex. To this end, we again performed a literature search in order to maximize our chances for success. In the same spirit as the previous chapter, the goal here was to check if repeating literature procedures with different lanthanide ions either yield new coordination polymers with different structures, or yield analogous structures where the only difference originates from a different ionic radius. As a second objective, we wanted to obtain decent luminescent properties.

3.2 Introduction

We looked at 2,5-pyridinedicarboxylic acid (H_2PDC, PDC^{2-} for the twice deprotonated ligand, PDC in formulas). The molecule is only different from the H_2BDC linker in that it features a nitrogen atom on the aromatic ring, but this has far-reaching consequences. The lone pair is also able to coordinate metal ions, which vastly increases the number of coordination modes when compared to the H_2BDC linker.

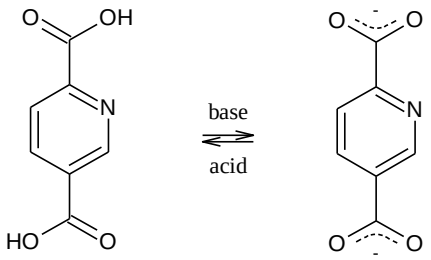

Figure 3-1: 2,5-Pyridinedicarboxylic acid (H_2PDC)

Specifically, there is the possibility to form a five-membered chelate ring, improving the stability of the formed coordinative bonds. The molecule is rigid and therefore fit to bridge ions.

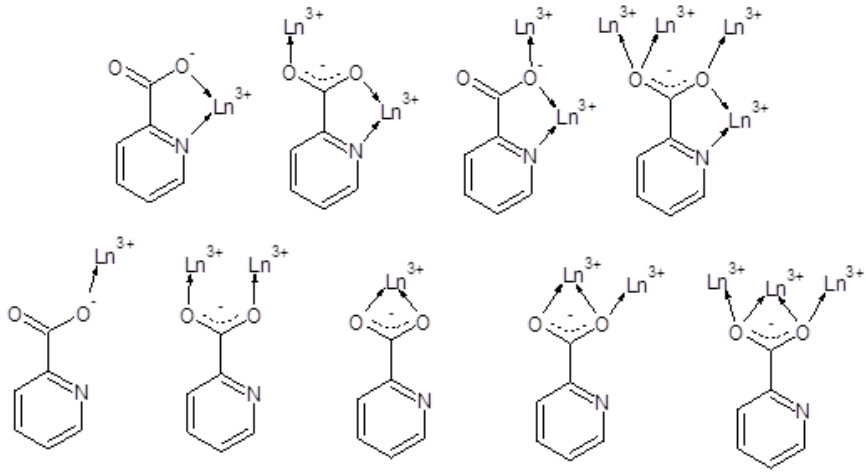

Figure 3-2: Coordination modes of the 2-pyridinecarboxylate motif

3.3 Reported relevant research

3.3.1 Combining lanthanides with PDC

Although younger and less extended than the group of lanthanide coordination polymers containing BDC^{2-}, the PDC^{2-} family is still quite large. Initially, the H_2PDC ligand was combined with transition metals or mixtures of transition metals and lanthanides. Only serendipitously was the first structure with just lanthanide ions obtained. The other earliest structures with only lanthanide ions were reported in 2005, making this Ln-PDC family half a decade younger than the first reported Ln-BDC compound by Reineke.

Trying to obtain a heterometallic coordination polymer with both Mn^{2+} and Nd^{3+}, Zhang *et al.* found that the neodymium ions had greater affinity for the oxygen coordination sites of the PDC ligand than the Mn had.[1] This led to a structure with molecular formula $Nd_2(PDC)_2(HPDC)_2(H_2O)_4 \cdot 2H_2O$, shown in Figure 3-3. The Nd^{3+} ions form a one-dimensional chain by carboxylate bridges. The PDC^{2-} ligands bridge chains together to form two-dimensional layers. Extended hydrogen bonds from the water molecules, together with π–π-stacking of the aromatic rings, add the third dimensionality in a supramolecular network. Half of the H_2PDC ligands are monoprotonated to account for charge balance and to participate in the hydrogen bonding. In previous years, mixed-metal compounds with 2,5-H_2PDC were already reported, but no Ln-only variants, so this is, to the best of my knowledge, the first one.

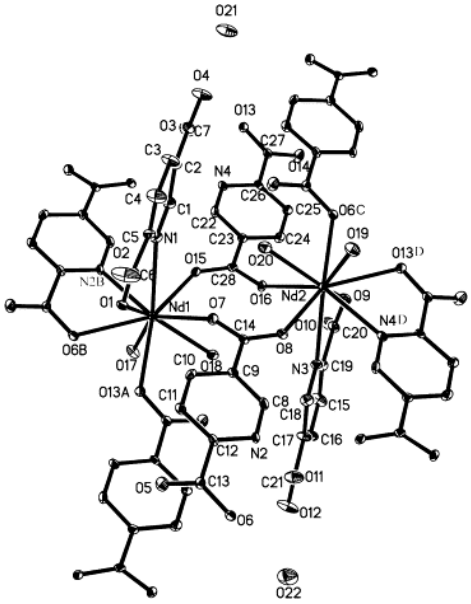

Figure 3-3: Unit cell of $Nd_2(PD^-)_2(HPDC)_2(H_2O)_4\}\cdot 2H_2O$ as taken from ref. 1

In the same year but chronologically later than this first compound, two other groups also reported Ln-only PDC compounds. Song *et al.* were probably unaware of the Zhang article since their hydrothermal synthesis is significantly different and they make no mention of the aforementioned compound.[2] They were able to obtain a crystal with molecular formula of $Eu(PDC)(HPDC)(H_2O)_5\cdot 4H_2O$, again half of the PDC ligands are monoprotonated. The Eu^{3+} luminescence is briefly described, no spectra are given.

This, however, is a complex and not a coordination polymer, as can be seen in Figure 3-4. It does signify that researchers were very close to obtaining, by design, an Ln-PDC compound without any other metals, added organic ligands or decomposition products.

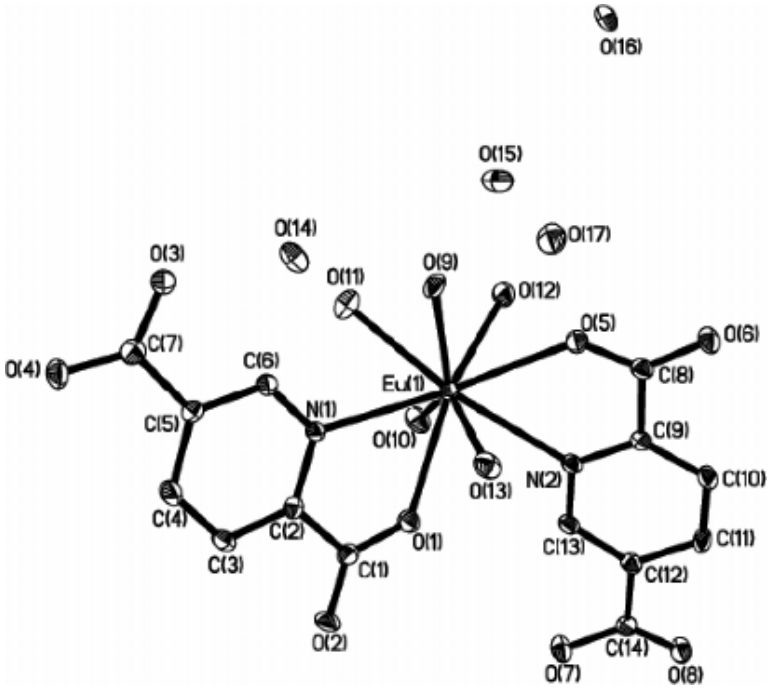

Figure 3-4: Crystal structure of the of $Eu(PDC^{2-})(HPDC^{-})(H_2O)_5 \cdot 4H_2O$ complex as taken from ref. 2

The third article appeared about half a year later[3], still in 2005; it contained the structures of $Ln(PDC^{2-})(HPDC^{-})$ where Ln = Sm, Eu and Gd. The Sm version is included in Figure 3-5. Written by Qin *et al.*, the article claims that these structures, and not the Zhang compound, are the first threedimensional Ln-PDC systems. The Eu luminescence is observed.

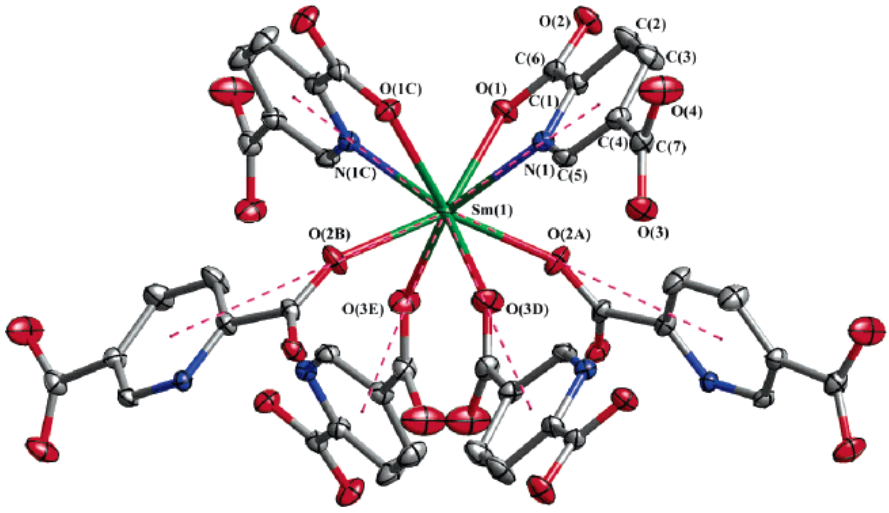

Figure 3-5: Crystal structure of Sm(PDC^{2-})(HPDC^{-}) as taken from ref. 3

In the same article, benzenecarboxylic (benzoic) acid (HBC) was mixed with the other reactants to obtain the mixed-ligand material with formula Ln(PDC)(BC)(H_2O) with Ln = Sm^{3+} and Gd^{3+}.

Several analogues have been found in the following years. Huang *et al.* hydrothermally synthesized $Pr_2(PDC)_3(H_2O)_2$ and Ln(PDC)(HPDC) with Ln = Eu^{3+}, Tb^{3+} and Er^{3+} in 2008.[4] They also observed partial decomposition of the H_2PDC molecule into nicotinic acid (H_2NIC), which was present as a building block in Gd(PDC)(NIC)(H_2O), a compound with the same architecture as Ln(PDC)(BC)(H_2O), mentioned above. Liu *et al.* found that the same decarboxylation of 2,5-H_2PDC happened when 4,4'-bipyridine was added to the reaction mixture, obtaining Ln(PDC)(NIC)(H_2O) for Ln = Nd^{3+} and Sm^{3+}.[5] The exact role of the 4,4'-bipyridine was not determined in that work.

Shi *et al.* published some variations on the theme.[6] Again, decomposition occurred during the solvothermal synthesis. Here, DMF underwent solvolysis into dimethylammonium anions, resulting in $[(CH_3)_2NH_2][Ln(PDC)_2]\cdot 0.5H_2O$ with Ln = Eu^{3+} and

Tb^{3+}. In the same publication, $[Er_4(OH)_4(PDC)_4(H_2O)_3]\cdot H_2O$ and $(Pr^{III})_2(Pr^{IV})_{1.25}O(OH)_3PDC$ frameworks were obtained by hydrothermal synthesis.

Two more species within the Ln^{3+}-PDC^{2-} theme were obtained by Huang *et al.* in 2009: $La_2(PDC)_3(H_2O)_2$ and $La(PDC)(HPDC)(H_2O)_2\cdot nH_2O$; this was done by changing the lanthanum ion source (oxide vs nitrate), lanthanum ion concentration and reaction pH.[7] The dependence on the pH was already shown two years prior by the same group.[8] They obtained $Ln_3(OH)_4(PDC)(HPDC)_3(H_2O)_4$ with Ln = Gd^{3+}, Dy^{3+}, Er^{3+}, Eu^{3+}, Sm^{3+}, Yb^{3+} and Y^{3+} (

Figure 3-6), by using the exactly the same method that was used to form Ln(PDC)(HPDC) corresponding to Figure 3-5, except they included an adjustment to the pH with HCl. This illustrates the drastic effect pH has on the formation of networks. The Eu^{3+}, Dy^{3+} and Sm^{3+} analogues showed characteristic lanthanide luminescence.

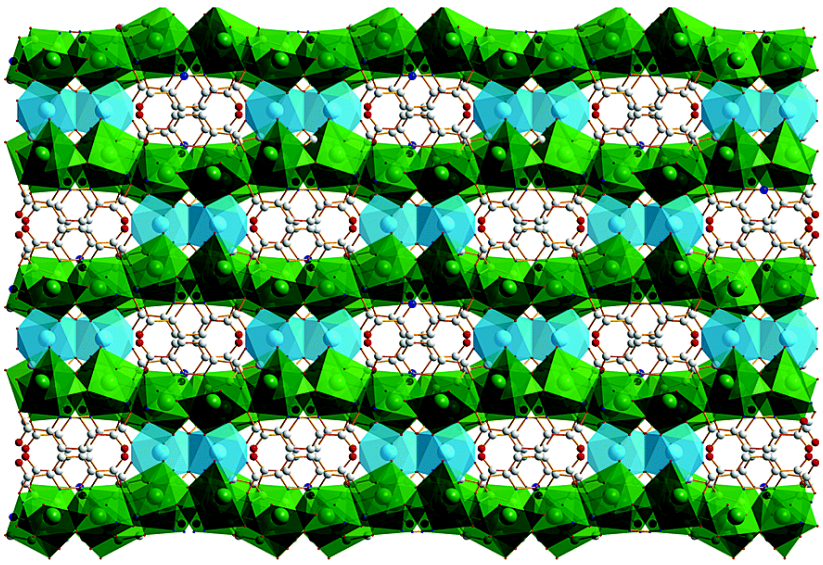

Figure 3-6: View of the $Eu_3(OH)_4(PDC)(HPDC)_3(H_2O)_4$ structure as taken from ref. 8 Blue and green polyhedra represent crystallographically unique Eu^{3+} sites

The Ce^{3+} and Pr^{3+} members of the $[Ln_2(PDC)_2(HPDC)_2(H_2O)_4]\cdot 2H_2O$ type were reported by Feng *et al.* in 2010.[9]

3.3.2 Mixing ligands

Mixing different ligands with PDC ligands is also possible. Song *et al.* did this with phenanthroline already in 2005 which is the same year the first materials were found that weren't a mix of either metals or ligands, obtaining $Dy(PDC)(HPDC)(phen)(H_2O)_2\cdot H_2O$.[10]

Soares-Santos *et al.* mixed 1,4-phenylenediacetic acid (1,4-H_2PDA) in the reaction mixture[11], resulting in $Ln_2(PDC)_2(1,4\text{-}PDA)(H_2O)_2$ where Ln = Eu^{3+}, Tb^{3+}, $(Eu_{0.2}Tb_{0.8})^{3+}$ and $(Eu_{0.1}Tb_{0.9})^{3+}$.

Huang *et al.* prepared $Nd(PDC)(OAc)(H_2O)\cdot 2H_2O$ by mixing neodymium nitrate and manganese acetate.[12] Interestingly, the Mn^{2+} ions are not taken up in the network here either. The La^{3+} variety of this was reported by Zeng *et al.* and is shown in Figure 3-7.[13]

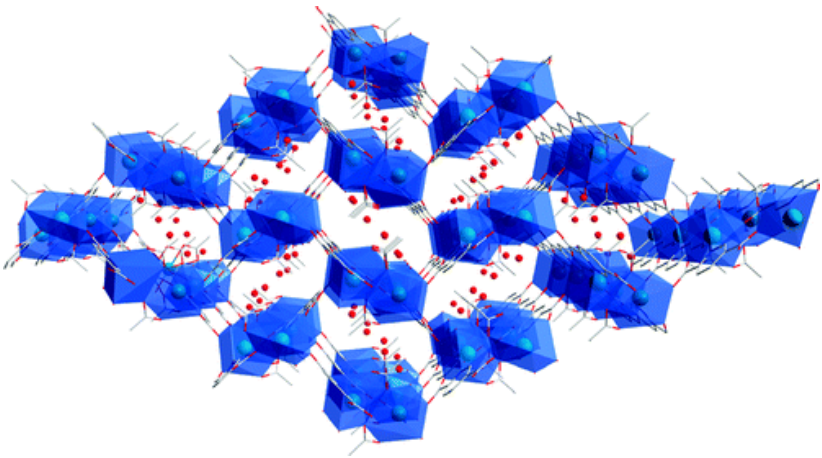

Figure 3-7: The $La(PDC)(OAc)(H_2O)\cdot 2H_2O$ network as taken from ref. 13

In 2009, Zhang *et al.* synthesized the first coordination polymer with a mix of PDC^{2-} and NIC^{2-} ligands by design, not by in situ degradation[14]. It has the same composition as the one mentioned above. Wang et al. used adipic acid (H_2ADP) in combination with PDC to obtain $Ln(PDC)(ADP)_{0.5}(H_2O)$ with Ln = Pr^{3+}, Nd^{3+}, Sm^{3+}, Eu^{3+} and Tb^{3+}, of which the Eu^{3+} version is shown in Figure 3-8.[15]

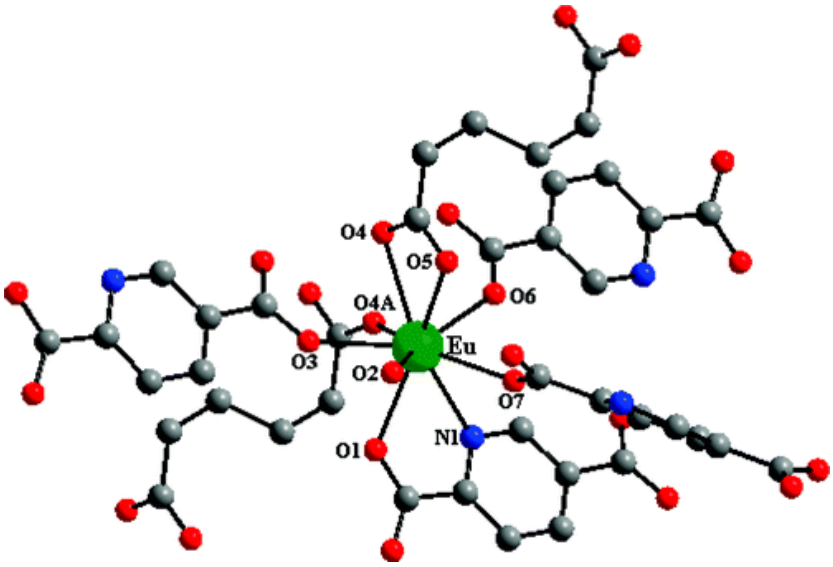

Figure 3-8: Coordination environment of Eu in $Eu(PDC)(ADP)_{0.5}(H_2O)$ as taken from ref. 15

In the same year, another mixed-ligand compound was made by Luo *et al.*, this time with the formic acid anion.

3.3.3 State of the art

Silva *et al.* were able to synthesize through microwave synthesis (MWAS) yet another novel member of the Ln-PDC family.[16] Shown in Figure 3-9 is $[Ce_2(PDC)_2(HPDC)(H_2O)_2)]Cl\cdot(9+y)H_2O$ (the y stands for water molecules that were unable to be refined into the crystal structure) was obtained in under 20 minutes,

alongside another phase identified as $Ce_2(PDC)_3(H_2O)_2$, an analogue of the Huang compound, upon which catalysis studies were performed. What is remarkable from a structural point of view is that slightly varying the reaction conditions produces three different phases. The La^{3+} homologue of the $Ce_2(PDC)_3(H_2O)_2$ side product was subsequently doped with Eu^{3+} and Tb^{3+} ions to study the luminescent properties of $Ln_2(PDC)_3(H_2O)_2$, where Ln = $(La_{0.95}Eu_{0.05})^{3+}$, $(La_{0.95}Tb_{0.05})^{3+}$ and $(La_{0.90}Eu_{0.05}Tb_{0.05})^{3+}$. This paves the way for fast and efficient synthesis of optically interesting compounds.

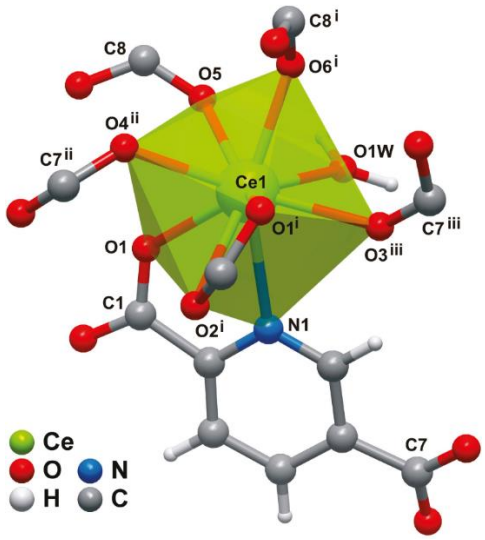

Figure 3-9: Coordination environment of the Ce^{3+} in the $[Ce_2(PDC)_2(HPDC)(H_2O)_2)]Cl\cdot(9+y)H_2O$ structure as taken from ref. 16.

3.4 This work

3.4.1 The crystal structures

3.4.1.1 Nd-PDC

We have been able to obtain single crystals of two unprecedented coordination polymers containing PDC and a lanthanide ion, namely Nd^{3+} and Lu^{3+}. The synthesis

method involves mixing appropriate quantities of lanthanide nitrate salt with H_2PDC in water and heating the mixture in a closed pyrex test tube to 160°C for three days. Afterwards, the mixture is cooled at the rate of 10°C/hour, upon which crystals precipitate.

The compound we have named Nd-PDC is, in fact, homologous to the reported structures by Zhang, Huang and Qin *et al.* and has the formula Nd(PDC)(HPDC). There is only one crystallographically unique Nd^{3+} centre in the asymmetric unit, positioned on a two-fold axis. The central ion is octacoordinated by a total of six ligands: twice by one pyridine nitrogen atom and one 2-carboxylate oxygen atom from two ligands each, twice by only a 2-carboxylate oxygen atom, and twice by a 5-carboxylate oxygen atom.

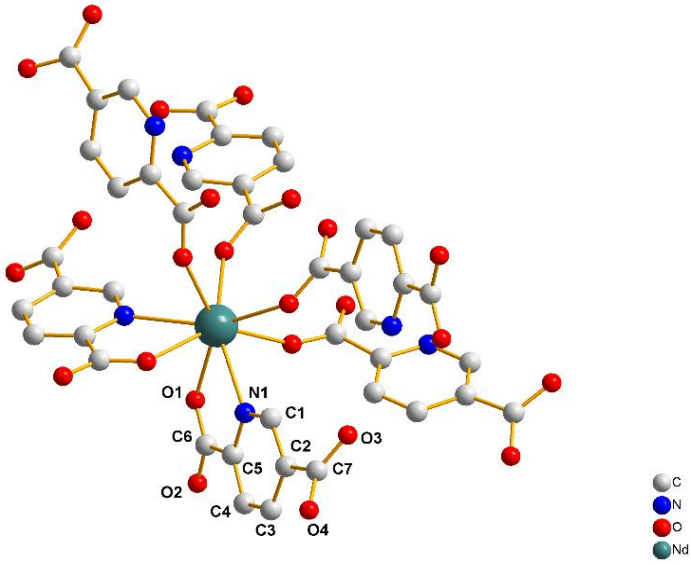

Figure 3-10: Coordination of the Nd ion in the Nd-PDC compound

There is actually only one crystallographically unique PDC^{2-} ligand. It coordinates to three Nd^{3+} ions, once in bidentate fashion with the nitrogen and one 2-carboxylate

oxygen, once monodentate with the other 2-carboxylate oxygen, and finally only one of the 5-carboxylate oxygen atoms is coordinated to a Nd^{3+} ion. There are, indeed, only three different Nd-O bond distances in the entire network. The remaining 5-carboxylate oxygen actually forms a hydrogen bond with its symmetry equivalent. This can be elucidated in two ways: stoichiometrically, every other PDC ligand needs to be only partially deprotonated instead of fully, to account for charge neutrality. It was also possible to determine the position of this hydrogen by modelling one on the relevant oxygen atoms. Its exact location could be retrieved from a difference Fourier electron density map; an additional peak was observed on the symmetry axis between the two oxygen atoms. This hydrogen bond adds an additional stabilizing factor to the coordination network.

The resulting network can be seen as being built in two steps. First, there is the formation of chains of octacoordinated Nd centres. These chains are linked by bridging PDC^{2-} ligands to form a threedimensional network.

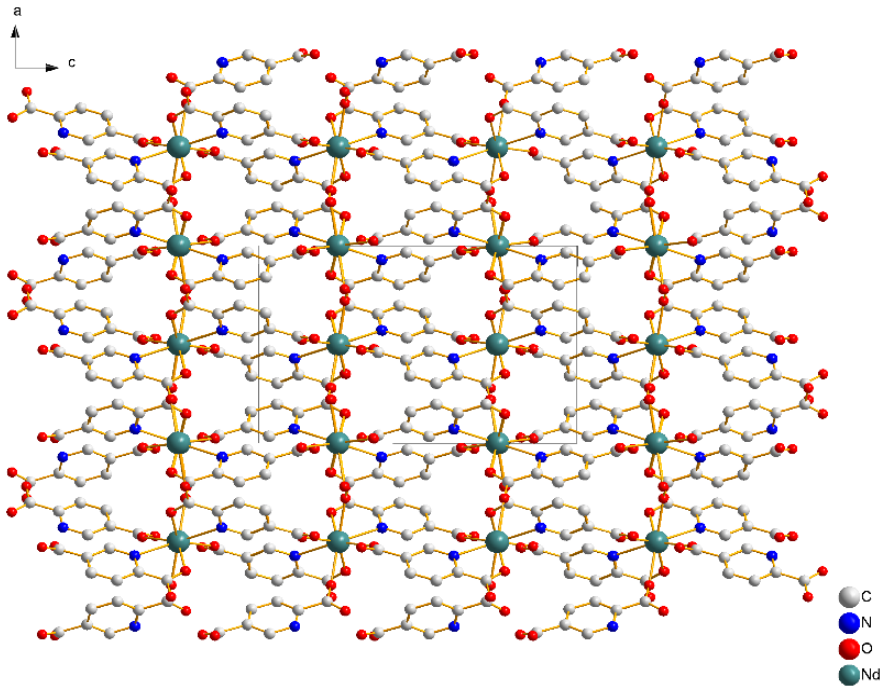

Figure 3-11: Packing of the Nd PDC compound

As can be seen, there are hardly any voids in the structure that are filled with solvent molecules. The result is a very dense, compact superstructure, with very low porosity. This is easily proven by TGA analysis, which reveals that there is no significant weight loss before complete degradation of the structure at 450°C. This means that there were no guest water molecules present, even though the synthesis was performed in water.

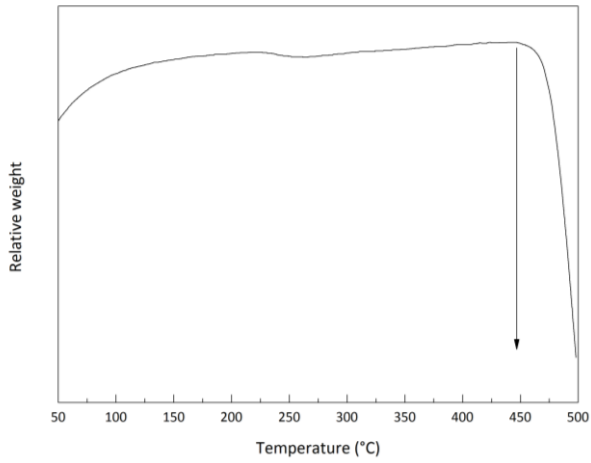

Figure 3-12: Thermogravimetric analysis of Nd(PDC)(HPDC)

Infrared analysis is somewhat less useful for these particular compounds. The identity of the organic PDC molecule does not change, so we can expect to see all aromatic ring and C-H vibrations, the 1,4 overtones and the carbonyl C-O relatively unchanged. The O-H stretch is still present since half of the PDC ligands is not fully deprotonated, however one must also not forget that there are now important hydrogen bonds contributing to this resonance signal.

3.4.1.1.1 Steady-state photoluminescence

Here, too, we were able to observe the characteristic Nd emission in the infrared region of the spectrum.

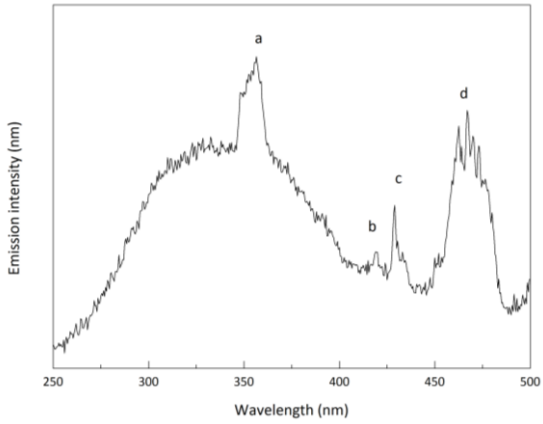

Figure 3-13: Excitation spectrum of Nd(PDC)(HPDC) monitoring the emission at 1061 nm

label	λ (nm)	ῡ (cm^{-1})	transition
a	356.5	27360	$^4D_{3/2}$, $^4D_{5/2}$, $^2I_{11/2}$, $^4D_{1/2} \leftarrow {}^4I_{9/2}$
b	419.5	23838	$^2D_{5/2} \leftarrow {}^4I_{9/2}$
c	429	23310	$^2P_{1/2} \leftarrow {}^4I_{9/2}$
d	467	21413	$^4G_{11/2}$, $^2D_{3/2}$, $^2P_{3/2}$, $^2G_{9/2}$, $^2K_{15/2} \leftarrow {}^4I_{9/2}$

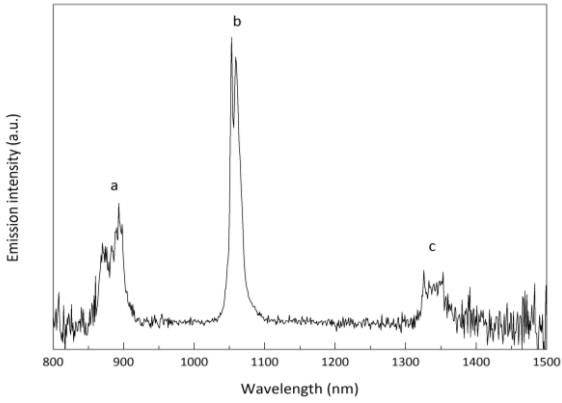

Figure 3-14: Emission spectrum of Nd(PDC)(HPDC)upon excitation at 300 nm

Table 3-1: Assignment of the peaks in Figure 3-14

label	λ (nm)	ῡ (cm^{-1})	transition
a	885	11300	$^4F_{3/2} \rightarrow {}^4I_{9/2}$
b	1055	9478	$^4F_{3/2} \rightarrow {}^4I_{11/2}$
c	1330	7519	$^4F_{3/2} \rightarrow {}^4I_{13/2}$

A comparison can be made between the Nd-BDC compound from the previous chapter and this one. The emission spectra are identical, save for a higher level of noise. In the excitation scan, we see one transition disappearing for the PDC compound, but a broader band at longer wavelengths and lower energies. If we attribute this transition to the excitation of the first excited singlet state S_1 from the ligand ground state S_0, it may indicate that the PDC^{2-} S_1 level is lower in energy than the BDC^{2-} S_1 level. Therefore the triplet level T_1 may also be possibly lower in energy, although this cannot be said for certain. We were unable to retrieve or determine values for this PDC triplet energy level, but since the structural difference between PDC^{2-} and BDC^{2-} is not that great, we can assume their triplet levels are very similar. The luminescent lifetime was found to be 0.32 μs, in good agreement with other compounds as previously described.

Table 3-2: Crystallographic data for Nd(PDC)(HPDC$^-$)

molecular formula	$C_{14}H_7N_2NdO_8$
fw (g mol^{-1})	475.46
cryst dimensions (mm^3)	0.4 x 0.1 x 0.1
cryst syst	orthorhombic
space group	Pbcn (No. 60)
a (Å)	9.9735(7)
b (Å)	8.7698(6)
c (Å)	15.787(1)
α (deg)	90
β (deg)	90
γ (deg)	90
V (Å^3)	1380.9(2)
Z	4
ρ_{calcd} (g cm^{-3})	2.287
$2\theta_{max}$ (deg)	135.4
T (K)	293(2)
F(000)	916
measured reflns	8600
unique reflns	1229
obsd reflns (I > 2σ(I))	1056
params refined	51
R1	0.0465
wR2	0.123
R1 (all data)	0.0526
wR2 (all data)	0.1321
GOF	1.097
μ (mm^{-1})	29.211

3.4.1.2 Lu-PDC

Another PDC-based coordination polymer was obtained after hydrothermal experiments. This time, the metal ion used was lutetium(III). This metal is one of the less frequently used lanthanides, mainly because its cost and difficulty to separate from the other lanthanides from the ores.

Based upon single crystal X-ray analysis and elemental analysis, the compound has the formula $Lu(PDC)(HPDC)(H_2O)_2 \cdot 4H_2O$. The central Lu^{3+} ion is octacoordinated by two nitrogen atoms and six oxygen atoms. The nitrogen atoms are obviously from one PDC^{2-} ligand each. Two oxygen atoms come from the corresponding PDC^{2-} ligand to coordinate in a bidentate fashion. Two more coordinating oxygen donor atoms are from two other carboxylate groups. The remaining two oxygen atoms come from water ligands. The first coordination sphere geometry can be observed as a distorted square antiprismatic polyhedron.

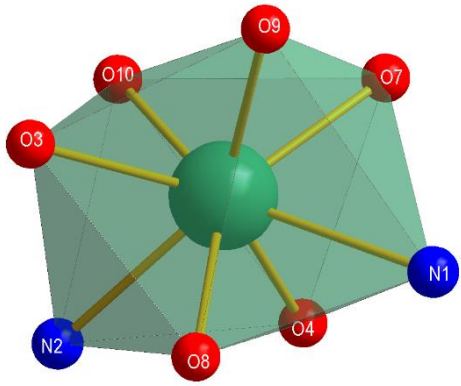

Figure 3-15: Coordination polyhedron of Lu in the Lu PDC compound

There are two independent PDC^{2-} ligands in the asymmetric unit. Both bidentately coordinate the central ion with the pyridyl nitrogen and one oxygen from the 2-carboxylate group. The other oxygen from the same carboxylate group bridges to

another lanthanide. This bridging functionality causes the formation of chains. To maintain a neutral network, half of the PDC^{2-} ligands need to be monoprotonated.

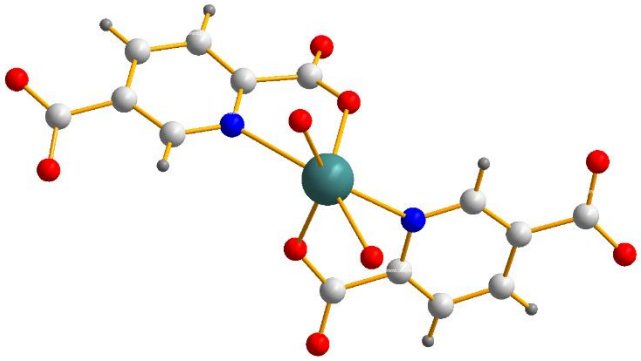

Figure 3-16: Coordination of the Lu^{3+} ion

These chains are linked together into a 2D-structure by hydrogen bonds from lattice water molecules with neutral or anionic carboxylates; these bonds are ordered in between the chains formed by Lu^{3+} ions.

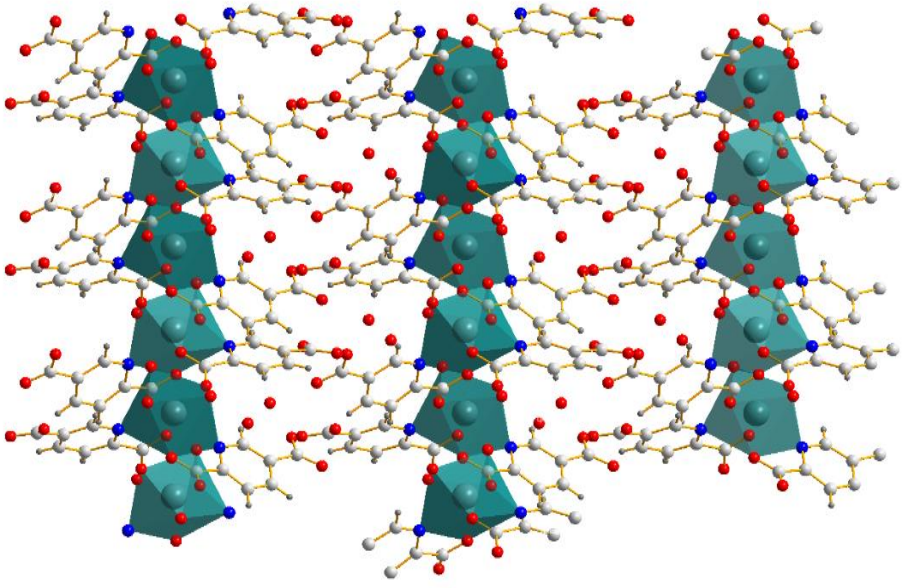

Figure 3-17: Packing of the Lu PDC compound

The presence of hydrogen-bonded lattice water is again confirmed by IR analysis, where broad O-H stretch vibration bands are visible at 3000 cm^{-1} and upwards.

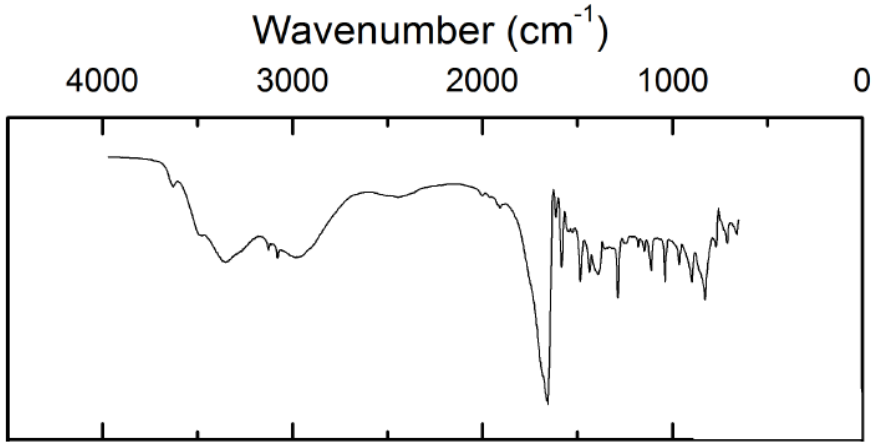

Figure 3-18: Diffuse Reflectance IR spectrum of Lu-PDC

Predicting structural properties for these compounds is very hard, as there are several factors that come into play when looking at the reagents and synthesis: Lutetium(III) has a smaller ionic radius than neodymium(III); the hydrothermal regime is beyond "classical" wet chemistry, the autoclave container was larger for the Nd^{3+} compound and so were the quantities. Again, the role of the ion itself must not be underestimated since there is more symmetry in this Lu-PDC network than in the Nd-PDC network.

Table 3-3: Crystallographic data for Lu(PDC)(HPDC)(H_2O)$_2$·4H_2O

molecular formula	$C_{14}H_6LuN_2O_{12}$
fw (g mol^{-1})	569.18
cryst dimensions (mm^3)	0.2255 x 0.0672 x 0.0425
cryst syst	monoclinic
space group	$P2_1$ (No. 4)
a (Å)	9.3606(3)
b (Å)	7.21044(16)
c (Å)	12.9030(3)
α (deg)	90
β (deg)	101.348(3)
γ (deg)	90
V (Å^3)	853.85(4)
Z	2
ρ_{calcd} (g cm^{-3})	2.214
$2\theta_{max}$ (deg)	52.74
T (K)	100(2)
F(000)	542
measured reflns	9685
unique reflns	3425
obsd reflns (I > 2σ(I))	2469
params refined	262
R1	0.0386
wR2	0.0647
R1 (all data)	0.0685
wR2 (all data)	0.0728
GOF	1.034
μ (mm^{-1})	5.854
CCDC entry	CCDC-999885

3.5 Conclusion and outlook

We have successfully synthesized two new compounds with formula Nd(PDC)(HPDC) and $Lu_2(BDC)_3(DMF)_3(H_2O)_2$. Their structures have been elucidated and the NIR luminescence of the Nd compound measured. Again, the Lu network could be interesting if it was able to dope other lanthanide ions in. From a structural viewpoint, it is remarkable to see that the Lu network has a more ordered structure than the Nd one. Unfortunately, due to the differences in structure that arise from slight variations it is very hard to see trends in structural properties dependent on the lanthanide ion size.

3.6 References

[1] Synthesis, structural characterization and magnetic property of metal 2,5-pyridine dicarboxylate complex, X. Zhang, D. Huang, C. Chen, Q. Liu, D. Liao, L. Li, Inorg. Chem. Comm., **2005**, Vol. 8, Issue 1, p. 22

[2] Hydrothermal synthesis and crystal structure of a novel luminescent europium complex of 2,5-pyridinedicarboxylic acid, Y. Song, B. Yan, Z. Chen, J. Coord. Chem., **2005,** Vol. 58, Issue 9, p. 811

[3] A Series of Three-Dimensional Lanthanide Coordination Polymers with Rutile and Unprecedented Rutile-Related Topologies, C. Qin, X.-L. Wang, E.-B. Wang, Z.-M. Su, Inorg. Chem., **2005**, Vol. 44, Issue 20, p. 7122

[4] Syntheses, structures, and photoluminescence of three-dimensional lanthanide coordination polymers with 2,5-pyridinedicarboxylic acid, Y. Huang, Y.-S. Song, B. Yan, M. Shao, J. Solid State Chem., **2008,** Vol. 181, Issue 8, p. 1731

[5] In situ hydrothermal decarboxylation for unprecedented three-dimensional lanthanide–organic frameworks, C.-M. Liu, D.-Q. Zhang, D.-B. Zhu, Inorg. Chem. Comm., **2008**, Vol. 11, p. 903

[6] Three-Dimensional Lanthanide−Organic Frameworks Based on Di-, Tetra-, and Hexameric Clusters, F.-N. Shi, L. Cunha-Silva, T. Trindade, F. A. Almeida Paz, J. Rocha, Cryst. Growth Des., **2009**, Vol. 9, issue 5, p. 2098

[7] Intricate 3D lanthanide–organic frameworks with mixed nodes nets, Y.-G. Huang, F.-L. Jiang, D.-Q. Yuan, M.-Y. Wu, Q. Gao, W. Wei, M.-C. Hong, J. Solid State Chem., **2009**, Vol. 182, Issue 2, p. 215

[8] New lanthanide hybrid as clustered infinite nanotunnel with 3D Ln-O-Ln framework and (3,4)-connected net, Y.-G. Huang, B.-L. Wu, D.-Q. Yuan, Y.-Q. Xu, F.-L. Jiang, M.-C. Chung, Inorg. Chem., **2007**, Vol. 46, Issue 4, p. 1171

[9] Synthesis, Structural Characterization and Luminescence of Lanthanide Coordination Polymers with Pyridine-2,5-dicarboxylic Acid, X. Feng, Q. Wei, S. Chen, S. Gao, Chin. J. Chem., **2010**, Vol. 28, p. 11

[10] Two novel lanthanide 1-D chain coordination polymers of pyridinedicarboxylic acids: hydrothermal synthesis, structure and luminescent properties, Y.-S. Song, B. Yan, Z.-X. Chen, J. Molec. Struct., **2005**, Vol. 750, Issue 1-3, p. 101

[11] Photoluminescent 3D Lanthanide−Organic Frameworks with 2,5-Pyridinedicarboxylic and 1,4-Phenylenediacetic Acids, P.C.R. Soares-Santos, L. Cunha-Silva, F. E. Almeida Paz,

R.A. Sá Ferreira, J. Rocha, T. Trindade, L.D. Carlos, H.I.S. Nogueira, Cryst. Growth Des., **2008**, Vol. 8, Issue 7, p. 2505

[12] A Prototypical Zeolitic Lanthanide–Organic Framework with Nanotubular Structure, Y.-G. Huang, F.-L. Jiang, D.-Q. Yuan, M.-Y. Wu, Q. Gao, W. Wei and M.-C. Hong, *Cryst. Growth Des.*, **2008**, Vol. 8, Issue 1, p. 166

[13] Synthesis, Structure and Properties Study of Two Lanthanide (Ⅲ) Coordination Polymers Constructed from 2,5-Pyridinedicarboxylic Acid, X.-Z. Zeng, A.-Y. Zhang, Y.-W. Li, Chin. J. Inorg. Chem., **2013**, Vol. 29, p.

[14] Hydrothermal synthesis, structure and rare ferromagnetic property of a 3-D Nd(III) metal–organic framework based on mixed pyridine-2,5-dicarboxylic acid/nicotinic acid ligands, D.-J. Zhang, T.-Y. Song, L. Wang, J. Shi, J.-N. Xu, Y. Wang, K.-R. Ma, W.-R. Yin, L.-R. Zhang, Y. Fan, Inorg. Chim. Acta, **2009**, Vol. 362, Issue 1, p. 299

[15] A Series of Three-Dimensional Lanthanide-Rigid-Flexible Frameworks: Synthesis, Structure, and Luminescent Properties of Coordination Polymers with 2,5-Pyridine Dicarboxylic Acid and Adipic Acid, C.-G. Wang, Y.-H. Xing, Z.-P. Li, J. Li, X.-Q. Zeng, M.-F. Ge, S.-Y. Niu, Cryst. Growth. Des., **2009**, Vol. 9, p. 1525

[16] Fast Microwave Synthesis of a Microporous Lanthanide–Organic Framework, P. Silva, A.A. Valente, J. Rocha, F.A. Almeida Paz, Cryst. Growth. Des., **2010**, vol. 10, p. 2025

4 Coordination polymers based on 2,6-naphthalenedicarboxylic acid and 1,2-cyclohexanedicarboxylic acid

4.1 Outline and goals

In this part of the work, a partnering lab synthesized two series of compounds; we determined the luminescence properties of those compounds. The structure of the linkers and of the networks are examined at first. Afterwards the measurements of the luminescence are discussed. The challenge here is to make rationalizations on the relation between these luminescence properties and the structure.

4.2 Introduction

In a collaboration with the UCCS group (Unité de Catalyse et Chimie du Solide) from Lille (France), led by prof. Thierry Loiseau, two series of new coordination polymers were obtained. These contained lanthanides and one of two dicarboxylic acids. We have measured the luminescence properties of these materials.

The organic spacers that were used here were either 2,6-napthalenedicarboxylic acid (H_2NDC, NDC^{2-} for the twice deprotonated form, NDC in formulas) or 1,2-cyclohexanedicarboxylic acid (H_2CDC, CDC^{2-} for the dianion, CDC in formulas). We can already make a few assumptions for the luminescent behaviour based on the structures of the organic molecules.

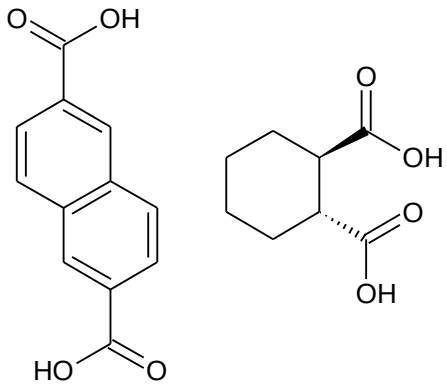

Figure 4-1: 2,6-Naphthalenedicarboxylic acid, H_2NDC (left) and trans-1,2-Cyclohexanedicarboxylic acid, H_2CDC (right)

2,6-napthalenedicarboxylic acid is quasi-linear with regard to the implementation of its carboxylic acid groups, giving it almost the same shape as terephthalate. One would suspect that the increase in size might lead to larger cavities inside the frameworks and larger unit cells. Furthermore, H_2NDC has a more extended aromatic structure than H_2BDC, which would mean that its peak of absorption is shifted towards lower energies, with the possible consequence of a lower triplet energy level.

1,2-cyclohexanedicarboxylic acid is an entirely different molecule. The implanting of the carboxylic acid groups is different, which should give rise to very different structural patterns. The aromatic π–π-stacking will not be available as a secondary structural determining factor. The loss of aromaticity has an effect on the absorptive properties. Since there is no conjugated system apart from the eventually deprotonated carboxylic acid groups, the absorption may lie at high energies, and even then have a low absorption coefficient. Thus, no appreciable antenna effect can be expected when using the standard wavelength range for excitation spectra.

4.3 Reported relevant research

4.3.1 NDC series

Lanthanide ions have been combined with 2,6 naphthalenedicarboxylic acid before. This section serves as a very brief overview.

In 2002, Wang et al. reported the structure of three compounds obtained at room temperature[1]. They have the formula $Ln_2(NDC)_3(DMF)_4 \cdot nH_2O$ with Ln = Eu^{3+}, Tb^{3+} and Ce^{3+} and n = 3, 4 and 2, respectively. Figure 4-2 shows the Eu^{3+} network. For the Eu^{3+} and Tb^{3+} analogue, steady state photoluminescence was recorded for the as-synthesized samples. However, they were found to deteriorate upon desolvation, rendering their use as sensors impossible.

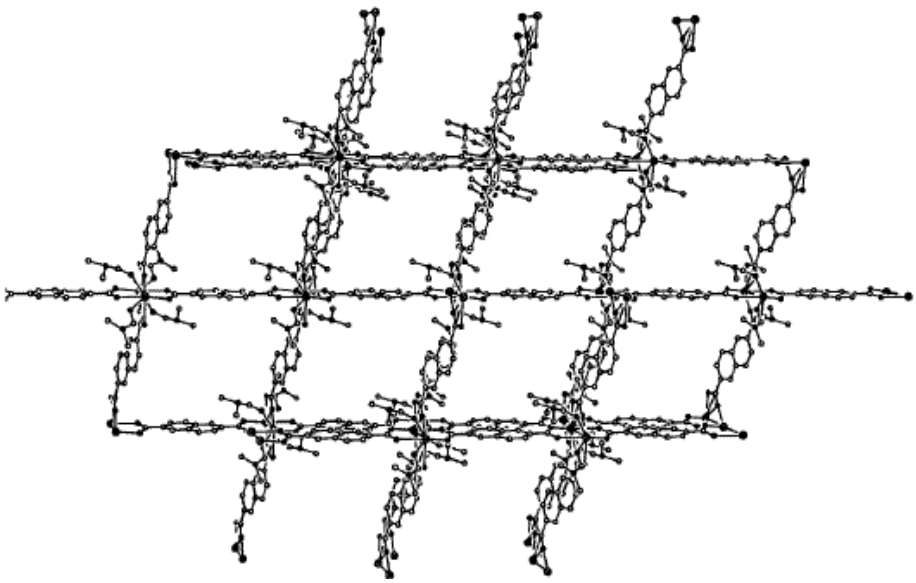

Figure 4-2: View of the $Eu_2(NDC)_3(DMF)_4 \cdot 3H_2O$ network as taken from ref. 1

In the same year, Min et al. reported a Tb^{3+}-containing coordination polymer obtained by hydrothermal synthesis.[2] This compound is noted as $[Tb_4(NDC)_6(H_2O)_5]\cdot 2H_2O$ and its structure is given in Figure 4-3. No luminescence is recorded.

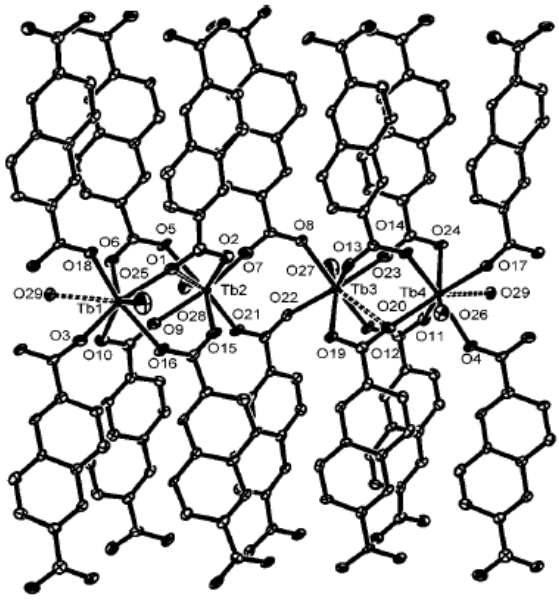

Figure 4-3: View of the $[Tb_4(NDC^{2-})_6(H_2O)_5]\cdot 2H_2O$ as taken from ref. 2

An Yb^{3+}-containing NDC^{2-} network was reported in 2003 by Almeida-Paz *et al.*[3] The structure with formula $Yb_2(NDC)_3(H_2O)\cdot(H_2O)_2$ was obtained by hydrothermal reaction and is given in Figure 4-4.

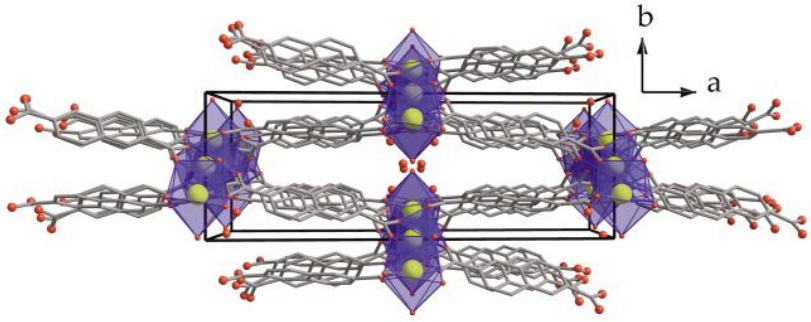

Figure 4-4: View of the $Yb_2(NDC)_3(H_2O)\cdot(H_2O)_2$ network as taken from ref. 3

In the same year, Daiguebonne *et al.* synthesized, by diffusion in gel media, the structure of $Er_2(NDC)_3(H_2O)_6$, given in Figure 4-5.[4]

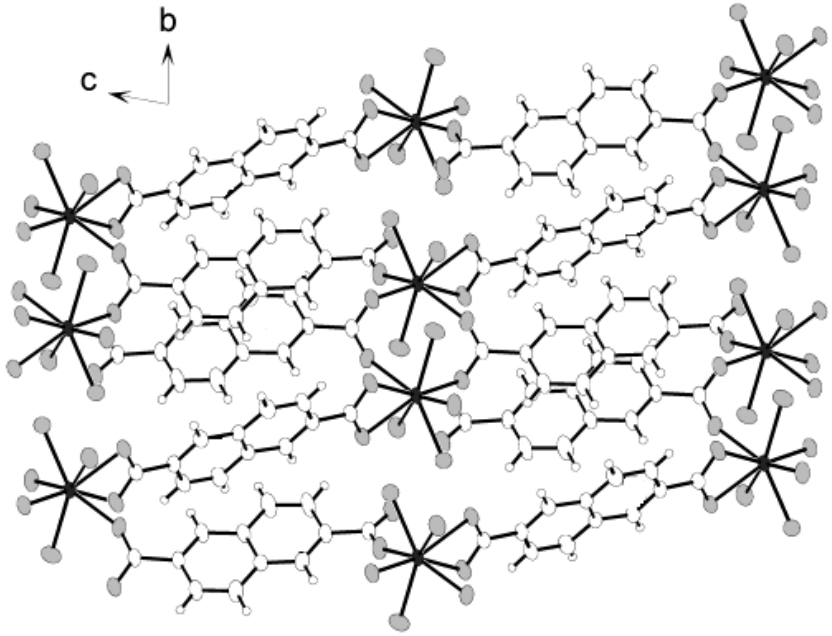

Figure 4-5: View of the $Er_2(NDC)_3(H_2O)_6$ network, adapted from ref.4

One year later, the Ln-NDC system was combined with the ancillary 1,10-phenanthroline ligand in a publication from Zheng *et al*. in order to create a ternary system.[5] In this work, the structures of $Ln_2(NDC)_3(phen)_2 \cdot H_2NDC$ with Ln = Tb^{3+}, Ho^{3+} and Yb^{3+} are reported, but not their luminescent properties.

Łyszczek *et al.* were able to use microwave synthesis to obtain $Ln_2(NDC)_3 \cdot nDMF$, with Ln = La^{3+} to Lu^{3+} except Pm and n ranges from 1.5 to 3.[6] For the Nd^{3+}, Eu^{3+}, Tb^{3+} and Er^{3+} analogues, the steady-state luminescence was recorded, as well as their luminescence lifetime.

Finally, in 2014, two articles appeared on this system. The first details the solvothermal synthesis of two Pr^{3+}-NDC^{2-} networks with formula $Pr_2(NDC)_2(NO_3)_2(DMA)_4$ (obtained in a DMA/CH_3CN medium) and $Pr_3(NDC)_{4.5}(DMF)_3(H_2O)$ (obtained in DMF) where DMA = dimethylacetamide.[7] Both structures show permanent porosity and are shown in Figure 4-6.

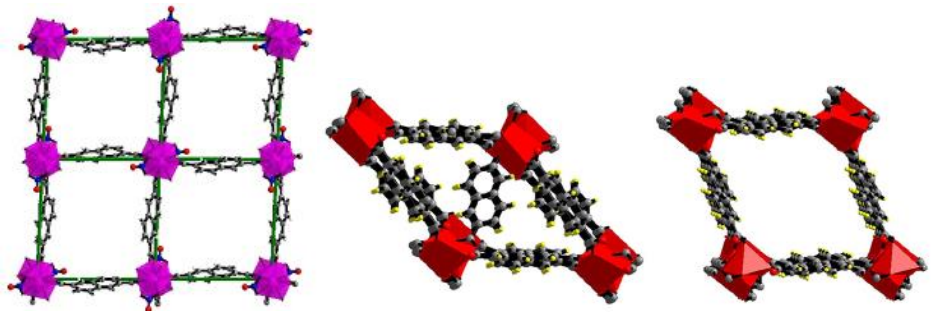

Figure 4-6: View of the $Pr_2(NDC)_2(NO_3)_2(DMA)_4$ (left) and $Pr_3(NDC)_{4.5}(DMF)_3(H_2O)$ (centre and right) networks as taken from ref. 7

The second article features five new structures with formula $[Ln(NDC)(NO_3)]\cdot(DMA)_2$ with Ln = La^{3+}, Pr^{3+}, Sm^{3+}, Eu^{3+} and Gd^{3+}.[8] The characteristic Eu^{3+} luminescence was recorded. The structures are isomorphous with the previously described $Pr_2(NDC)_2(NO3)_2(DMA)_4$ networks. This is not mentioned, probably because the articles appeared so close besides each other.

4.3.2 CDC series

The combination of lanthanide ions with 1,2-cyclohexandicarboxylic acid is much more rare. Only transition metal coordination polymers containing this ligand have been successfully characterized.[9,10,11,12.]

4.4 Structural properties

4.4.1 NDC series

These compounds were solvothermally synthesized by combination of H_2NDC and the hydrated lanthanide chloride salt in DMF, heating to 200°C under autogenous pressure for 24 hours and subsequent washing with water. The general formula of these series is LnCl(NDC)(DMF) where Ln = Ce^{3+}, Nd^{3+}, Tb^{3+} or Eu^{3+}. Each lanthanide ion is nonacoordinated by six carbonyl oxygen atom, two chloro ligands and one oxygen from DMF and adopts a tricapped trigonal prismatic shape.

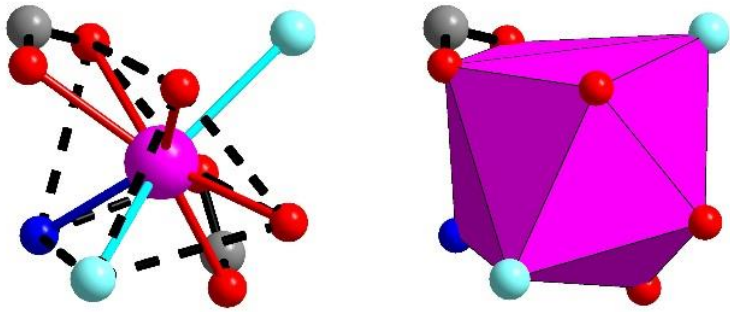

Figure 4-7: Representation of the first coordination sphere in ball & stick and polyhedral view of the Ln cation in the LnCl(NDC)(DMF) series

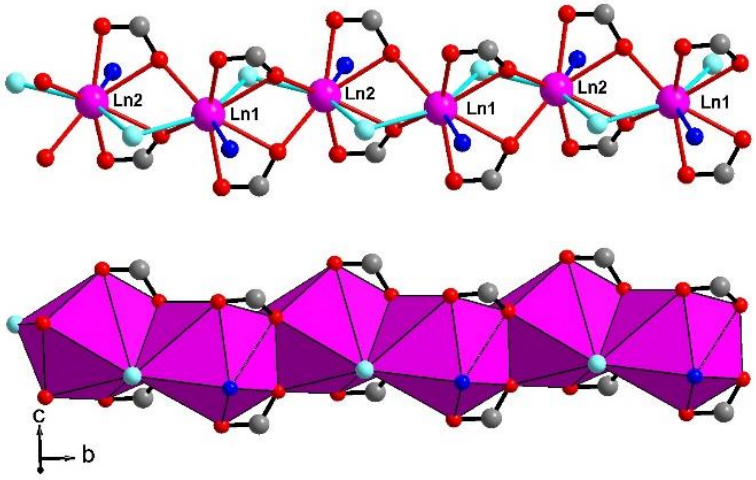

Figure 4-8: Representation of the connection modes through chlorine and chelating carboxylate groups creating infinite chains of lanthanide ions

The carbonyl oxygen atoms are bidentate and chelating in order to link two polyhedrons. The chloride ions also bridge the polyhedra, giving rise to a face-sharing mode of connection.

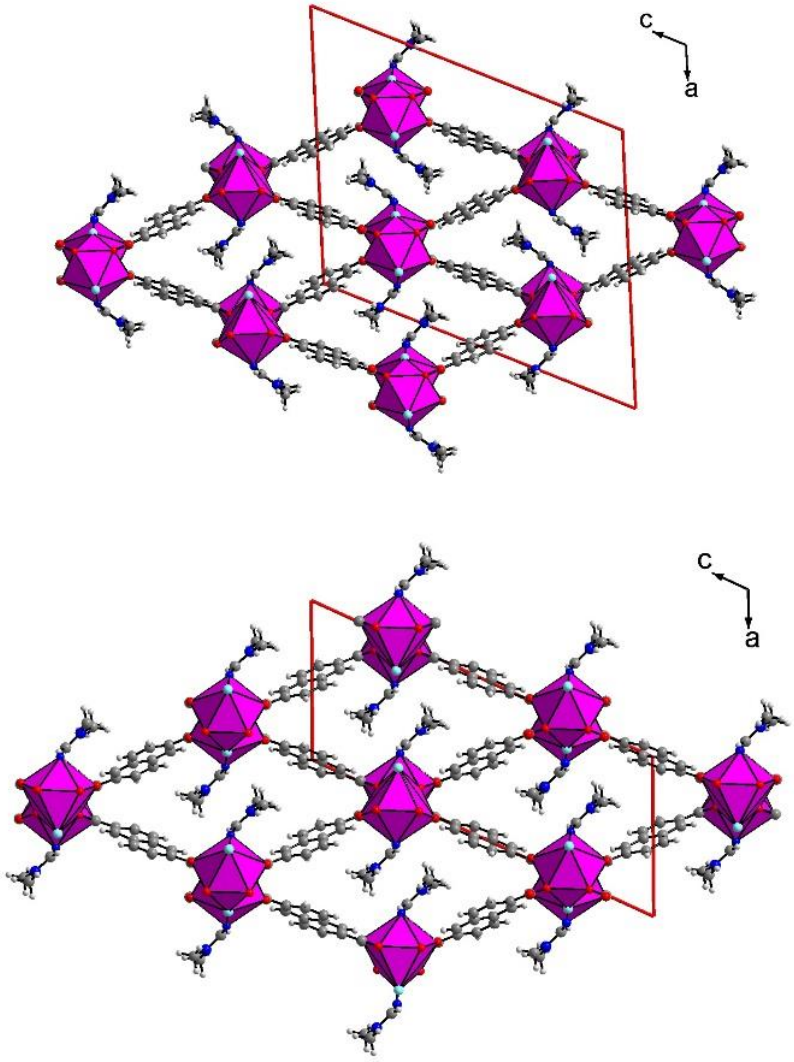

Figure 4-9: View of the LnCl(NDC)(DMF) structures where Ln = Nd^{3+} or Ce^{3+} (top) and Ln = Eu^{3+} or Tb^{3+} (bottom) and their respective unit cells

While the crystal structures within the series are closely similar to each other, there are some subtle differences. For example, the cell volumes of the Nd^{3+} and Ce^{3+} analogues are about double the value of the others; as seen in Figure 4-9.

This is because of the orientation of the DMF molecules in the channels. Interestingly, the oxychloride lanthanide chains created by linking coordination spheres and the network topology created by the connecting ditopic NDC ligands remains the same. The backbone of the DMF ligands for the lighter lanthanides are tilted away from the tricapped trigonal prism. For the lighter lanthanides (Ce^{3+}, Nd^{3+}), the tilting angles result in a geometry reminiscent of a *cis* conformation (Figure 4-9, top), whereas the rest of the series exhibits a *trans* conformation (Figure 4-9, bottom). This difference is the cause for the double cell volume and the second crystallographic independent lanthanide ion site.

For the Tb^{3+} and Dy^{3+} analogues, the structure is similar to $La_2(NDC)_3(DMF)_2$, which was submitted to the CCDC in a private communication by Long *et al*.

4.4.2 CDC series

These compounds were solvothermally synthesized by combination of the hydrated lanthanide chloride salt, H_2CDC and formic acid in DMF, heating to 200°C under autogenous pressure for 24 hours and subsequent washing with water. This series has eight identical structures with formula Ln(CDC)(form)(H_2O), where $form^-$ is the formate anion and Ln = Ce^{3+}, Pr^{3+}, Nd^{3+}, Sm^{3+}, Eu^{3+}, Gd^{3+}, Tb^{3+} and Dy^{3+}. There is only one unique crystallographic site, it is nonacoordinated by oxygen atoms only, and has a tricapped trigonal prism as its coordination polyhedron.

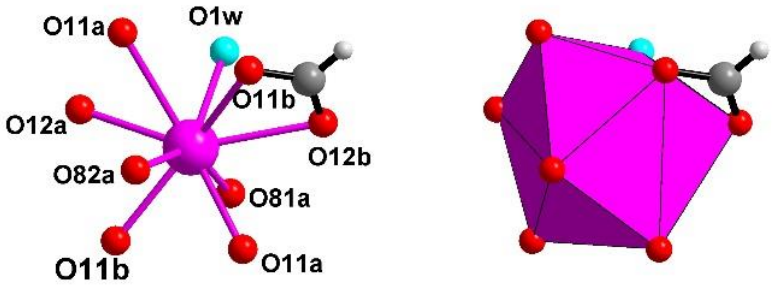

Figure 4-10: Representation of the first coordination sphere in ball & stick and polyhedral view of the Ln cation in the Ln(CDC^{2-})(form)(H_2O) series

Three oxygen atoms come from formate carboxylate groups, five from the CDC^{2-} molecules and the ninth oxygen is from a coordinated water molecule. The formate is both chelating and bidentate. One of the CDC^{2-} carboxylates adopts a symmetric chelating mode with one lanthanide centre, the other carboxylate bidentately bridges two centres.

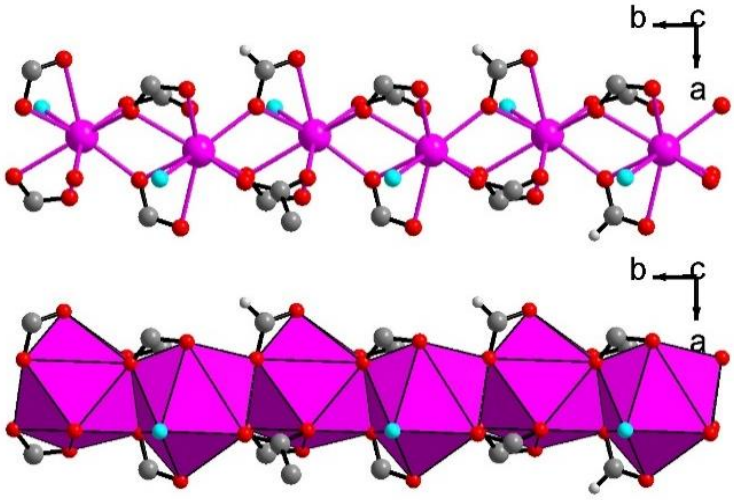

Figure 4-11: Representation of the connection modes through chelating carboxylate groups creating infinite chains

The bridging and chelating modes lead to one-dimensional chains of face-sharing coordination polyhedral (Figure 4-11), which are linked through the CDC^{2-} dianion in sheets (Figure 4-12, top).

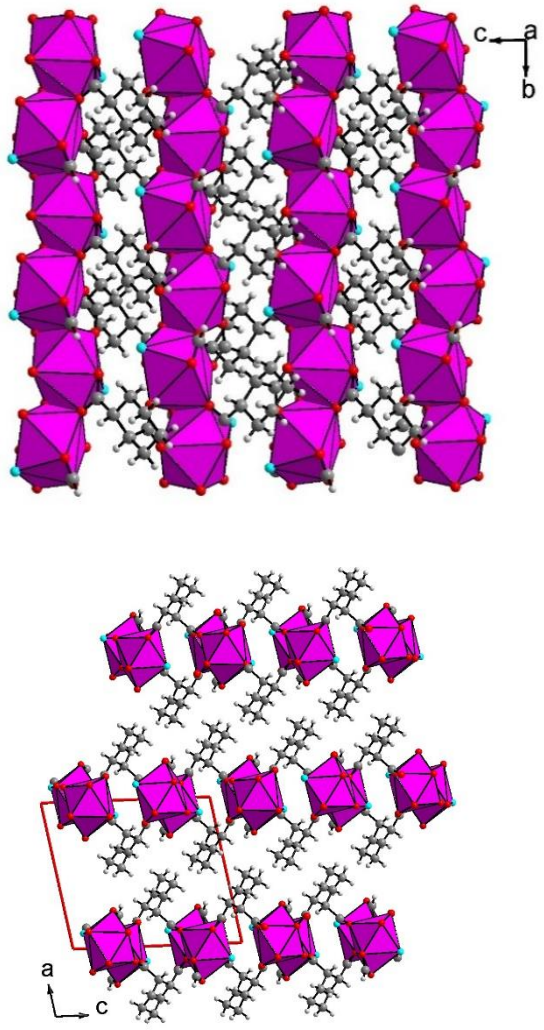

Figure 4-12: View of the Ln(CDC)(form)(H_2O) structures, showing layers of infinite chains (top) linked together by the CDC molecules (bottom)

The threedimensional structure is achieved through stacking of these sheets by van der Waals-interactions (Figure 4-12, bottom).

4.5 Luminescence

4.5.1 NDC series

We were able to obtain the luminescence spectra of the Ce^{3+} and Nd^{3+} analogues in the NDC series. The steady-state excitation and emission spectra are presented below and are corrected for detector sensitivity unless otherwise noted.

4.5.1.1 CeCl(NDC)(DMF)

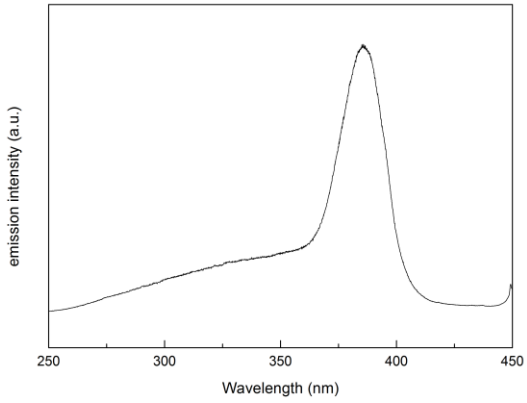

Figure 4-13: Excitation spectrum of CeCl(NDC)(DMF)

Upon monitoring the emission at 466 nm, the excitation wavelength was varied from 250 to 450 nm. A single peak was observed at 385 nm. This corresponds to a 5d ← 4f transition. The presented spectrum is not corrected, because the correction overcompensates for the low intensity of the emitted light from the Xe-lamp in this wavelength range; this causes the baseline to erroneously appear relatively more intense.

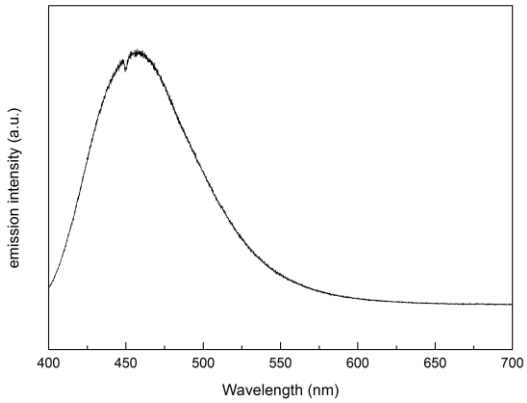

Figure 4-14: Emission spectrum of CeCl(NDC)(DMF)

Upon excitation of the sample at 385 nm in the 5d ← 4f transition found in the above excitation spectrum, the emission spectrum shows a band centred around 456 nm. This corresponds to the 5d → 4f transition, specifically from the lowest 5d state to the terminal $^2F_{5/2}$ and $^2F_{3/2}$ ground states of Ce^{3+}.

4.5.1.2 NdCl(NDC)(DMF)

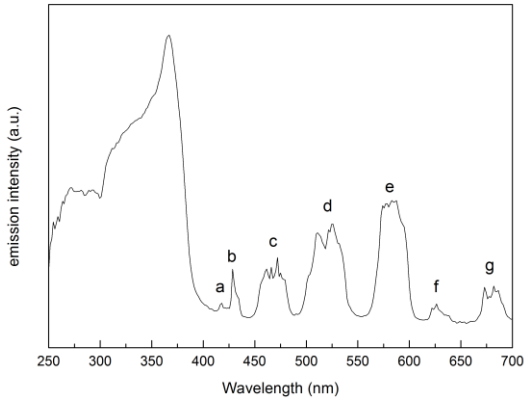

Figure 4-15: Excitation spectrum of NdCl(NDC)(DMF)

Monitoring the emission of the sample at 1055 nm, the excitation wavelength was varied from 250 to 700 nm to record an excitation spectrum. The peaks labelled a-g can be assigned to the corresponding transitions in the Nd^{3+}-ion's 4f-shell.

Table 4-1: Assignment of the peaks in Figure 4-15

label	λ (nm)	$\bar{\upsilon}$ (cm^{-1})	Transition
a	418	23923	$^2D_{5/2} \leftarrow {}^4I_{9/2}$
b	428	23364	$^2P_{1/2} \leftarrow {}^4I_{9/2}$
c	466	21459	$^2K_{15/2}, {}^2D_{3/2}, {}^2P_{3/2}, {}^4G_{11/2}, {}^2G_{9/2} \leftarrow {}^4I_{9/2}$
d	526	19011	$^2K_{13/2}, {}^4G_{7/2}, {}^4G_{9/2} \leftarrow {}^4I_{9/2}$
e	580	17241	$^2G_{7/2}, {}^4G_{5/2} \leftarrow {}^4I_{9/2}$
f	626.5	15692	$^2H_{11/2} \leftarrow {}^4I_{9/2}$
g	679	14859	$^4F_{9/2} \leftarrow {}^4I_{9/2}$

The broad excitation band at lower wavelengths with a maximum at 367 nm is attributed to ligand sensitization of the neodymium ion, as described in ref. 6. This band is lower in energy when compared to the BDC^{2-} excitation spectra (in for example Figure 2-33), which was centred below 300 nm.

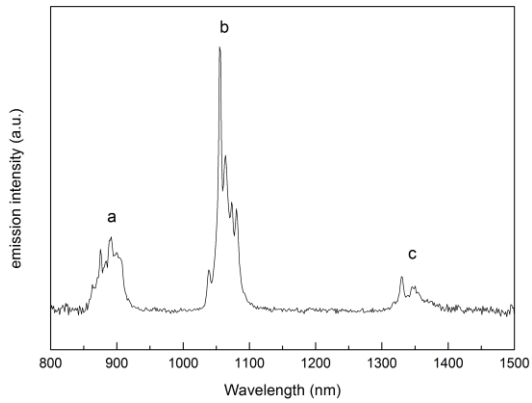

Figure 4-16: Emission spectrum of NdCl(NDC)(DMF)

This is logical since the conjugated system in NDC^{2-} is larger than that of BDC^{2-}, and with larger conjugated systems the absorption wavelengths tend to shift towards longer wavelengths and lower energies.

Upon excitation at 355 nm, the sample shows the typical narrow Nd^{3+} emission peaks a-c, corresponding to the electronic transitions listed below.

Table 4-2: Assignment of the peaks in Figure 4-16

label	λ (nm)	ῡ (cm^{-1})	Transition
a	890	11236	$^4F_{3/2} \rightarrow {}^4I_{9/2}$
b	1055	9479	$^4F_{3/2} \rightarrow {}^4I_{11/2}$
c	1330	7519	$^4F_{3/2} \rightarrow {}^4I_{13/2}$

For this compound, sensitization can occur for the Nd^{3+} analogue of the LnCl(NDC)(DMF) series. The intensity of the characteristic Nd^{3+} emission is relatively higher when excited through the broad band at shorter wavelengths. The typical Nd^{3+} absorption bands, however, are significantly present in the excitation spectrum, meaning that the antenna effect is not the only pathway to excitation for the ions in this case. This means that one or more of the energy transfer processes is not fully efficient.

The luminescent lifetime was also measured and calculated at 1.38 µs. When comparing this to the Łyszczek reference where the lifetime of the two Nd^{3+} sites in $Nd_2(NDC)_3 \cdot 2.5DMF$ were calculated at 1.66 µs and 10.13 µs, respectively, it is apparent that our value is within the same order of magnitude.

4.5.2 CDC series

For the CDC series, we were able to record the luminescence spectra of the Ce^{3+}, Nd^{3+}, Pr^{3+}, Eu^{3+}, Tb^{3+} and Dy^{3+} analogues. Presented below are the steady state excitation and emission spectra. Although we expect no large absorption (except at very low wavelength) from CDC^{2-} and therefore no large energy transfer to the lanthanide ions, we still present these spectra for the sake of completeness.

4.5.2.1 Ce(CDC)(form)(H_2O)

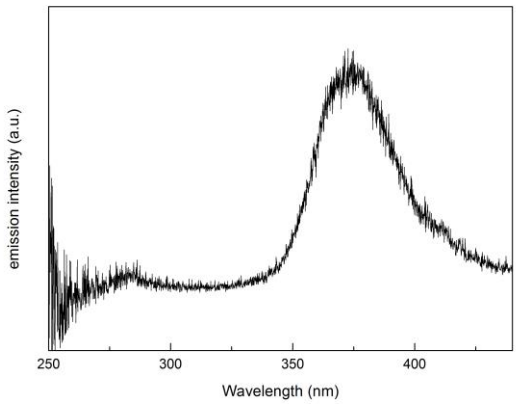

Figure 4-17: Excitation spectrum of Ce(CDC)(form)(H_2O)

Upon monitoring the emission at 466 nm, the excitation wavelength was varied from 250 to 450 nm. A single peak was observed at 375 nm. This corresponds to a 5d ← 4f transition.

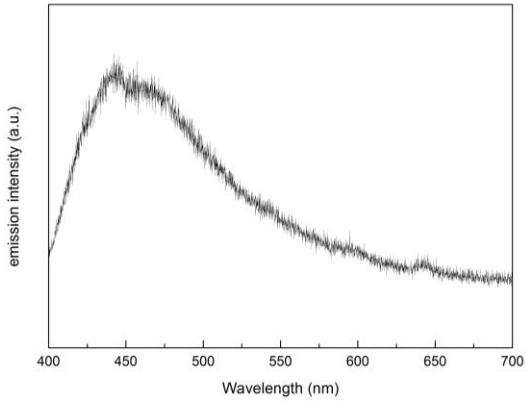

Figure 4-18: Emission spectrum of Ce(CDC)(form)(H_2O)

Upon excitation of the sample at 375 nm in the 5d ← 4f transition, the emission spectrum shows a peak centred around 450 nm. This corresponds to a 5d → 4f transition, specifically from the lowest 5d state to the terminal $^2F_{5/2}$ and $^2F_{3/2}$ ground states of Ce^{3+}.

4.5.2.2 Nd(CDC)(form)(H_2O)

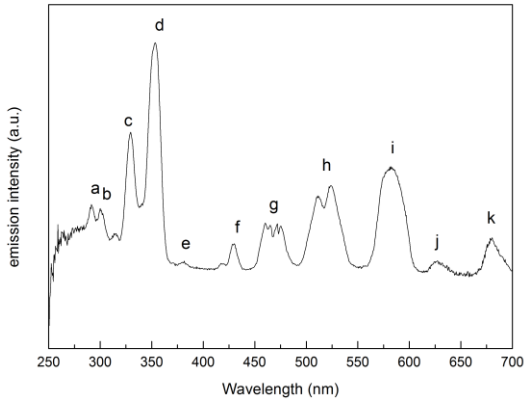

Figure 4-19: Excitation spectrum of Nd(CDC)(form)(H_2O)

Monitoring the emission of the sample at 1055 nm, the excitation wavelength was varied from 250 to 700 nm to record an excitation spectrum. The peaks labelled a-k are assigned to corresponding transitions in the Nd^{3+}-ion's 4f-shell.

Table 4-3: Assignment of the peaks in Figure 4-19

Label	λ (nm)	ῡ (cm^{-1})	Transition
a	291	34364.26	$^2D_{5/2} \leftarrow {}^4I_{9/2}$
b	300	33333.33	$^2D_{3/2} \leftarrow {}^4I_{9/2}$
c	329	30395.14	$^2L_{17/2}, {}^4D_{7/2} \leftarrow {}^4I_{9/2}$
d	353	28328.61	$^2L_{15/2}, {}^4D_{1/2}, {}^2I_{11/2}, {}^4D_{5/2}, {}^4D_{3/2} \leftarrow {}^4I_{9/2}$
e	381	26246.72	$(^2P,{}^2D)_{3/2} \leftarrow {}^4I_{9/2}$
f	439	22779.04	$^2D_{5/2}, {}^2P_{1/2} \leftarrow {}^4I_{9/2}$
g	467	21413.28	$^4G_{11/2}, (^2P,{}^2D)_{3/2}, {}^2G_{9/2} \leftarrow {}^4I_{9/2}$
h	523	19120.46	$^2K_{13/2}, {}^4G_{9/2}, {}^4G_{7/2} \leftarrow {}^4I_{9/2}$
i	582	17182.13	$^2G_{7/2}, {}^4G_{5/2} \leftarrow {}^4I_{9/2}$
j	627	15948.96	$^2H_{11/2} \leftarrow {}^4I_{9/2}$
k	680	14705.88	$^4F_{9/2} \leftarrow {}^4I_{9/2}$

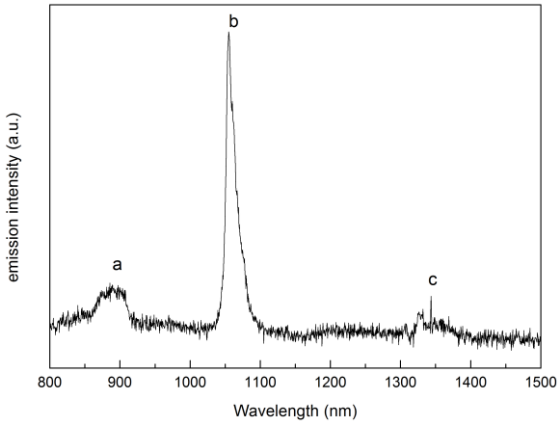

Figure 4-20: Emission spectrum of Nd(CDC)(form)(H_2O)

Upon excitation at 355 nm in the $^4D_{5/2} \leftarrow {}^4I_{9/2}$ band, the sample shows the typical narrow Nd^{3+} emission peaks a-c in the NIR range, corresponding to the electronic transitions listed below. Here as well, only the uncorrected spectrum is shown. Near the visible region, the correction overcompensates for the insensitivity of the NIR-PMT detector.

Table 4-4: Assignment of the peaks in Figure 4-20

Label	λ (nm)	ῡ (cm^{-1})	transition
a	880	11364	$^4F_{3/2} \rightarrow {}^4I_{9/2}$
b	1053	9497	$^4F_{3/2} \rightarrow {}^4I_{11/2}$
c	1327	7536	$^4F_{3/2} \rightarrow {}^4I_{13/2}$

4.5.2.3 Sm(CDC)(form)(H_2O)

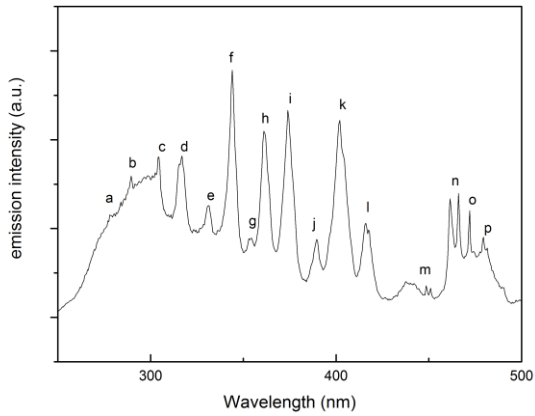

Figure 4-21: Excitation spectrum of Sm(CDC)(form)(H_2O)

Monitoring the emission intensity of the sample at 595 nm, the excitation wavelength was varied from 250 to 500 nm to record an excitation spectrum. The peaks labelled a-p can be assigned to the corresponding transitions in the Sm^{3+}-ion's 4f-shell.

Table 4-5: Assignment of the peaks in Figure 4-21

Label	λ (nm)	ῡ (cm^{-1})	transition
a	279.5	35971	$^4I_{11/2} \leftarrow {}^6H_{5/2}$
b	289.5	34542	$(^4I, {}^4F)_{9/2} \leftarrow {}^6H_{5/2}$
c	304.5	32840	$^4P_{5/2} \leftarrow {}^6H_{5/2}$
d	317	31545	$^4P_{3/2} \leftarrow {}^6H_{5/2}$
e	331	30211	$^4G_{9/2}, {}^4G_{5/2} \leftarrow {}^6H_{5/2}$
f	344	29069	$^4H_{9/2}, {}^4D_{7/2} \leftarrow {}^6H_{5/2}$
g	354	28248	$^4H_{7/2} \leftarrow {}^6H_{5/2}$
h	361	27700	$^4D_{3/2}, (^4D, {}^6P)_{5/2} \leftarrow {}^6H_{5/2}$
i	374	26737	$^4P_{7/2} \leftarrow {}^6H_{5/2}$
j	389	25706	$^4L_{15/2} \leftarrow {}^6H_{5/2}$
k	402	24875	$^6P_{3/2}, {}^4F_{7/2}, {}^4L_{13/2} \leftarrow {}^6H_{5/2}$
l	416	24038	$(^6P, {}^4P)_{5/2} \leftarrow {}^6H_{5/2}$
m	448.5	22296	$^4F_{5/2} \leftarrow {}^6H_{5/2}$

n	464	21551	$^4I_{13/2} \leftarrow {}^6H_{5/2}$
o	472	21186	$^4I_{11/2} \leftarrow {}^6H_{5/2}$
p	479	20876	$^4I_{9/2}$, $^4M_{15/2} \leftarrow {}^6H_{5/2}$

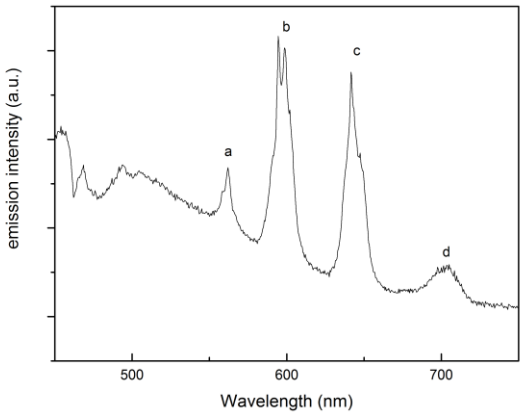

Figure 4-22: Emission spectrum of Sm(CDC)(form)(H_2O)

Upon excitation at 344 nm in the $^4H_{9/2}$, $^4D_{7/2} \leftarrow {}^6H_{5/2}$ band, the sample shows the typical narrow Sm^{3+} emission peaks a-d in the visible range, corresponding to the electronic transitions listed below. These peaks are superimposed on a broad band, which is probably the phosphorescence of the ligands in the structure.

Table 4-6: Assignment of the peaks in Figure 4-22

Label	λ (nm)	ῡ (cm^{-1})	transition
a	279.5	35971	$^4G_{5/2} \rightarrow {}^6H_{5/2}$
b	289.5	34542	$^4G_{5/2} \rightarrow {}^6H_{7/2}$
c	304.5	32840	$^4G_{5/2} \rightarrow {}^6H_{9/2}$
d	317	31545	$^4G_{5/2} \rightarrow {}^6H_{11/2}$

4.5.2.4 *Eu(CDC)(form)(H_2O)*

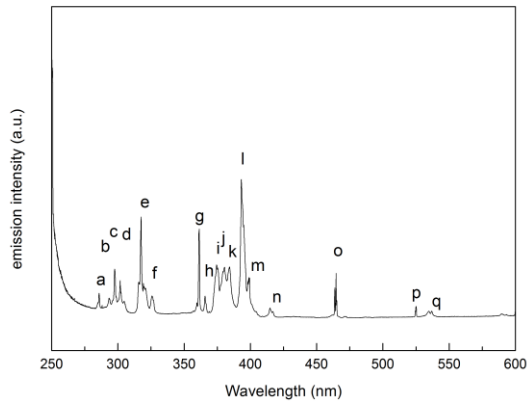

Figure 4-23: Excitation spectrum of Eu(CDC)(form)(H_2O)

Monitoring the emission of the sample at 618 nm (16181 cm^{-1}), the excitation wavelength was varied from 250 to 600 nm to record an excitation spectrum. The peaks labeled a-q can be assigned to the corresponding transitions in the Eu^{3+}-ion's 4f-shell. It is worth noting that the Eu^{3+} emission will only be caused by direct excitation of the ion itself, there is no sign of sensitization or charge transfer. This makes the CDC^{2-} /formate combination poor for luminescent enhancement of Eu^{3+}.

Table 4-7: Assignment of the peaks in Figure 4-23

label	λ (nm)	ῡ (cm^{-1})	Transition
a	285	35087.72	$(^5I, {}^5H)_6 \leftarrow {}^7F_0, {}^5I_7 \leftarrow {}^7F_1$
b	293.5	34071.55	$^5F_5 \leftarrow {}^7F_0, (^5I, {}^5H)_5 \leftarrow {}^7F_1$
c	297.5	33613.45	$^5F_4 \leftarrow {}^7F_0, {}^5I_4 \leftarrow {}^7F_1$
d	301.7	33145.51	$^5F_2 \leftarrow {}^7F_0, {}^5F_1 \leftarrow {}^7F_1$
e	317.5	31496.06	$^5H_6 \leftarrow {}^7F_0$
f	325.7	30703.1	$^5H_7 \leftarrow {}^7F_1$
g	361.4	27670.17	$^5D_4 \leftarrow {}^7F_0$
h	365.8	27337.34	$^5D_4 \leftarrow {}^7F_1$
i	374.5	26702.27	$^5G_6 \leftarrow {}^7F_0$

j	380.4	26288.12	$^5G_2 \leftarrow {}^7F_0$, $^5G_3 \leftarrow {}^7F_1$
k	384.1	26034.89	$^5L_7 \leftarrow {}^7F_1$
l	393.2	25432.35	$^5L_6 \leftarrow {}^7F_0$
m	399.3	25043.83	$^5L_6 \leftarrow {}^7F_1$
n	414.7	24113.82	$^5D_3 \leftarrow {}^7F_1$
o	464.6	21523.89	$^5D_2 \leftarrow {}^7F_0$
p	525.2	19040.37	$^5D_1 \leftarrow {}^7F_0$
q	535.1	18688.1	$^5D_1 \leftarrow {}^7F_1$

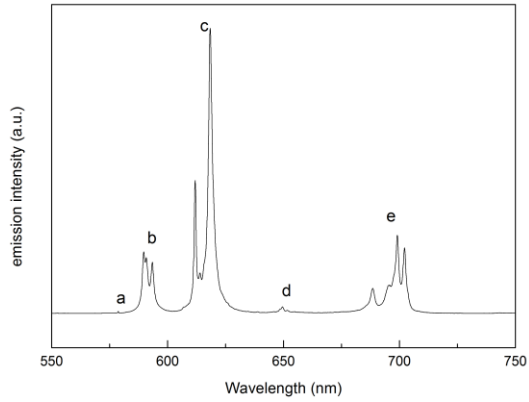

Figure 4-24: Emission spectrum of Eu(CDC)(form)(H_2O)

Upon excitation at 394 nm in the $^5L_6 \leftarrow {}^7F_0$ band, the sample shows the typical narrow Eu^{3+} emission peaks a-e in the visible range, corresponding to the electronic transitions listed below.

Table 4-8: Assignment of the peaks in Figure 4-24

label	λ (nm)	ῡ (cm^{-1})	transition
a	578.8	17277	$^5D_0 \rightarrow {}^7F_0$
b	591.4	16909	$^5D_0 \rightarrow {}^7F_1$
c	618.4	16170	$^5D_0 \rightarrow {}^7F_2$
d	649.5	15396	$^5D_0 \rightarrow {}^7F_3$
e	699.2	14302	$^5D_0 \rightarrow {}^7F_4$

4.5.2.5 *Tb(CDC)(form)(H_2O)*

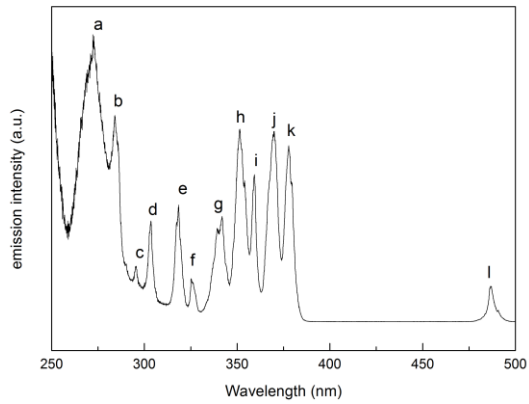

Figure 4-25: Excitation spectrum of Tb(CDC)(form)(H_2O)

Monitoring the emission of the sample at 545 nm (18349 cm^{-1}), the excitation wavelength was varied from 250 to 500 nm to record an excitation spectrum. The peaks labelled a-l can be assigned to the corresponding transitions in the Tb^{3+}-ion's 4f-shell.

Table 4-9: Assignment of the peaks in Figure 4-25

label	λ (nm)	ῡ (cm-1)	transition
a	272.2	36738	$^5I_7 \leftarrow {}^7F_6$
b	284	35211	$^5I_8 \leftarrow {}^7F_6$
c	295.6	33829	$^5H_5 \leftarrow {}^7F_6$
d	303.5	32949	$^5H_6 \leftarrow {}^7F_6$
e	318.5	31397	$^5H_7 \leftarrow {}^7F_6$
f	325.3	30741	$^5D_1 \leftarrow {}^7F_6$
g	341.9	29248	$^5L_8, {}^5L_7 \leftarrow {}^7F_6$
h	351.4	28458	$^5L_9 \leftarrow {}^7F_6$
i	359.3	27832	$^5G_5 \leftarrow {}^7F_6$
j	370	27027	$^5L_{10} \leftarrow {}^7F_6$
k	377.8	26469	$^5G_6 \leftarrow {}^7F_6$
l	486.7	20547	$^5D_4 \leftarrow {}^7F_6$

The $^5I_7 \leftarrow {}^7F_6$ and $^5I_8 \leftarrow {}^7F_6$ appear to be broader and superimposed on a broad band that can be seen as absorption from the ligand. However, this may also be attributed to the correction. It is therefore not possible to say whether the CDC^{2-}/formate matrix is suitable for Tb^{3+} excitation.

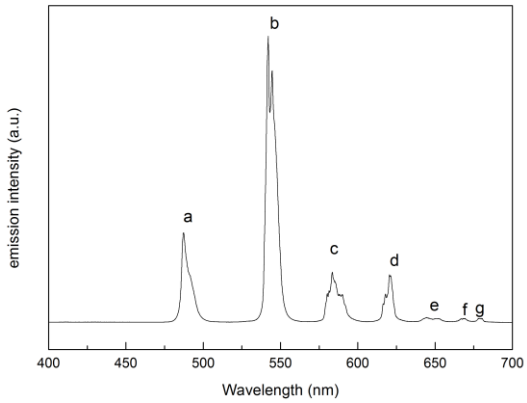

Figure 4-26: Emission spectrum of Tb(CDC)(form)(H_2O)

Upon excitation at 350 nm in the $^5L_9 \leftarrow {}^7F_6$ band, the sample shows the typical narrow Tb^{3+} emission peaks a-g in the visible range, corresponding to the electronic transitions listed below.

Table 4-10: Assignment of the peaks in Figure 4-26

label	λ (nm)	ῡ (cm^{-1})	transition
a	487.3	20521	$^5D_4 \rightarrow {}^7F_6$
b	545	18348	$^5D_4 \rightarrow {}^7F_5$
c	583.5	17137	$^5D_4 \rightarrow {}^7F_4$
d	620.5	16116	$^5D_4 \rightarrow {}^7F_3$
e	646.6	15465	$^5D_4 \rightarrow {}^7F_2$
f	668.2	14965	$^5D_4 \rightarrow {}^7F_1$
g	680.2	14701	$^5D_4 \rightarrow {}^7F_0$

4.5.2.6 Dy(CDC)(form)(H_2O)

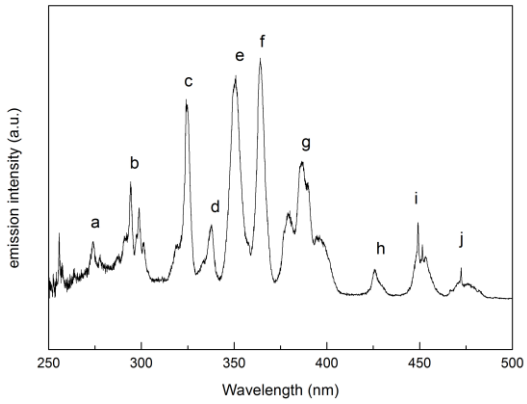

Figure 4-27: Excitation spectrum of Dy(CDC)(form)(H_2O)

Monitoring the emission of the sample at 545 nm (17931 cm^{-1}), the excitation wavelength was varied from 250 to 500 nm to record an excitation spectrum. The peaks labelled a-j can be assigned to the corresponding transitions in the Dy^{3+}-ion's 4f-shell.

Table 4-11: Assignment of the peaks in Figure 4-27

label	λ (nm)	ῡ (cm^{-1})	transition
a	274.1	36483	$^4G_{9/2}$, (^4G, $^4H)_{7/2} \leftarrow {}^6H_{15/2}$
b	294.2	33990	$^4L_{17/2}$, $^4G_{11/2}$, $^4G_{9/2}$, $^4H_{11/2}$, $^4D_{7/2}$, (^4K, $^4L)_{13/2}$, $^4H_{13/2} \leftarrow {}^6H_{15/2}$
c	324.1	30855	$^4L_{19/2}$, $^4K_{15/2}$, (^4G, $^2F)_{7/2} \leftarrow {}^6H_{15/2}$
d	337.8	29603	$^4M_{17/2}$, $^6P_{3/2}$, $^4G_{9/2}$, $^4I_{9/2}$, (^4F, $^4D)_{5/2} \leftarrow {}^6H_{15/2}$
e	350.9	28498	(^4M, $^4I)_{15/2}$, $^5P_{7/2}$, $^4I_{11/2} \leftarrow {}^6H_{15/2}$
f	364.1	27465	$^6P_{5/2}$, (^4P, $^4D)_{3/2}$, $^4M_{19/2} \leftarrow {}^6H_{15/2}$
g	386.3	25887	$^4K_{17/2}$, $^4M_{21/2}$, $^4I_{13/2}$, $^4F_{7/2} \leftarrow {}^6H_{15/2}$
h	425.6	23496	$^4G_{11/2} \leftarrow {}^6H_{15/2}$
i	449.1	22267	$^4I_{15/2} \leftarrow {}^6H_{15/2}$
j	472.4	21169	$^4F_{9/2} \leftarrow {}^6H_{15/2}$

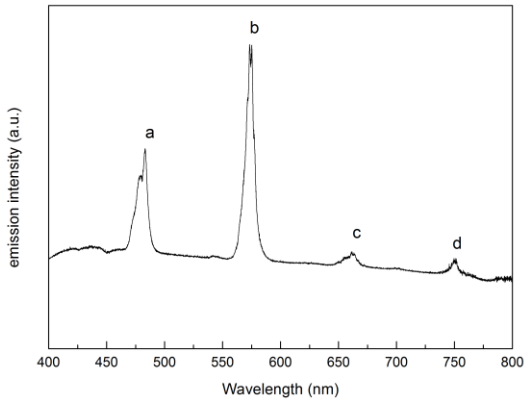

Figure 4-28: Emission spectrum of Dy(CDC)(form)(H_2O)

Upon excitation at 350 nm in the (^{4}M, ^{4}I)$_{15/2}$, $^5P_{7/2}$, $^4I_{11/2} \leftarrow {}^6H_{15/2}$ band, the sample shows the typical narrow Dy^{3+} emission peaks a-d in the visible range, corresponding to the electronic transitions listed below.

Table 4-12: Assignment of the peaks in Figure 4-28

label	λ (nm)	ῡ (cm^{-1})	transition
a	478.4	20903	$^4F_{9/2} \rightarrow {}^6H_{15/2}$
b	573.3	17443	$^4F_{9/2} \rightarrow {}^6H_{13/2}$
c	661.8	15110	$^4F_{9/2} \rightarrow {}^6H_{11/2}$
d	750	13333	$^4F_{9/2} \rightarrow {}^6H_{9/2}$, $^6F_{11/2}$

4.6 Conclusion and outlook

For these compounds, we have been able to record the steady state luminescence spectra without difficulty. The NDC series as expected showed excitation via the ligand. For the CDC series, no broad bands are visible in any of the excitation spectra. The emission was caused by direct excitation of the metal ion itself. This means that the CDC

ligand, as expected, is a poor sensitizer when using light from the selected excitation wavelength range. For this, one should perform absolute quantum yield measurements with the help of an integrating sphere.

4.7 References

[1] Synthesis, structures, and luminescence properties of a new family of three-dimensional open-framework lanthanide coordination polymers, Z. Wang, C.-M. Jin, T. Shao, Y.-Z. Li, K.-L. Zhang, H.-T. Zhang, X.-Z. You, Inorg. Chem. Comm., **2002,** vol. 5, p. 642

[2] 3-Dimensional Terbium Coordination Polymers: $[Tb_4(NDC)_6(H_2O)_5]\cdot 2H_2O$ and $[Tb_2(BPDC)_3(H_2O)_3]\cdot H_2O$ (NDC = 2,6-Naphthalenedicarboxylate; BPDC = 2,2'-Bipyridine-4,4'-dicarboxylate), D. Min, S.W. Lee, Bull. Korean Chem. Soc., **2002**, Vol 23, No. 7, p. 948

[3] Hydrothermal synthesis of a novel thermally stable three-dimensional ytterbium-organic framework, F.A. Almeida-Paz, J. Klinowski, Chem. Commun., **2003**, p. 1484

[4] Interplane Distances Modulation in Lanthanide-Based Coordination Polymers, A. Deluzet, W. Maudez, C. Daiguebonne, O. Guillou, Cryst. Growth Des., **2003**; Vol. 3, No.4, p. 475

[5] Hydrothermal Syntheses, Structures, and Properties of Three 3-D Lanthanide Coordination Polymers that Form 1-D Channels, X.-J. Zheng, Z.-M. Wang, S. Gao, F.-H. Liao, C.-H. Yan,L.-P. Jin, Eur. J. Inorg Chem., **2004**, p. 2968

[6] Microwave-assisted synthesis of lanthanide 2,6-naphthalenedicarboxylates: Thermal, luminescent and sorption characterization, R. Łyszczek, A. Lipke, Micropor. Mesopor. Mat., **2013**, Vol. 168, p. 81

[7] Two structurally different praseodymium-organic frameworks with permanent porosity, O. Alduhaish, B. Li, V. Nesterov, H.D. Arman, K. Alfooty, A.M. Asiri, H. Wang, B. Chen, Inorg. Chem. Commun, **2014**, Vol. 45, p. 89

[8] The syntheses, structures, magnetic and luminescent properties of five new lanthanide(III)–2,6-naphthalenedicarboxylate complexes, Y.-B. Lu, S. Jin, Z.-G. Zhou, S.-Y. Zhang, G.-T. Lou, Y.-R. Xie, Inorg. Chem. Commun., **2014**, vol 48, p. 73

[9] Zinc(II) and cadmium(II) complexes with mixed 1,3-di(1H-imidazol-4-yl)benzene and cyclohexanedicarboxylate ligands: Synthesis, structure and property, Z.-H. Chen, Y. Zhao, P. Wang, S.-S. Chen, W.-Y. Sun, Polyhedron, **2014**, vol. 67, p. 253

[10] Tuning the Supramolecular Structure through Variation of the Ligand Geometry and Metal Substituents−Diorganotin Macrocycles and Coordination Polymers Derived from cis- and trans-1,2-, 1,3-, and 1,4-Cyclohexanedicarboxylic and cis,cis-1,3,5-Cyclohexanetricarboxylic Acid, I. F. Hernández-Ahuactzi, J. Cruz-Huerta, H. Tlahuext, V. Barba, J. Guerrero-Alvarez, H. Höpfl, Cryst. Growth Des., **2015**, Vol 15, p. 829

[11] Construction of coordination frameworks based on 4-imidazolyl tecton 1,4-di(1*H*-imidazol-4-yl)benzene and varied carboxylic acids, S.-S. Chen, Y. Zhao, J. Fan, T. Okamura, Z.-S. Bai, Z.-H. Chena, W.-Y. Sun, CrystEngComm, **2012,** Vol. 14, p. 3564

[12] Synthesis, crystal structures, photoluminescence, and catalytic reactivity of novel coordination polymers (0-D, 1-D, 2-D to 3-D) constructed from *cis*-1,2-cyclohexanedicarboxylic acid and various bipyridyl ligands , Y.J. Lee, E.Y. Kim, S.H. Kim, S.P. Jang, T.G. Lee, C. Kim, S.-J. Kim, Y. Kim New J. Chem., **2011**, vol. 35, p.833

5 Towards coordination polymers containing lanthanides and β-diketonates

5.1 Outline and goals

Though in volume somewhat shorter than the other chapters, this part of the work has actually been the most time- and labour intensive. As the title partially displays, we have tried to go from mononuclear lanthanide β-diketonate complexes towards coordination polymers. The literature on this topic is rather limited. All synthetic efforts and attempts are based on classic procedures described in literature, both from articles in this and in previous chapters.

The big challenge here is to "simply" find crystalline materials that are suitable for analysis. Without them, there is no way to establish the identity and connectivity of newly-formed ordered coordination polymers, if they are formed at all. There are no similar structures to reasonably compare with, so Rietveld refinement is not an option. X-ray powder diffraction combined with TGA may show that an ordered structure was formed, but would yet again be unable to elucidate the structure.

5.2 The β-diketonate network

In coordination polymers, a cluster of ions or one central ion is coordinated, and this coordination sphere is linked to others.

So far in this work, the common organic functionality that coordinates the lanthanide metal has been a deprotonated carboxylic acid anion, combined with a pyridine nitrogen in the chapter concerning pyridinedicarboxylates. We will not be paying any attention

to these in this chapter, even though they are ideal for the formation of these compounds. Other functional groups, however, have also been employed. To list up and classify all of them would be beyond the scope of this work. Suffice to say that the easiest way of categorizing alternatives to carboxylates is by the identity of the coordinating functionality. Some examples of alternative ligands being used are: phosphonates (P), sulphonates (S), polypyridines (N), dioxane (O).

We sought to use yet other kinds of moieties that were previously unused or, at the very least, extremely rare.

To this end, we looked at some of the most studied functional groups in lanthanide coordination chemistry, namely β-diketones. Mononuclear complexes containing these ligands have been studied for 50 years already; their properties are well known.[1,2,3] For an exhaustive compilation on the subject, see Binnemans' review in reference 3.

The hydrogens on the α-position are easily removed (pKa = 8.95 for acetylacetone). The resulting deprotonated system is stabilized through resonance and, like the enol form, can form stable six-membered rings when both oxygen atoms coordinate a metal ion.

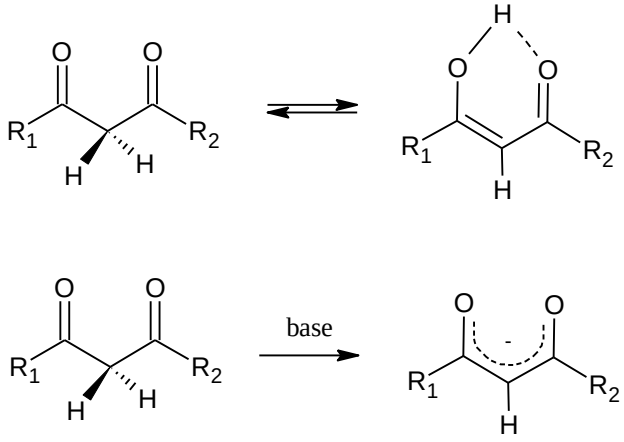

Figure 5-1: β-diketonate tautomerisation (top) and deprotonated conjugation (bottom)

Usually, depending on the synthesis conditions, three to four negatively charged β-diketonate ligands coordinate one lanthanide ion in mononuclear complexes. If there are three β-diketonates, additional ligands may be introduced to increase the coordination number to 8 and expel undesired water molecules from the first coordination sphere. 1,10-Phenanthroline or 2,2'-bipyridine are often chosen due to their bulky size and broad absorption bands. When no additional ligands are added, oftentimes water or solvent molecules complete the coordination sphere. This is detrimental to the luminescent efficiency, since vibronic coupling with OH vibrations quenches the luminescence. That is why a competing ligand needs to expel the water molecules from the first coordination sphere. If there are four β-diketonates, a positive counterion needs to be present to account for charge balance.

The luminescent properties of these complexes are tuneable by changing the substituents on the carbon chain, which can make them shine quite bright. The thermal and chemical stabilities of the complexes are fair, and the affinity of the diketonate group for a lanthanide ion is significant (see

Table 5-1). A β-diketonate ligand bidentately coordinates to one, two or three metal ions (see Figure 5-2), in that regard the group can be easily compared to carboxylates.

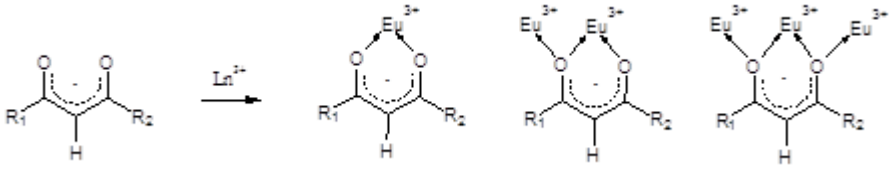

Figure 5-2: Coordination modes for β-diketonates

This means that metallocluster formation is possible. For discrete clusters involving β-diketonates, we refer to the work of Roesky *et al.*[4,5,6,7].

All the mentioned reasons combined leave us no doubt that using the motif in coordination chemistry and, by extension, coordination polymers, would be a good idea. It would literally embody the step from mononuclear coordination chemistry to coordination polymer and even metal-organic framework synthesis. If one would be able to obtain a functionalized molecule featuring two β-diketone coordination sites, this would be the bridging linker molecule from which we could start.

5.2.1 The linkers

To start with, we looked at two of the simplest molecules that fulfil the shape requirement we were searching for.

5.2.1.1 1,1',2,2'-tetraacetylethane

5.2.1.1.1 The structure

1,1',2,2'-Tetraacetylethane (H_2TAE, TAE^{2-} for the dianion and TAE for the dianion in formula) is a molecule that has been long known and easy to synthesize.[8] It has the two diketone groups opposite from one another, attached through their α-positions. Similar to oxalic acid, which is known as an efficient building block in coordination polymers, the groups are close to each other (Figure 5-3). The added benefit to TAE^{2-} however, is that the coordination sites are further apart than those of oxalic acid.

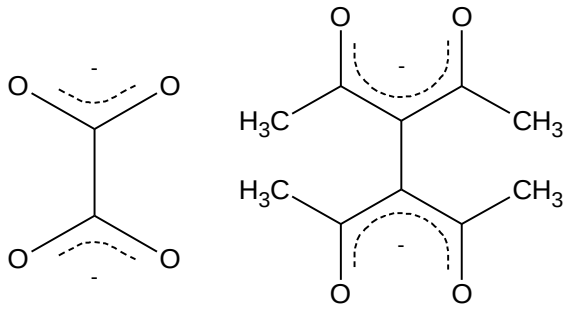

Figure 5-3: Oxalate and the tetraacetylethane dianion

This means that there will be less steric hindrance and more opportunity to make a framework in three dimensions. Substituted H_2TAE ligands can be synthesized, for example 1,2-diacetyl-1',2'-dibenzoylethane or 1,1',2,2'-tetrabenzoylethane[9], but these may ultimately prove to be too bulky for network formation. TAE^{2-} already adapts a non-planar structure due to steric hindrance of the four methyl groups, the dihedral angle being about 90°.

5.2.1.1.2 Reported relevant research

What has been achieved so far with H_2TAE pertains to transition metal ions instead of lanthanide ions, and to discreet mono, di, tri or tetranuclear complexes, but never to higher nuclearities. One of the oldest articles reporting research on this was written by Bailar *et al*. in 1962.[10] Coincidentally, Bailar may have been the first to coin the term coordination polymer.[11] In their work, they described four methods for combining the H_2TAE bis-β-diketone with metal salts or complexes of Be(II), Cu(II), Co(II), Ni(II) and Zn(II). They obtain compounds that they suggest have three different chain-like properties. The assumptions were based solely on thermogravimetric studies and elemental analysis including only carbon, hydrogen and the metal ion, oxygen is excluded. No crystal structures are presented, either because this technique was

unavailable or because no crystalline materials were found anyway. Shortly after, Charles *et al.* attempted something similar, again without reporting crystal structures.[12] Cu(II), Ni(II), Co(II), Zn(II), Cd(II) and Mg(II) were used in their divalent state, so the formation of chains is to be expected since the TAE linker has one negative charge at each end. Their main analysis techniques were thermogravimetry, spectrophotometric titration and elemental analysis. It was found that the degree of polymerization was rather low. Emara *et al.* also made the effort to characterize these polymers.[13] Via mass spectrometry, they found dinuclear (for Ni(II) and Co(III)), trinuclear (for Cu(II)) and polymeric (Fe(III) and Cr(III)) compounds. Again, extended order in the form of crystal structures was not found.

With TAE^{2-}, still, some dinuclear complexes were made and structurally characterized. Fukuda *et al.* synthesized a family of three compounds of the $[Ni_2(TAE)(TMED)_2]X_2 \cdot nH_2O$ family with X = BPh_4^-, ClO_4^- or NO_3^- and TMED = N, N, N', N'-tetramethylethylenediamine.[14] Costes *et al*. reported the Cu^{2+} analogue crystal structure of the.ClO_4^- compound.[15] Lim *et al.* completed the Cu^{2+} analogue group by reporting the structures of $[(Cu_2(TAE)(TMED)_2]X_2$, where X = NO_3^- or BPh_4^-, presented in Figure 5-4. [16]

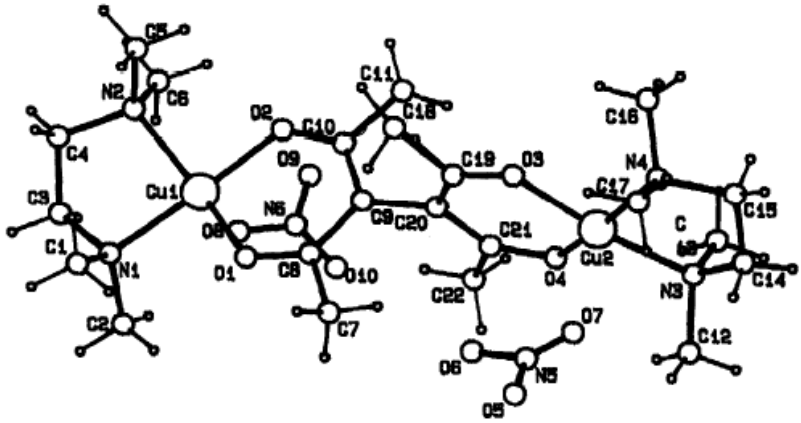

Figure 5-4: Crystal structure of $[(Cu)_2TAE(TMED)_2](NO_3)_2$ as taken from ref. 16

Very similar to this was the work of Golchoubian *et al.*, where four compounds were synthesized: $Cu_2(L)_2(TAE)]X_2$ with X = BPh_4^-, ClO_4^-, and L = N,N-dimethyl-N'-benzylethylenediamine or N,N'-dibenzylethylenediamine.[17] Continuing the list of dinuclear complexes, Zhang *et al.* also made three structures: $Cu_2(TAE)(DPA)_2(O_2CCF_3)_2$, $[Co_2(TAE)(DPA)_4](O_2CCH_3)_2(H_2O)_2$ and $[Cu_2(TAE)(DPA)_2(4,4'\text{-bipy}](O_2CCF_3)_2$ where DPA is dipiridylamine.[18] The last one is actually polymeric in nature, with the 4,4'-bipyridyl molecule linking two dinuclear complexes in zig-zag like chains. Koiwa *et al.* used TAE to bridge ruthenium complexes; their results include $Ru_2(TAE)(acac)_4$ which is shown in Figure 5-5, $Ru_2(TAE)(phpa)_4$ and $[Ru_2(TAE)(2,2'\text{-bipy})_4]^{2+}$ where acac = acetylacetonate and phpa = dipivaloymethanate.[19]

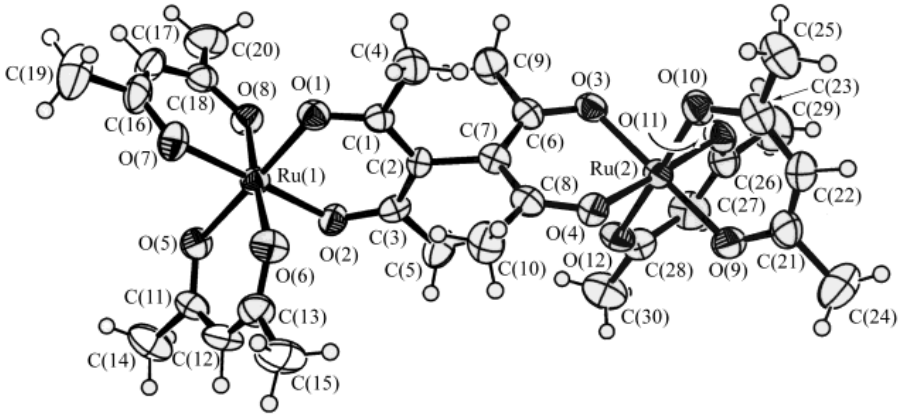

Figure 5-5: Crystal structure of $Ru_2TAE(acac)_4$ as taken from ref. 18

In 1998, a remarkable Co(II) molecular square complex was reported by Zhang *et al.*[20] The near 90° twisting of the TAE ligands make this square chiral. As end-capping ligands, it featured di-2-pyridylamine on the octahedral Co(II) corners (Figure 5-6).

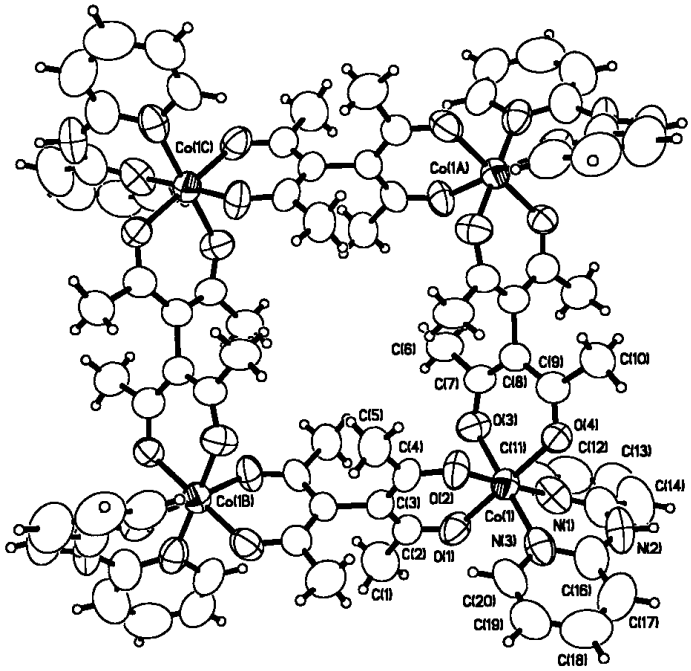

Figure 5-6: Crystal structure of the $[Co_4(TAE)_4(DPA)_4]$ molecular square as taken from ref. 20

Coordination polymers containing TAE^{2-} that have been characterized by single crystal X-ray diffraction, however, are very rare. To the best of my knowledge, only one article actually reports success in this regard.[21] Burrows *et al.* have isolated six different networks, all in low yield (less than a milligram); three of them were obtained from the same reaction mixture so reproducibility cannot be proven and phase purity optimization was not done. One can argue that even the one crystal is enough to classify as the successful very first synthesis. The reaction usually proceeded in a timespan of eight weeks; Zn^{2+} and Cd^{2+} nitrate salts were dissolved and reacted with TAE in the presence of triethylamine vapours. The precipitates that formed were filtered off and the filtrate was allowed to stand for several weeks until, in the lowest of yields, crystals formed. Depending on the solvents used, the one-dimensional chains $[Zn(TAE)(DMF)]\cdot 0.65CHCl_3\cdot 0.35DMF$ (in $CHCl_3$/DMF) and $[Zn_3(TAE)_3(MeOH)(DMSO)_{4.2}]\cdot 0.8DMSO$ (in MeOH/DMF) were found. Switching the reaction medium to methanol, three structures were found that consist of Zn-TAE dimers linked into two-dimensional networks: $[Zn_2(TAE)_2(MeOH)_2]\cdot 2MeOH$ (Figure 5-7), $[Zn_2(TAE)_2(MeOH)]\cdot 2H_2O$ and $Zn_2(TAE)_2(OH_2)_2$. A Cd analogue with formula $[Cd_2(TAE)_2(H_2O)_2]\cdot 2.5H_2O$ was also made, the general network connectivity remains the same but the spectator solvent ligands are different. The difficulty, lengthy reaction times and low yields of these syntheses suggest sub-optimal reaction conditions.

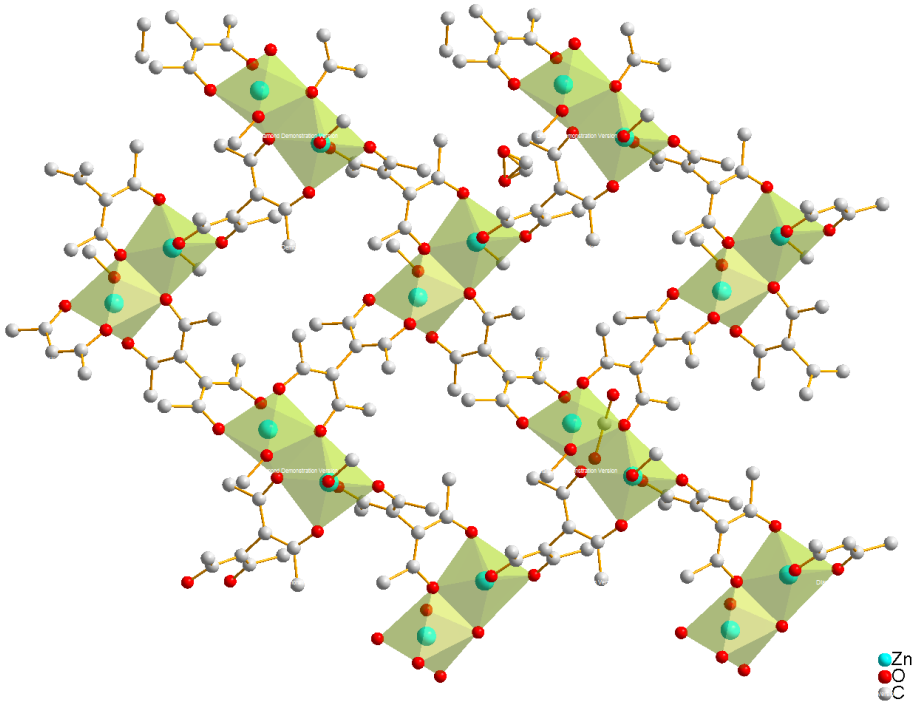

Figure 5-7: Two-dimensional network of $[Zn_2(TAE)_2(MeOH)_2]\cdot 2MeOH$, adapted from ref. 21. Hydrogen atoms omitted for clarity.

5.2.1.2 1,4-bis-(3-acetylacetone)-benzene

5.2.1.2.1 The structure

Another molecule of interest is 1,4-bis-(3-acetylacetone)-benzene (also 1,4-bis(2,4-dioxopentan-3-yl)benzene, henceforth H_2BAB unless specifically noted otherwise, BAB^{2-} for the dianion, BAB for the dianion in formulas), which is structurally reminiscent of terephthalic acid in that the two functional groups are placed on *ortho*-positions with respect to each other on a benzene ring (Figure 5-8). This could allow for rod-like behaviour when using this molecule as a building block, with a 180° angle between the negative charges on the deprotonated ligand.

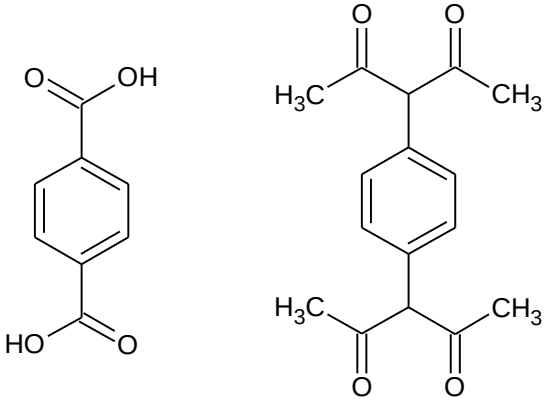

Figure 5-8: Comparison between terephthalic acid (H_2BDC, left) and 1,4-bis-(3-acetylacetone)-benzene (BAB, right)

5.2.1.2.2 Reported relevant research

The 1,2- and 1,3- isomers of BAB are also easily synthesized and, together with the 1,4 isomer, were used to make a series of three dinuclear Cu^{2+} complexes, capped with 2,2'-bipy (Figure 5-9).[22]

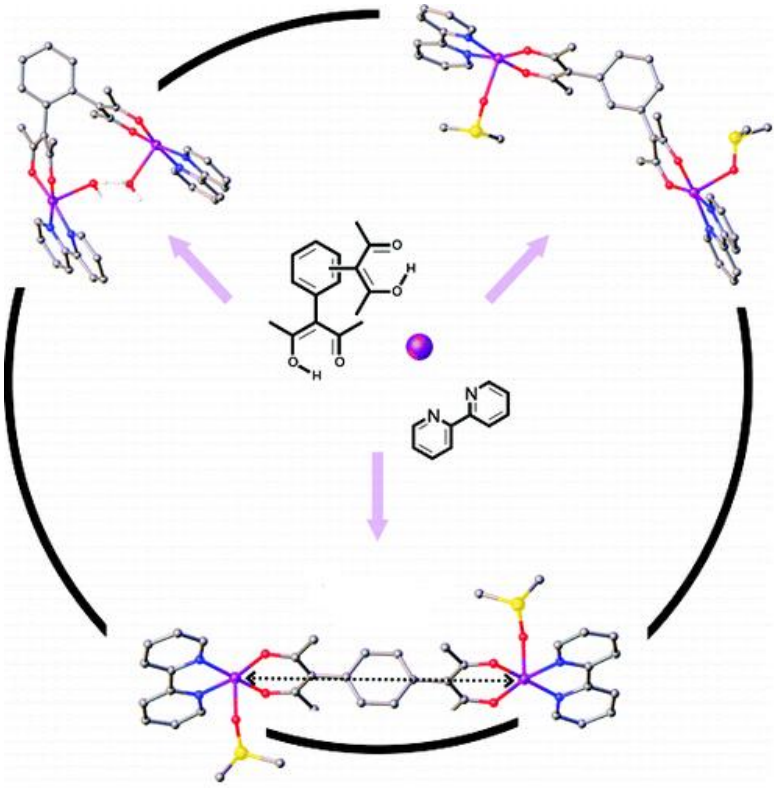

Figure 5-9: Isomeric dinuclear complexes of bis-(3-acetylacetonate)benzene, Cu^{2+} and 2,2'-bipyridine, as taken from ref. 22

With the 1,2-substitued BAB one would expect the formation of trinuclear triangles since the *ortho* angles of the functionalities are at 60°, and a hexanuclear molecular hexagon with the *meta* isomer. However, distortion of the 60° and 120° angles occurs and instead dinuclear dimeric[23] and tetranuclear tetrameric[24] copper complexes were made; the latter is depicted below in Figure 5-10.

Figure 5-10: The molecular square formed by Cu^{2+} and 1,3-BAB^{2-} as taken from ref. 24

Contrast this tetranuclear complex to the molecular TAE square previously described; either the metal or the organic linker serves as the vertex point and vice versa for the sides. Rancan *et al.* found that for the 1,2-BAB, however, a dynamic equilibrium was found between a dimeric and a trimeric compound, with template assistance from hexamethylenetetramine (HMT) favouring the trimeric form, depicted below in Figure 5-11.[25]

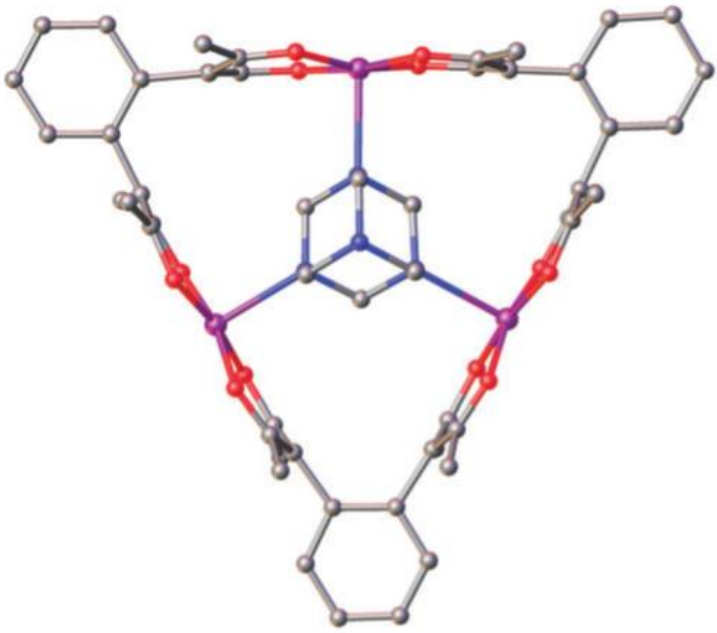

Figure 5-11: Crystal structure of the trimeric [Cu_3(1,2BAB)$_3$(HMT)] as taken from ref. 25

Lambert and Liu have also synthesized two dinuclear complexes with BAB^{2-} and Cu^{2+}; one was capped with TMED (tetramethylethylenediamine) and with two ClO_4^- counterions bound to the Cu(II) ions; the other was capped with 2,2'-bipy and with two DMSO molecules coordinated to one Cu(II) ion each, two ClO_4^- counterions are present but not coordinating.[26] The bipy molecules form a chain through π–π stacking (Figure 5-12).

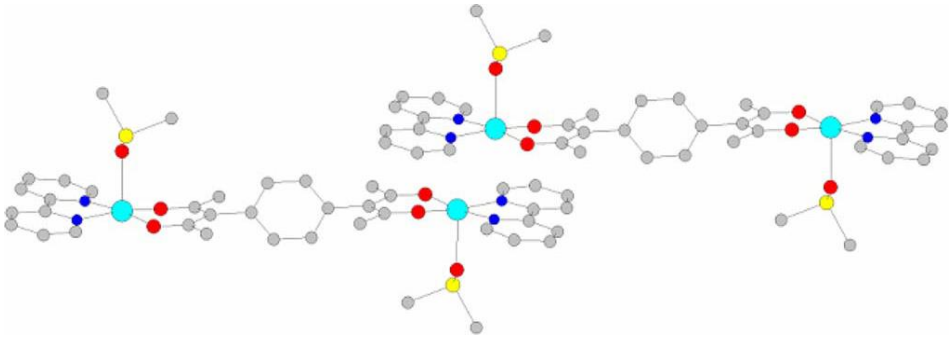

Figure 5-12: Crystal structure of $Cu_2(BAB^{2-})(DMSO)_2(2,2'bipy)_2$ as taken from ref. 26

Although, again to the best of my knowledge, no actual coordination polymers have been made with BAB^{2-}, several honourable mentions for attempts need to be noted. The first would be found in the aforementioned paper by Lambert and Liu, who specifically attempted this by mixing Cu^{2+} salts and H_2BAB together. They did not achieve crystalline materials with BAB^{2-}. They did, however, make a one-dimensional chain with 4-(3'acetylacetonato)pyridine, 1,10-phenanthroline and Cu^{2+} ions (Figure 5-13), which technically is a coordination polymer containing the β-diketonate ligand.

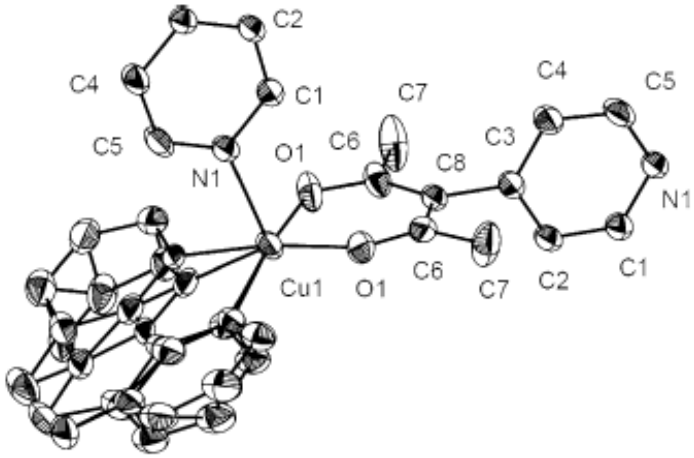

Figure 5-13: Unit cell of the Cu^{2+}, phen and 4-(3'acetylacetonato)pyridine coordination polymer as taken from ref. 24

The second mention is that of a Master Thesis work by B.T. Nguyen Pham.[27] In it, this researcher describes the synthesis of a one-dimensional chain using Zn^{2+} and 3,3'-(biphenyl-4-4'-diyl)dipentane-2,4-dione (H_2BABP) with formula $Zn(BABP)(DMSO)_2(CH_3OH)$ (Figure 5-14 and Figure 5-15). This linker molecule is strikingly similar to H_2BAB but has one extra benzene ring between both β-diketone functionalities. Although the synthesis of this chain was reproducible, an unidentifiable insoluble solid precipitated alongside the crystals every time.

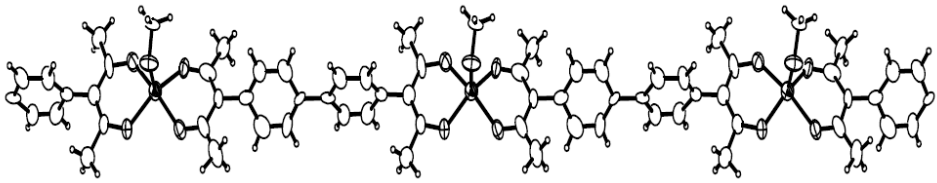

Figure 5-14: One-dimensional chain, $Zn(BABP)(DMSO)_2(CH_3OH)$ as taken from ref. 27

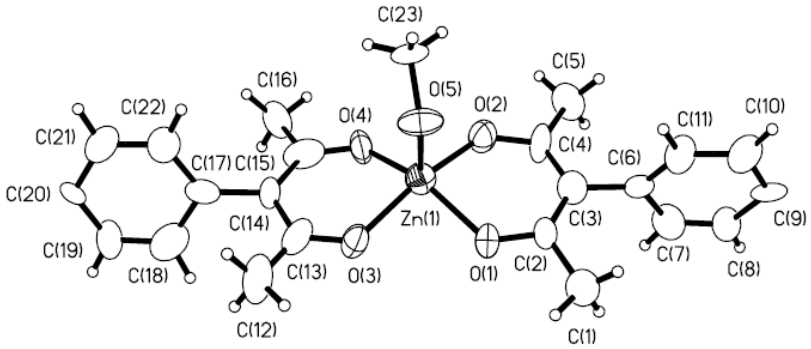

Figure 5-15: Unit cell of the one-dimensional chain as taken from ref. 27. C9 and C20 are connected through a single covalent bond.

As a side note, he also made the dinuclear complex $Zn_2(BABP)(phen)_2(OAc)_2$ (Figure 5-16), which might count as similar to the TAE^{2-} and DAB^{2-} dinuclear complexes.

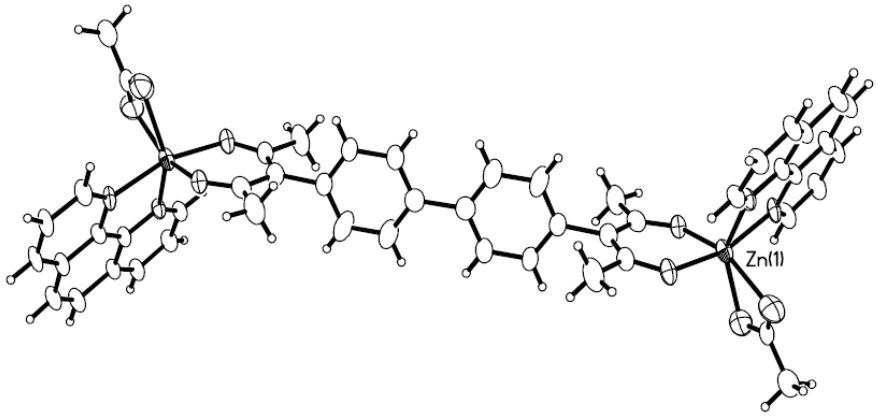

Figure 5-16: Crystal structure of $Zn_2(BABP)(phen)_2(OAc)_2$. as taken from ref. 27. The coordination polyhedron changes slightly upon resolvation and recrystallization.

A thorough search of the literature has revealed that only very few examples exist that apply the ideas (coordination polymers of lanthanide containing β-diketonate ligands) and molecules (specifically, TAE and BAB) presented in this chapter. Whether this is because nothing of the sorts has proven to be successful or efficient before, or truly because nobody has ever attempted it remains to be seen.

There are three more pieces of research that should be mentioned. One is the work of Carlucci *et al.*(ref. 30), the other is the work of Andrews *et al.* (ref. 31). These will be viewed in a following subchapter for relevancy. The reason is that in there, networks are formed using the β-diketonate groups but without TAE^{2-} or BAB^{2-} (similar to the 4-(3'acetylacetonato)pyridine-containing structure).

Finally, an interesting review about similar bis-β-diketonates and their coordination chemistry was published by Bray *et al.*[28]

5.2.2 Predictions and hurdles

A few remarks need to be made here, concerning the successes and failures in all previously described work.

1. The stability constants for complexes containing β-diketonate ligands and transition metal ions and, by extension, lanthanide ions are generally up to three times higher than those of analogous carboxylate complexes.[29] Some $acac^-$ and OAc^- stability constants are noted in
2. Table 5-1.

Table 5-1: Selected stability constants for acetylacetonate and acetate complexes

	La^{3+}	Lu^{3+}	Y^{3+}	Cu^{2+}	Fe^{3+}
Aqueous stability constants for acetylacetonate complexes					
Log β_1	4.94	6.15	5.89	8.16	10
Aqueous stability constant for acetate complexes					
Log β_1	1.82	1.85	1.86	1.83	3.38

Furthermore, the acidity of acetic acid in water is higher than that of acetylacetone ($pK_{a,HOAc}$ = 4.75, $pK_{a,\ Hacac}$ = 8.95). The reason for both acidity and stability constant values is structural mainly. When either of the two oxygens from β-diketonate ligands binds to a metal ion, the other one is close by to form the six-membered ring, which functions as a stabilizing factor. The same is possible for the proton in the tautomeric protonated form, whereas a stabilization in carboxylic acids by resonance is only present in the deprotonated carboxylate form, hence the higher acidity of carboxylic acid. The tendency for carboxylate groups to form bridges, however, shows that there is more flexibility in crystal growth. Usually, complex formation is entropy driven by the release of coordinated aquo ions. The use of different solvents and the formation of entropy-unfavoured ordered networks decrease this influence.

The increased affinity for β-diketones, therefore, gives rise to stronger metal-ligand bonds. This is a problem. During the growth of crystal structures, a certain degree of reversibility is needed, allowing bonds to form, break, realign or rotate, and form again to achieve long-distance order. If one part of a growing crystal structure is dislocated or wrongfully connected, this error will

propagate throughout the structure, destroying the long-range order and consequentially the crystallinity. This will give rise to amorphous insoluble products that one cannot structurally characterize, as described by both Lambert & Liu and Pham, evidenced by the synthesis method of Burrows' TAE^{2-} networks, and reported by the early works of Bailar, Charles and Emara.

One could remedy this by using lengthy synthesis methods, in which the reactants have ample time to grow in the correct manifold, and in dilute conditions, in which the reactants' opportunities to bond one another are reduced and insoluble oligo- and polymer formation is avoided.

3. Another subtle difference between carboxylates and β-diketonates is to be found in steric hindrance. Carboxylate moieties are built from three atoms. β-diketonates, on the other hand, have at least five atoms (two carbonyl C=O groups and one α carbon) to which are attached two R groups on the 1 and 3 α' positions. The smallest of these would be the methyl group, creating acetylacetone. However, this expands the bulk of the functionality even more. If three or four acac groups would all coordinate the same lanthanide ion bidentately, the coordination environment would look like that of mononuclear complexes. We cannot assume this, however, since there are other coordination modes possible, and this is where one can expect the network construction to be hindered due to sterical interactions.
4. Since all parties have employed transition metals, it should be possible to make some educated assumptions on what lanthanide ions would do to the outcome of the reactions. Most of the ions in the reported source are quite small and

typically have low coordination numbers. This limits the dimensionality of the networks as evidenced by the formation of one-dimensional chains or two-dimensional sheets.

Increasing the ionic radius to lanthanide proportions should increase the coordination number, the number of linkers attached to it and consequently, the network dimensionality.

5. However, the often unpredictable coordination geometry of lanthanide ions might impede the formation of ordered networks, mainly because the angles are distorted from “ideal” ones frequently seen in larger arrays. This means that crystallization might be an even harder task and difficult to steer.
6. It is definitely worth noting that the use of lanthanides in itself does not guarantee desired luminescent properties. The ligand triplet levels may be unsuitable, any additional coordinated solvent or guest solvent molecules may quench the luminescence, there can be self-absorption due to the proximity of many luminescent ions and there may be back-transfer to the ligand itself. However, the rigidity of the suggested molecules should prove to decrease radiationless deactivation. The fact that the coordination spheres of lanthanides can be filled quite quickly before additional water ligands will attach themselves, for example in the case of tetrakis-modes of coordination, can also prove to be a benefit.

5.2.3 Our attempts

After taking all these difficulties and warnings into account, the next step would be to find an efficient synthesis method that generates phase-pure crystalline materials, ideally suitable for single crystal X-ray analysis.

We have invested a lot of effort into finding a suitable way to obtain materials for which the syntheses were reproducible and where crystalline networks were formed of reasonable qualities in order to characterize them. To that purpose, we have attempted all of the conventional methods: hydro- and solvothermal syntheses, milder synthesis at increased temperature, experiments where a base enters the reaction medium through gaseous diffusion, layering solutions on top of each other, slow evaporation of reaction mixtures, dropwise addition of solutions to each other and the addition of diluted reaction mixtures.

In the end, amid a sea of unwanted powders that were unfit for characterization and solvent mixtures that showed absolutely no precipitation, only two kinds of crystals were formed. One was the starting product TAE, meaning that any equilibria in those mixtures were shifted to the side of the starting product. The other was the formate salt of neodymium, which comes from degradation from the bis-β-diketone.

When working with quantities of starting products that are comparable to literature values, usually precipitation occurs very quickly.

To find the reason why our attempts were unsuccessful is not easily done. One could just say that the ideal reaction conditions weren't met during the experiments and be done with explaining. This is not unreasonable, since even the slightest variations in the conditions indeed have this profound effect on the outcome. On the other hand, we

have outsourced this specific topic to the Unité de Catalyse et Chimie du Solide research group from Lille (Université de Lille) mentioned in a previous chapter, where solvothermal synthesis methods were intensively attempted. They, too, found similar results: the crystals of the starting products and the formate salt. In the Innovative Molecular Materials research group in Belfast (Queen's University), unconventional ionic liquid syntheses were attempted on this system. Again the same undesired products were formed.

If one takes the time to review the few networks thus far reported, one will see that they:

a. consisted of transition metals and TAE,
b. were obtained in very low yield,
c. were not part of a pure phase,
d. only crystallized after an unspecified amount of initial product was filtered off,
e. took several weeks to form

Since it is usually less difficult to achieve ordered structures for transition metals than for lanthanides, one should be able to appreciate both the difficulty with which the networks from Burrows *et al.* were obtained and the increase in challenge when making the step to lanthanides.

Given this, we could say that for this goal, the TAE^{2-} and BAB^{2-} ligands are simply unfit for combination with lanthanide metals:

a. possibly because of their high affinity for the ions which leaves no room for errors and corrections in the network construction,

b. possibly because of the unpredictable, low symmetry coordination modes in lanthanide ions,
c. possibly because of the high coordination number and consequentially the sterical hindrance that arises from network building in such a tight space,
d. possibly because of their tendency to degrade in solution
e. possibly because the parameters for the reaction are very specific and weren't found during the attempts
f. most likely a combination of all of the above

5.3 A heteronuclear alternative

5.3.1 Concept

Directly building networks with our simple linker molecules and lanthanides using conventional methods has proven to be unsuccessful. There is an indirect way of making networks that feature lanthanide ions coordinated by β-diketonate ligands. This method uses a "building-block" approach.

First, simple mononuclear complexes are synthesized. This complex can be seen as the building block. The story does not end there, because the complexes are functionalized in order to be able to coordinate to a secondary metal ion, which is added in a subsequent step. If all goes well, combination of building blocks may yield an ordered network structure.

In practice, such a ligand needs to have two distinct bonding sites that preferentially coordinate either a lanthanide ion or a secondary metal ion. The answer to this problem may be found in Pearson's hard-soft-acid-base theory; if we can find a ligand that has

both a moiety that exhibits great affinity for hard ions such as lanthanides and a soft group that may preferentially bond to soft metal ions, we have one of our modular building blocks.

To this end, we have tried to perform something akin to the work of Carlucci *et al.*[30], where some transition metal ions form complexes with substituted dibenzoylmethanato ligands. The substitution in question consisted of a pair of nitrile functions on the 4-positions on the benzene rings (see Figure 5-17). The name of this molecule is 1,3-bis(4'-cyanophenyl)-1,3-propanedione, we have given it the code HCNDBM.

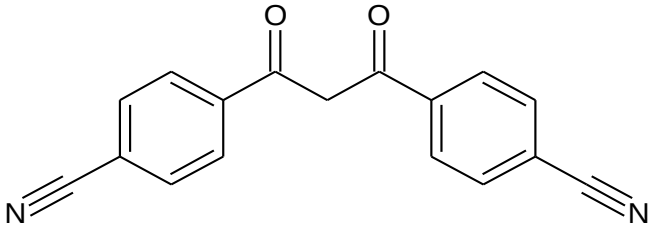

Figure 5-17: 1,3-bis(4-cyanophenyl)-1,3-propanedione, HCNDBM

The negatively charged β-diketonate groups are known to be "hard" and coordinated to transition metal ions such as Fe^{3+}, Co^{3+}, Zn^{3+}, Mn^{3+} and Cd^{3+} whereas the cyano groups can be classified as "soft" and connected the mononuclear complexes through coordination with "soft" Ag^{+} ions. The combination of these building blocks yielded threedimensional networks for those researchers, as shown in Figure 5-18.

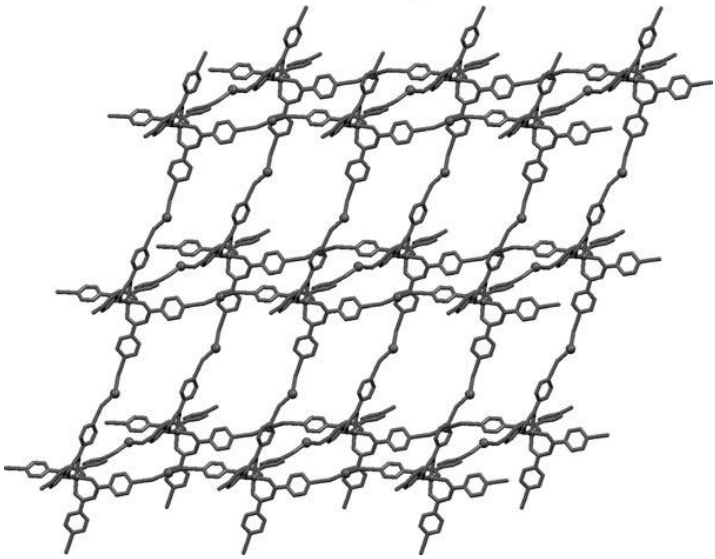

Figure 5-18: The heterometallic framework $[Zn(CNDBM)_3Ag_3](ClO_4)_2 \cdot solv$ adapted from ref. 30

We sought to try the same thing, but while using lanthanide ions instead of transition metal ions. This would give us, although not in its most rudimentary binary form, the network we sought: lanthanides coordinated by β-diketonates within a metal-organic rigid framework.

5.3.2 Our attempts

Facile Claisen condensation yielded the ligand in high yield. The synthesis and purification was followed by combination with lanthanide salts in the presence of a base. Depending on the relative stoichiometries in the reaction medium, we were able to crystallize three distinct classes of compounds: the $[LnCNDBM_3(phen)] \cdot solv$ with Ln = Nd^{3+}, Tb^{3+}, Y^{3+}, Ho^{3+} and Er^{3+} (Figure 5-19, Figure 5-20, Figure 5-21, Figure 5-22 and Figure 5-23 respectively), $[LnCNDBM_3(DMF)_2]$ with Ln = Nd^{3+} and Er^{3+} (Figure 5-24 and Figure 5-25) and $[Sm(CNDBM)_4](Et_4N)_2Cl$ (Figure 5-26) varieties.

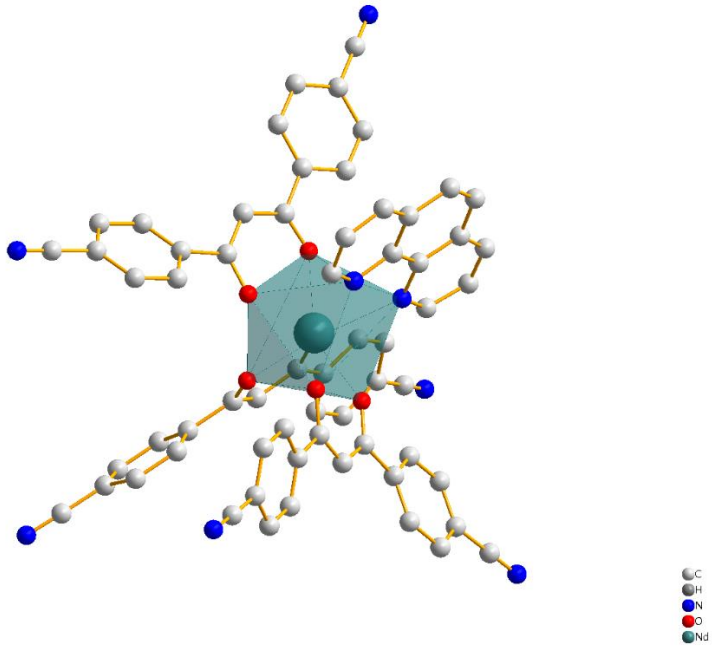

Figure 5-19: Crystal structure of [Nd(CNDBM)$_3$phen]

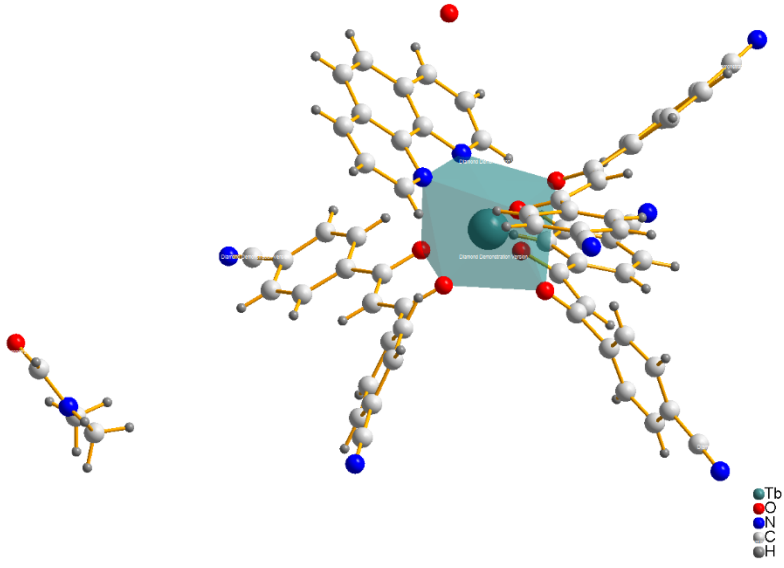

Figure 5-20: Crystal structure of [Tb(CNDBM)$_3$phen]·(DMF)(H$_2$O)

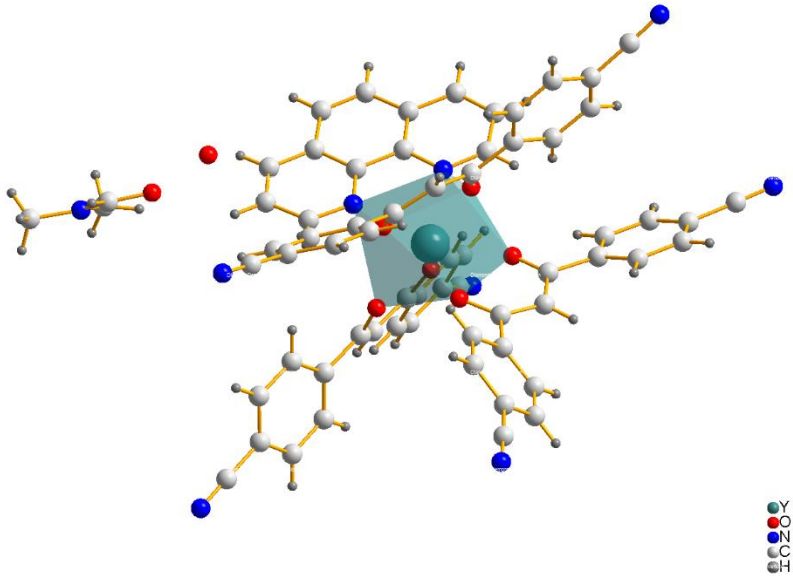

Figure 5-21: Crystal structure of [Y(CNDBM)$_3$phen]·(DMF)(H$_2$O)

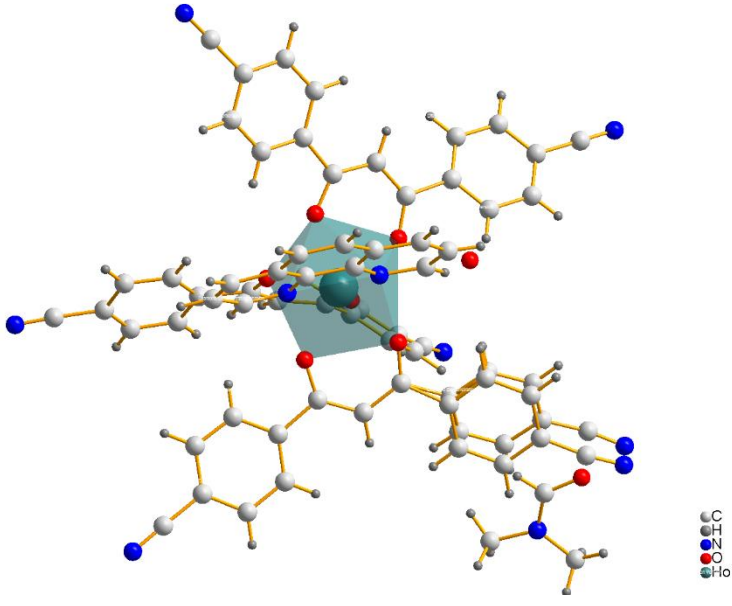

Figure 5-22: Crystal structure of [Ho(CNDBM)$_3$phen]·(DMF)(H$_2$O).
One of the benzene rings is disordered in the crystal structure.

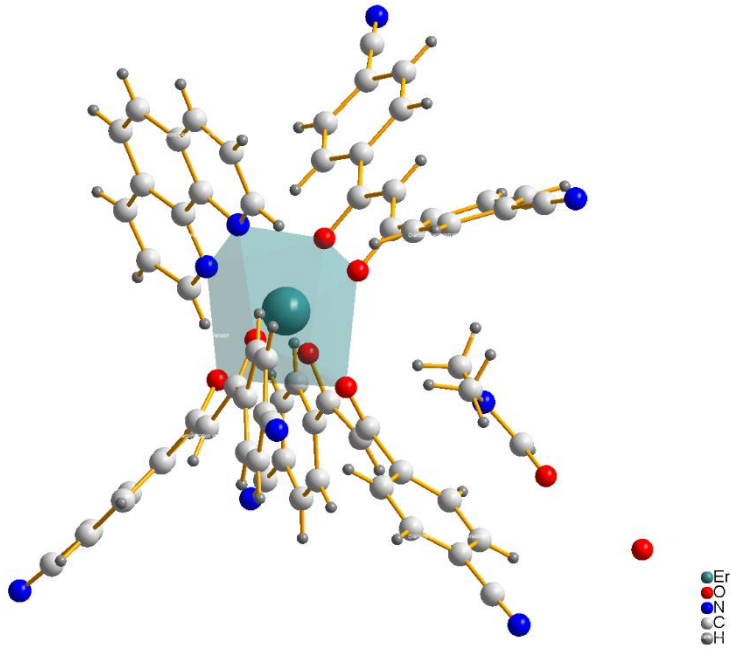

Figure 5-23: Crystal structure of [Er(CNDBM)$_3$phen]·(DMF)(H_2O)

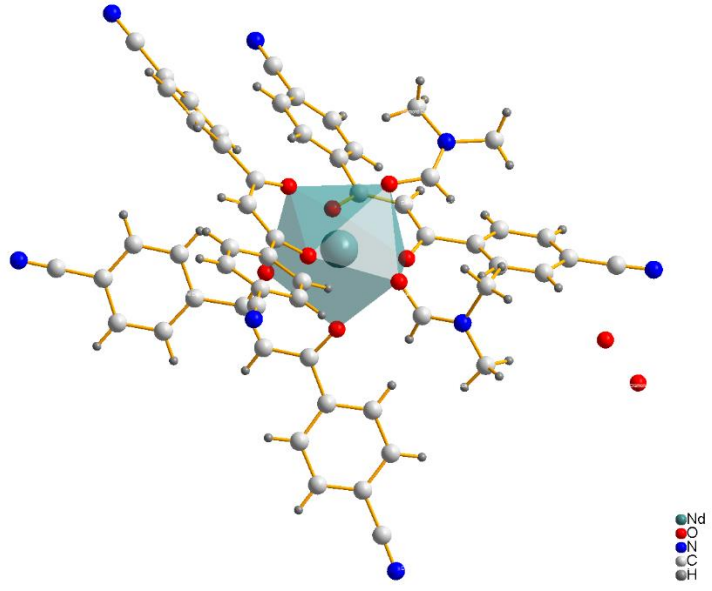

Figure 5-24: Crystal structure of [Nd(CNDBM)$_3$(DMF)$_2$]·H_2O.
The water molecule is disordered in the crystal structure.

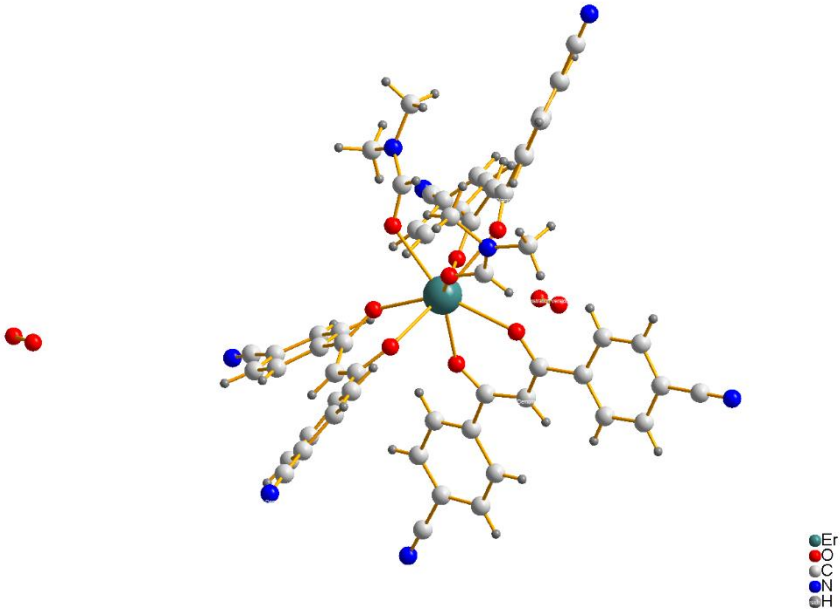

Figure 5-25: Crystal structure of $[Er(CNDBM)_3(DMF)_2]\cdot H_2O$. The water molecule is disordered in the crystal structure.

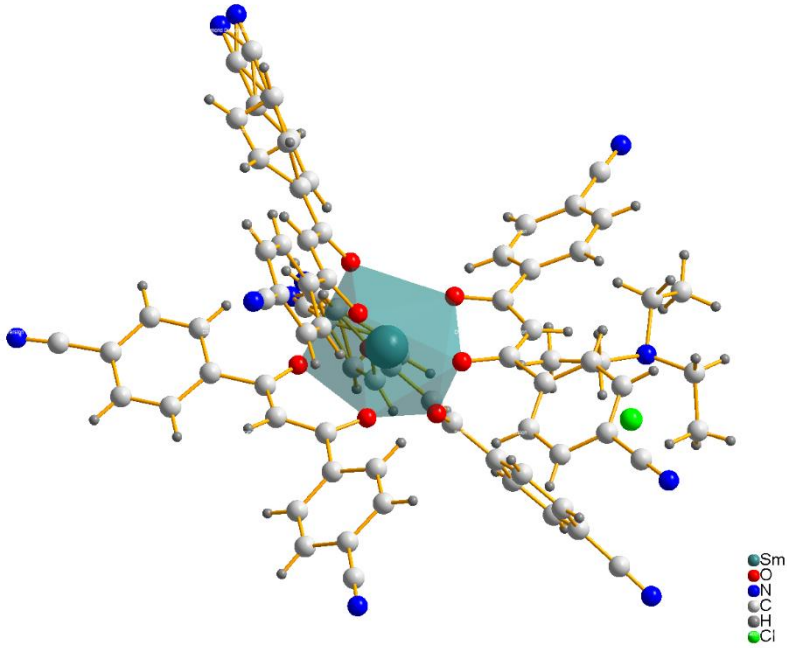

Figure 5-26: Crystal structure of $[Sm(CNDBM)_4](Et_4N)_2Cl$.
One of the benzene rings is disordered in the crystal structure.

The synthesis of clusters was also attempted but this did not yield results.

Crystallographic data on these complexes is found in Table 5-2.

Table 5-2: Crystallographic data of Ln-CNDBM complexes

	[Nd(CNDBM)$_3$phen]	[Tb(CNDBM)$_3$phen]·(DMF)(H$_2$O)
molecular formula	$C_{63}H_{35}N_8NdO_6$	$C_{66}H_{42}N_9O_8Tb$
fw (g mol^{-1})	1144.23	1248.00
cryst dimensions (mm^3)	0.50 x 0.13 x 0.11	0.32 x 0.233 x 0.1963
cryst syst	monoclinic	monoclinic
space group	$P2_1/c$ (No. 14)	$P2_1/c$ (No. 14)
a (Å)	14.9401(7)	14.80525(19)
b (Å)	21.4367(6)	20.9592(3)
c (Å)	17.8516(8)	18.8093(3)
α (deg)	90	90
β (deg)	10.772(4)	102.1800(15)
γ (deg)	90	90
V (Å^3)	5616.5(4)	5705.26(15)
Z	4	4
ρ_{calcd} (g cm^{-3})	1.353	1.453
2θmax (deg)	51.66	58.614
T (K)	150(2)	100.0
F(000)	2308	2520.0
measured reflns	36406	40434
unique reflns	9811	13644
obsd reflns (I > 2σ(I))	8135	10873
params refined	703	759
R1	0.0409	0.0454
wR2	0.0938	0.1126
R1 (all data)	0.0538	0.0625
wR2 (all data)	0.0993	0.1258
GOF	1.066	1.050
μ (mm^{-1})	0.983	1.306

	[Y(CNDBM)$_3$phen]·(DMF)(H$_2$O)	[Ho(CNDBM)$_3$phen]·(DMF)(H$_2$O)
molecular formula	$C_{66}H_{42}N_9O_8Y$	$C_{66}H_{42}HoN_9O_8$
fw (g mol^{-1})	1178.00	1252.85
cryst dimensions (mm^3)	0.4347 x 0.3882 x 0.2356	0.3083 x 0.1270 x 0.0828
cryst syst	monoclinic	monoclinic
space group	$P2_1/c$ (No. 14)	$P2_1/c$ (No. 14)
a (Å)	14.8230(3)	14.8152(4)
b (Å)	20.9857(4)	21.0711(6)
c (Å)	18.7014(4)	18.1605(9)
α (deg)	90	90
β (deg)	102.350(2)	102.043(3)
γ (deg)	90	90
V (Å^3)	5682.8(2)	5544.4(4)
Z	4	4
ρ_{calcd} (g cm^{-3})	1.377	1.434
2θmax (deg)	58.946	58.4928
T (K)	100.0	100(2)
F(000)	2416.0	2405.6
measured reflns	30393	37061
unique reflns	13499	11328
obsd reflns (I > 2σ(I))	9880	
params refined	759	834
R1	0.0584	0.654
wR2	0.1422	0.1388
R1 (all data)	0.0900	0.0805
wR2 (all data)	0.1612	0.1459
GOF	1.025	1.195
μ (mm^{-1})	1.093	1.489

	$[Er(CNDBM)_3phen]\cdot(DMF)(H_2O)$	$[Sm(CNDBM)_4](Et_4N)_2Cl$
molecular formula	$C_{66}H_{42}ErN_9O_8$	$C_{80}H_{66}ClN_{10}O_8Sm$
fw (g mol^{-1})	1256.35	1481.24
cryst dimensions (mm^3)	0.3651 x 0.2314 x 0.1908	0.1887 x 0.1724 x 0.1023
cryst syst	monoclinic	monoclinic
space group	$P2_1/c$ (No. 14)	C2/c (No. 15)
a (Å)	14.8110(2)	19.8912(9)
b (Å)	21.0024(3)	21.6320(7)
c (Å)	18.5898(4)	17.7406(8)
α (deg)	90	90
β (deg)	102.4087(18)	110.833(5)
γ (deg)	90	90
V ($Å^3$)	5647.58(17)	7134.5(6)
Z	4	4
ρ_{calcd} (g cm^{-3})	1.478	1.379
2θmax (deg)	59.066	140.44
T (K)	100.0(1)	100.0(1)
F(000)	2532.0	3036.0
measured reflns	31829	19552
unique reflns	13524	6623
obsd reflns ($I > 2\sigma(I)$)	11083	5603
params refined	759	471
R1	0.0521	0.0411
wR2	0.1222	0.0831
R1 (all data)	0.0674	0.0625
wR2 (all data)	0.1315	0.1069
GOF	1.063	1.127
μ (mm^{-1})	1.553	7.044

	$[Nd(CNDBM)_3(DMF)_2]\cdot(H_2O)$	$[Er(CNDBM)_3(DMF)_2]\cdot(H_2O)$
molecular formula	$C_{57}H_{43}NdN_8O_9$	$C_{57}H_{41}ErN_8O_9$
fw (g mol^{-1})	1126.22	1149.24
cryst dimensions (mm^3)	0.3341 x 0.1758 x 0.1344	0.6163 x 0.2595 x 0.1514
cryst syst	triclinic	triclinic
space group	P-1	P-1
a (Å)	12.9570(9)	12.9747(5)
b (Å)	13.6255(10)	13.5782(7)
c (Å)	17.7436(10)	17.7502(7)
α (deg)	89.302(5)	89.766(4)
β (deg)	73.598(6)	73.479(3)
γ (deg)	80.792(6)	81.067(4)
V ($Å^3$)	2966.1	2959.0(2)
Z	2	2
ρ_{calcd} (g cm^{-3})	1.261	1.290
2θmax (deg)	133.202	133.2
T (K)	293.15	293.15
F(000)	1142.0	1158
measured reflns	24337	23551
unique reflns	10452	10406
obsd reflns ($I > 2\sigma(I)$)	7084	4562
params refined	685	685
R1	0.0604	0.1171
wR2	0.1564	0.2927
R1 (all data)	0.0887	0.1978
wR2 (all data)	0.1797	0.3833
GOF	0.988	1.061
μ (mm^{-1})	7.152	3.107

It is worth noting that the lanthanide ions and the nitrile functions do not come into close proximity of one another, not even in the packing of the crystal structure. This is the case for all reported structures and means that the requirements for a primary building block are fulfilled: a functionalized β-diketonate having lanthanide ions inside and the functionalities pointing outwards.

It could have been otherwise as evidenced by the work of Andrews *et al.*[31] In their article, they use a very similar β-diketone: 1,3-bis(pyridine-4-yl)propane-1,3-dione (BPPD), which can be described as dibenzoylmethane but with pyridine nitrogens on the para positions. When combined with Gd^{3+} in the presence of triethylamine, a coordination polymer is formed. In it, the Gd^{3+} ions are octacoordinated by three times two chelating diketonate oxygens, one water molecule and most importantly, one nitrogen from another BPPD unit.

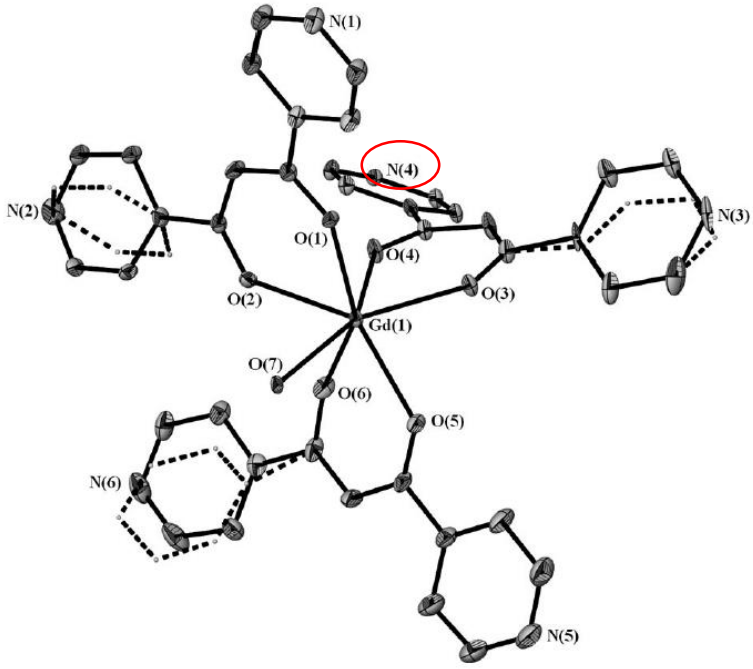

Figure 5-27: Crystal structure of $Gd(BPPD)_3H_2O$ as taken from ref. 31
N(4), red circle, also coordinates to the Gd^{3+} centre after symmetry operations are applied.

This gives rise to one-dimensional chains. Furthermore, the coordinated water molecule participates in two hydrogen bonds with two more pyridyl groups. Together with intermolecular π–π–stacking, this interlocks the chains and creates a threedimensional network.

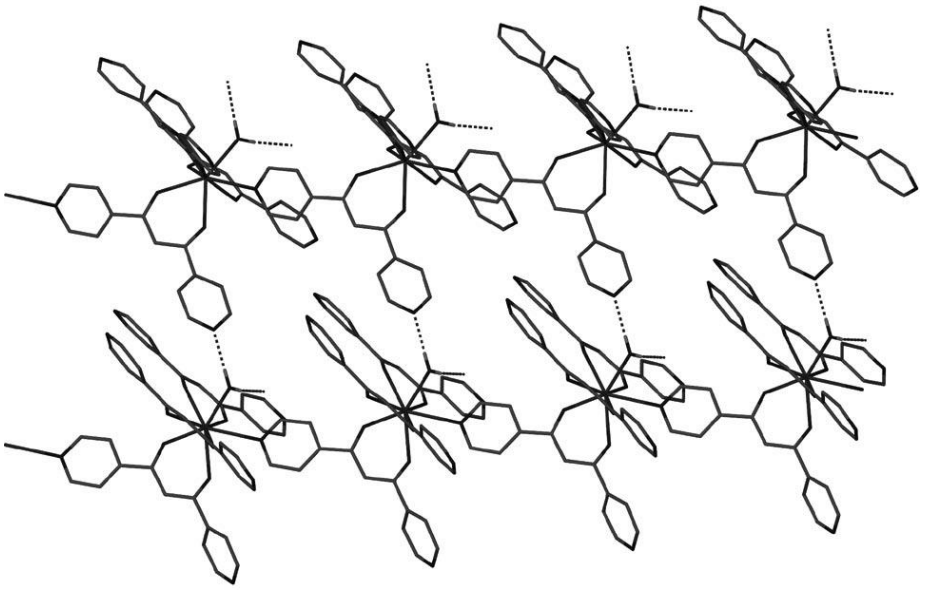

Figure 5-28: Polymeric structure of $Gd(BPPD)_3H_2O$ as taken from ref. 31, all H atoms are omitted except those on the coordinated water molecule

Were this network formation to happen for our particular subject, we would have been able to omit the secondary step using the soft Ag(I) ion and have arrived at the goal of making an extended network. As proven by the crystal structures of the three kinds of mononuclear complexes, this is not the case. The 7th and 8th coordination sites are either taken up by 1,10-phenanthroline, by DMF molecules or by the fourth CNDBM ligand. The cyano groups do not point to the lanthanide ions of neighbouring complexes.

The next step, then, should be the formation of ordered networks. Again, this proved to be the bottleneck in the research. Taking a “soft” metal ion such as Ag(I), dissolving its salt, and mixing this solution with a solution of mononuclear complex should yield, after some time, the desired crystals. Indeed, this did not go as planned, and unidentifiable products were formed.

Trying to find why this failed, one could compare the similar work of Carlucci to our attempts.

Intuitively, the answer lies in the symmetry. In that work, Fe(III), Co(III), Zn(II), Mn(II) and Cd(II) were used as central metal ions. The obtained monomer complexes crystals approximate a D_3 symmetry, putting the CN groups at the vertices of a near-perfect octahedron. This is ideal for combination with silver ions. Since these act as a linear bridging function, not much deviation from "ideal" angles can be tolerated.

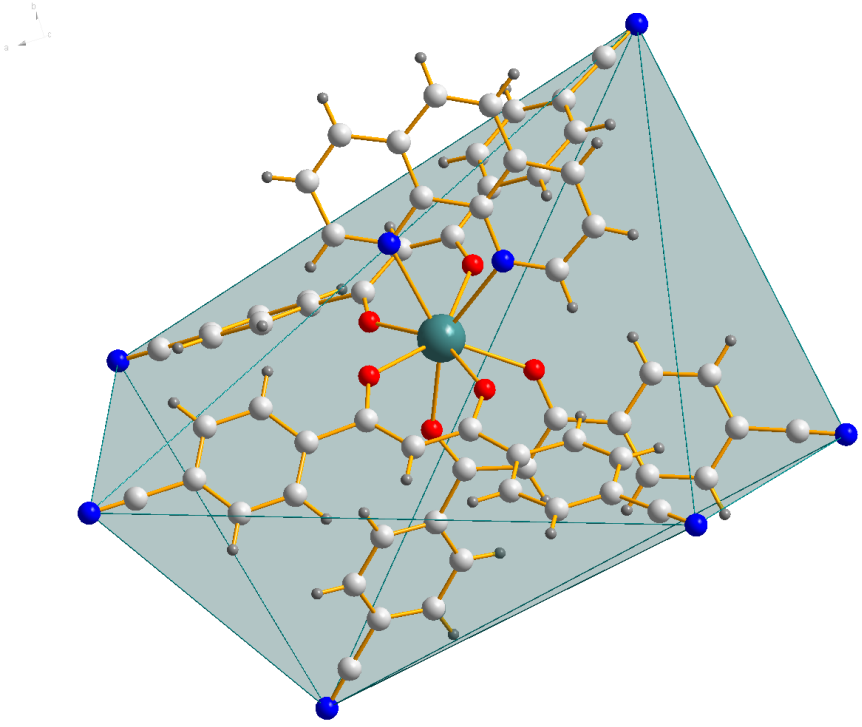

Figure 5-29: Crystal structure of the [Nd(CNDBM)$_3$(phen)] monomer connecting the cyano group nitrogen atoms to form a distorted trigonal antiprismatic polyhedron

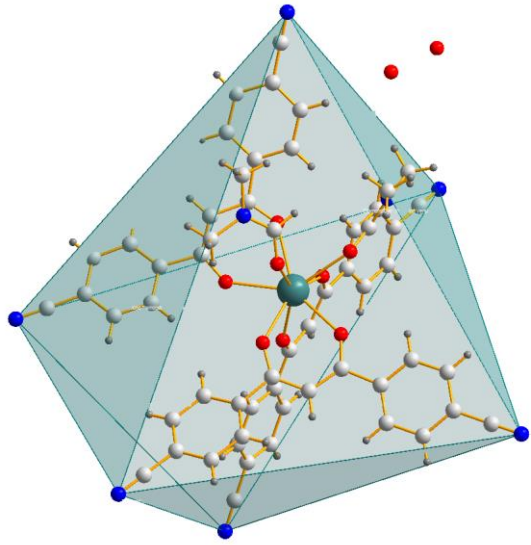

Figure 5-30: Crystal structure of the $[Nd(CNDBM)_3(DMF)_2]\cdot 2H_2O$ monomer, connecting the cyano group nitrogen atoms to form a distorted octahedron

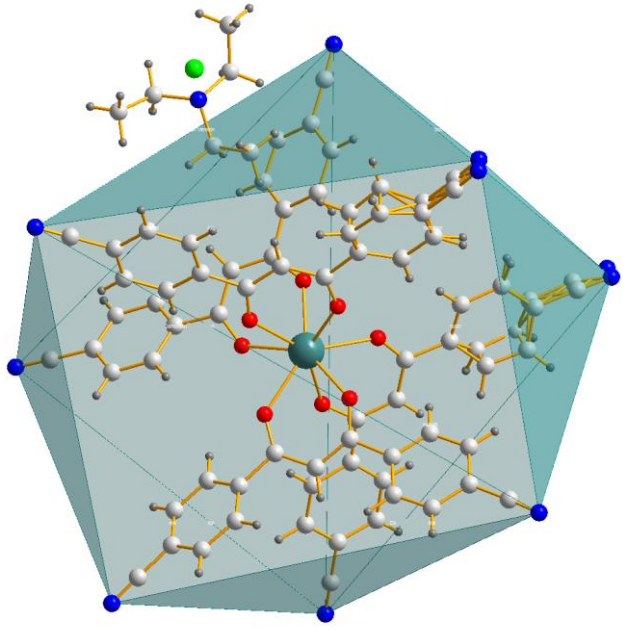

Figure 5-31: Crystal structure of the $[Sm(CNDBM)_4](Et_4N)_2Cl$ monomer, connecting the cyano group nitrogen atoms to form a distorted square antiprismatic polyhedron

Below, the values for cyano N-N-N polyhedron angles (Figure 5-32 and Figure 5-33) and cyano N-N distances (Figure 5-34 and Figure 5-35) from $[Nd(CNDBM)_3(phen)]$, $[Er(CNDBM)_3(phen)]\cdot(DMF)(H_2O)$, $[Nd(CNDBM)_3(DMF)_2]$ and $[Er(CNDBM)_3(DMF)_2]$ are compared with those of the monomers $[Co(CNDBM)_3]\cdot$acetone, $[Zn(CNDBM)_3]NEt_4\cdot CH_2Cl_2$ and $[Cd(CNDBM)_3]NEt_4\cdot CH_2Cl_2$ that have been used to create polymeric networks in the referenced work.

In all of the four following figures, the data is grouped as follows: 1: $[Nd(CNDBM)_3(phen)]$, 2 = $[Er(CNDBM)_3(phen)]\cdot(DMF)(H_2O)$, 3 = $[Nd(CNDBM)_3(DMF)_2]$, 4 = $[Er(CNDBM)_3(DMF)_2]$, 5 = $[Co(CNDBM)_3]\cdot$acetone, 6 = $[Zn(CNDBM)_3]NEt_4\cdot CH_2Cl_2$ and 7 = $[Cd(CNDBM)_3]NEt_4\cdot CH_2Cl_2$. This means that 5, 6 and 7 correspond to transition metal tris-CNDBM complexes.

One can immediately see that the range of N-N-N angles in these last complexes is smaller than that in the lanthanide tris-CNDBM complexes. This is not surprising given the low contribution of 4f-orbitals in coordination geometry, but what it does show is that the distortion from ideal octahedral angles (90° for N-N-N angles for non-face-sharing-edges and 60° for face-sharing N-N-N-angles) is quite significant.

Comparing the N-N-distances is slightly less straightforward due to the difference in ionic radius (even though the values lie within the same order of magnitude), but the same observation holds: the range of N-N distances is again larger in the lanthanide complexes.

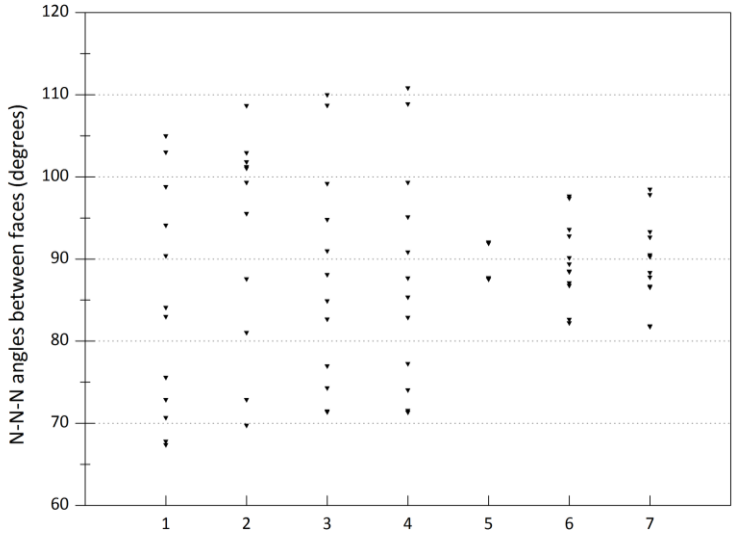

Figure 5-32: Compiled values for N-N-N vertex angles between the faces of the polyhedra obtained by connecting the six cyano-N atoms from seven tris-CNDBM complexes.

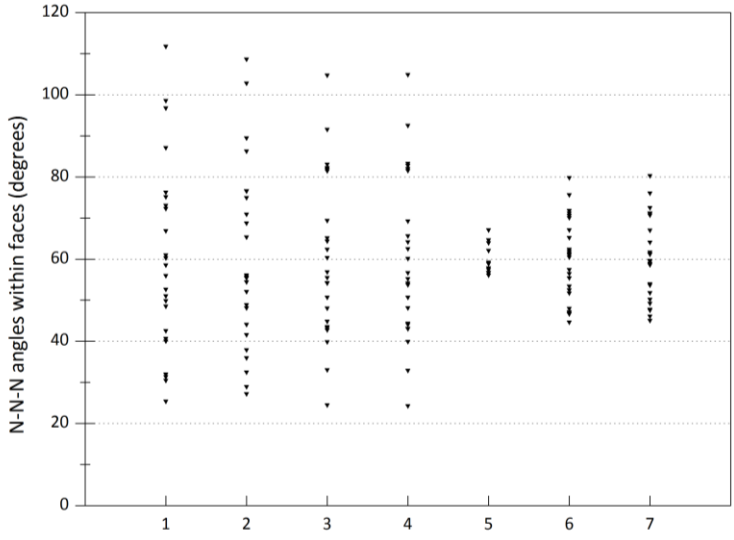

Figure 5-33: Compiled values for N-N-N vertex angles in the faces of the polyhedra obtained by connecting the six cyano-N atoms from seven tris-CNDBM complexes.

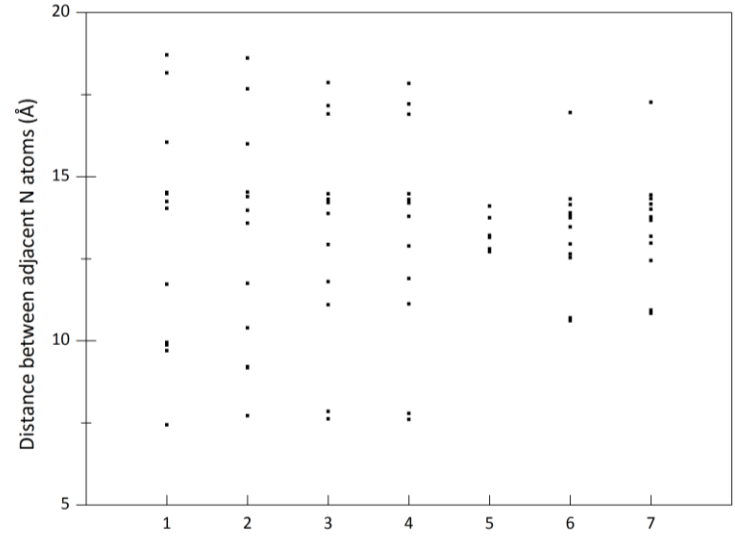

Figure 5-34: Compiled values for distances between edge-sharing N atoms in the polyhedra obtained by connecting the six cyano-N atoms from seven tris-CNDBM complexes

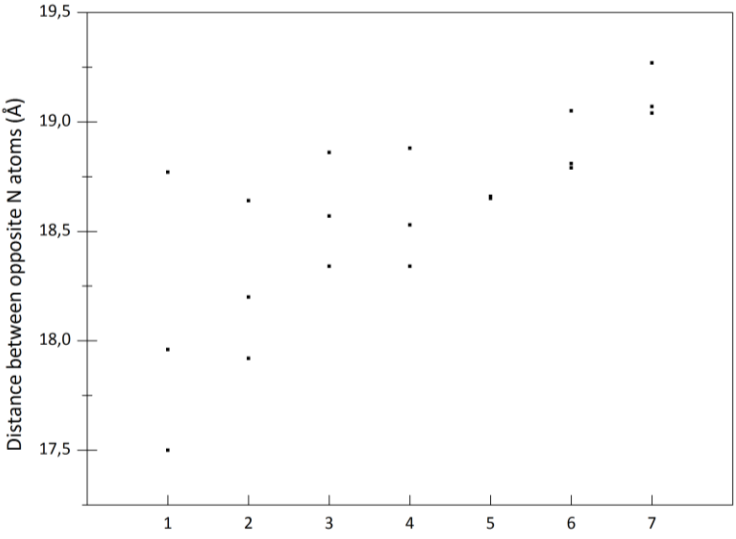

Figure 5-35: Compiled values for distances between opposite N atoms in the polyhedra obtained by connecting the six cyano-N atoms from seven tris-CNDBM complexes

As a result, creating long-range order by combination with linearly connecting soft Ag(I) ions becomes less feasible. In other words: if the building block is as heavily distorted as these prove to be, it does not bode well for the entire building.

5.4 Conclusion and outlook

It seems that the combination of lanthanides and poly-β-diketonates is either very difficult if not impossible to achieve. An attempt to rationalize this has been made. We do believe it remains possible, however to optimize any synthesis that would result in suitable structures is an undertaking that deviates away from design and more towards trial and error.

In a second series of attempts, we have tried to apply a building block approach to the concept, using mononuclear complexes that feature *exo* ligands in order to make heterometallic networks. The synthesis of the building block succeeded, however the assembly into an extended ordered network again proved to be the difficult point. This is perhaps due to the lack of symmetry in this building block. Again, we do believe the idea remains viable, however the exact requirements in terms of conditions but also in terms of structural properties for the building blocks are what need to be determined.

Finding new structures with new ligands has proven to be something that one would need high-throughput equipment for. All too often, we have found that it is a subtle combination of multiple interactions that ultimately lead to crystal formation. Varying all of the relevant parameters for all the described systems would take time, money and luck but it might just be the method that eventually proves to be successful.

5.5 References

[1] Synthesis and Fluorescene of Some Trivalent Lanthanide Complexes, L.R. Melby, N.J. Rose, E. Abramson, J.C. Caris, J. Am. Chem. Soc., **1964**, Vol. 86, p. 5118

[2] Octacoordinate Chelates of Lanthanides. Two Series of compounds, H. Bauer, J. Blanc, D.L. Ross, J. Am. Chem. Soc., **1964,** Vol. 86, p. 5125

[3] RARE-EARTH BETA-DIKETONATES, chapter 225 in the Handbook on the Physics and Chemistry of Rare Earths, K. Binnemans, Vol. 35, **2005**, Elsevier, and all references contained therein

[4] Pentanuclear Dysprosium Hydroxy Cluster Showing Single-Molecule-Magnet Behavior, M.T. Garner, Y. Lan, P.W. Roesky, A.K. Powell, R. Clérac, Inorg. Chem., **2008,** Vol 46, p. 6581

[5] New amino acid ligated yttrium hydroxy clusters, D.T. Thielemann, I. Fernandéz, P.W. Roesky, Dalton Trans**, 2010**, Vol. 39, p. 6661

[6] Lanthanide hydroxide cubane clusters anchoring ferrocenes: model compounds for fixation of organometallic fragments on a lanthanide oxide surface, V. Baskar, P.W. Roesky, Dalton Trans., **2006**, p. 676

[7] Luminescent Cell-Penetrating Pentadecanuclear Lanthanide Clusters, D.T. Thielemann, A.T. Wagner, E. Rösch, D. K. Kölmel, J.G. Heck, B. Rudat, M. Neumaier, C. Feldmann, U. Schepers, S. Bräse, P.W. Roesky, J Am. Chem. Soc., **2013**, Vol. 135, p. 7454

[8] Tetraacetylethane, R.G. Charles, Organic Syntheses, **1963**, Coll. Vol. 4, p. 869

[9] The Conformation of Some 1,1,2,2-Tetraacylethanes in the Solid-State: Crystal-Structures of 1,1,2,2-Tetrabenzoylethane, 1,2-Diacetyl-1,2-Dibenzoylethane and 1,1,2,2-Tetraethoxycarbonylethane, J.R. Cannon, V.A. Patrick, A.H. White, Aus. J. Chem., **1986**, Vol. 39, Issue 11, p. 1811

[10] Some Coordination Polymers Prepared from Bis-ß-Di-ketones, J.S. Oh, J. C. Bailar, Jr., J. Inorg. Nuclear Chem., **1962**, Volume 24, p. 1225

[11] "Coordination Polymers," A Chapter in "Inorganic Polymers, An International Symposium," J.C. Bailar, Jr., p. 51, The Chemical Society, London, **1961**

[12] Metal chelate polymers derived from tetraacetylethane, R. G. Charles, J. Polymer Science, Part A: General Papers, **1963**, Vol. 1, Issue 1, p. 267

[13] Di-, tri- and polynuclear transition metal complexes of 3,4-diacetyl-2,5-hexanedione, A.A.A. Emara, S.M.E. Khalil, K.A.R. Salib, J. Coord. Chem, **1995**, Vol. 36, Issue 4, p. 1995

[14] Syntheses of Nickel(II) Dinuclear Complexes with Tetraketone and the Effect of Anions on Coordination Geometries, Y. Fukuda, K. Mafune, Chem. Lett., **1988**, Vol. 17, Issue 4, 697

[15] Intermolecular versus Intramolecular Exchange Interactions. Magnetic Properties of (Tetraacetylethanato(2-)) bis(*(N,N,N',N'*- tetramethylethylenediamine)copper(II)) Diperchlorate Hydrate (I) and of (Tetraacetylethanato(2-)) bis((N,N,N',N'-tetramethylethylenediamine)copper(II))Bis(tetraphenylborate) Hydrate (II). Crystal and Molecular Structure of I, J.-P. Costes, F. Dahan, J.-P. Laurent, Inorg. Chem. **1992,** Vol. 31, p. 284

[16] X-ray crystal, magnetic and spectroscopic studies of dicopper mixed-ligand complexes containing bridged bis(β-diketonate) and tetramethylethylenediamine ligands, Y.Y. Lim, W. Chen, L.L. Tan, X.Z. You, T.M. Yao, Polyhedron, **1994**, Vol. 13, p. 2861

[17] Synthesis and solvatochromism studies of new mixed-chelate dinuclear copper(II) complexes with different counter ions, H. Golchoubian, E. Razaee, G. Bruno, H.A. Rudbari, Inorg. Chim. Acta, **2011**, Vol. 366, p. 290

[18] Polynuclear Co(II) and Cu(II) Complexes of Tetraacetylethane: $Cu_2(dpa)_2(tae)(O_2CCF_3)_2$, {$[Cu_2(dpa)_2(tae)(4,4'\text{-bipy})](O_2CCF_3)_2$ and $[Co_2(dpa)_4(tae)](O_2CCH_3)_2(H_2O)_2$, dpa = 2,2'dipyridylamine, tae = tetraacetylethane dianion, Y. Zhang, S.R. Breeze, S. Wang, J.E. Greedan, N.P. Raju, L.J. Li, Can. J. Chem., **1999**, Vol. 77, p. 1424

[19] Synthesis, Characterization, and Detailed Electrochemistry of Binuclear Ruthenium(III) Complexes Bridged by Bisacetylacetonate. Crystal and Molecular Structures of [{$Ru(acac)_2$}$_2$(tae)] (acac = 2,4-Pentanedionate Ion, tae = 1,1,2,2-Tetraacetylethanate Dianion), T. Koiwa, Y. Masuda, J. Shono, Y. Kawamoto, Y. Hoshino, T. Hashimoto, K. Natarajan, K. Shimizu, Inorg. Chem., **2004,** Vol. 43, p. 6215

[20] Tetraacetylethane Dianion (Tae) As a Bridging Ligand for Molecular Square Complexes: $Co^{II}_4(Tae)_4(Dpa)_4$, Dpa = Di-2-pyridylamine, a Chiral Molecular Square in the Solid State, Y. Zhang, S. Wang, G.D. Enright, S.R. Breeze, J. Am. Chem. Soc., **1998**, Vol. 120, p. 9398

[21] Synthesis and characterisation of metal–organic frameworks containing bis(β-diketonate) linkers, A.D. Burrows, K. Cassar, M.F. Mahon, S.P. Rigby, J.E. Warren, CrystEngComm, **2008,** Issue 10, p. 1479

[22] Dinuclear Cu(II) Complexes of Isomeric Bis-(3-acetylacetonate)benzene Ligands: Synthesis, Structure, and Magnetic Properties, M. Rancan, A. Dolmella, R. Seraglia, S. Orlandi, S. Quici, L. Sorace, D. Gatteschi, L. Armelao, Inorg. Chem. **2012**, Vol. 51, p. 5409

[23] Bis(*o*-phenylenebis(acetylacetonato))dicopper(II): A Strained Copper(II) Dimer Exhibiting a Wide Range of Colors in the Solid State, C. Pariya, F.R. Fronczek, A.W. Maverick, Inorg. Chem., **2011**, Vol. 50, p. 2748

[24] Copper β-Diketonate Molecular Squares and Their Host–Guest Reactions**,** C. Pariya,C.R. Sparrow, C.-K. Back, G. Sandí, F.R. Fronczek, A.W. Maverick, Angew. Chem. Int. Ed., **2007**, Vol. 46, Issue 33, p. 6305

[25] A templating guest sorts out a molecular triangle from a dimer–trimer constitutional dynamic library, M. Rancan, A. Dolmella, R. Seraglia, S. Orlandi, S. Quici, L. Armelao, Chem. Commun., **2012**, Vol. 48, p. 3115

[26] Dinuclear Complexes and a One-dimensional Chain Involving Difunctional Ligands Containing the Acetylacetonate Functionality, J.B. Lambert, Z. Liu, J. Chem. Cryst., **2007**, Vol. 37, Issue 9, p. 629

[27] Construction of Multi-Dimensional Metal-Organic Framework via Self-Assembly Approach: the Harvest of Interesting Molecular Structures, B.T.N. Pham, **2008**, retrieved from https://tspace.library.utoronto.ca/bitstream/1807/11157/1/Nguyen_Pham_Bich_Tram_200806_MSc._thesis.pdf

[28] Self-assembled Metallo-supramolecular Systems Incorporating β-diketone motifs as Strucutral Elements, D.J. Bray, J.K. Clegg, L.F. Lindoy, D. Schilter, Adv. Inorg. Chem, **2007**, vol. 59, ISSN 0898-8838

[29] Lanthanide and Actinide Chemistry, S. Cotton, **2006**, John Wiley & Sons Ltd., The Atrium, Southern Gate, Chichester, West Sussex PO19, England,

[30] Heterometallic Modular Metal–Organic 3D Frameworks Assembled via New Tris-β-Diketonate Metalloligands: Nanoporous Materials for Anion Exchange and Scaffolding of Selected Anionic Guests, L. Carlucci, G. Ciani, S. Maggini, D.M. Proserpio, M. Visconti, Chemistry Eur. J., **2010**, Vol. 16, Issue 41, p. 12328

[31] Formation of Ho^{III} Trinuclear Clusters and Gd^{III} Monodimensional Polymers Induced by *ortho* and *para* Regioisomers of Pyridyl-Functionalised β-Diketones: Synthesis,

Structure, and Magnetic Properties, P.C. Andrews, G.B. Deacon, R. Frank, B.H. Fraser, P.C. Junk, J.G. MacLellan, M. Massi, B. Moubaraki, K.S. Murray, M. Silberstein, Eur. J. Inorg. Chem., **2009**, Issue 6, p. 744

6 General conclusion and outlook

We have attempted to further the understanding of lanthanide coordination polymers and MOFs in terms of synthesis, structural properties and luminescence activity.

First, a series of compounds where lanthanides were combined with terephthalic acid were synthesized and found to be fit for structural and luminescent analysis. Second, new structures were found with pyridinedicarboxylic acid and analysed as well.

In a third step, luminescent spectra were successfully recorded from two series of synthesized compounds with 2,6-naphthalenedicarboxylic and 1,2-cyclohexanedicarboxylic acid.

Finally, we have taken considerable efforts into creating a binary bis-β-diketonate-based lanthanide coordination polymer using “classical” synthesis methods. This did not produce suitable results. An alternative route was attempted via a building block approach, using monomeric lanthanide β-diketonate complexes with functional exo ligands that could coordinate to a second ion in order to create a ternary network. The construction of the monomers was successful, the formation of networks once again proved to be the bottleneck. We have tried to rationalize these failures.

For future research into the topic of lanthanide poly-β-diketonate networks I would strongly advise using a top quality high-throughput synthesis setup. The term “trial and error” contains only three words and “success” is not one of them, to achieve it one should at least minimize the effort spent on “trial” in order to reduce the frustration that comes with perpetual “error”.

7 Instrumental and experimental

7.1 Instrumental

Listed here are the used apparati for structural determination and characterization. For a detailed description of the advantages of the techniques, refer to the chapter on terephthalates.

For X-ray single crystal analysis, X-ray intensity data were collected at 100 K on a Agilent SuperNova dual source diffractometer equipped with an Atlas CCD detector using Mo Kα radiation (λ = 0.710 73 Å), and ω scans. The images were interpreted and integrated with the program CrysAlis PRO from Agilent Technologies[1]. The structures were solved by direct methods and refined by full-matrix least-squares on F^2 using the SHELXTL program package[2].

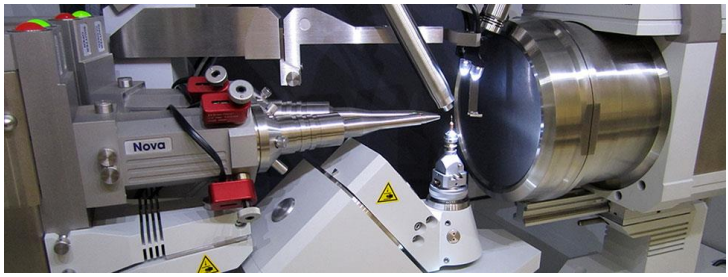

Figure 7-1: Sample chamber for single crystals. Left: dual source, middle bottom: rotating goniometer with mounted crystal, middle top: cooling jet, right: detector

Typically, a single crystal was fixed on a silicon loop using parabar (previously known as paratone) as cryoprotectant. The mounted crystal was then manually aligned and the data was recorded if the crystal was of sufficient quality.

For X-ray powder diffraction, diffractograms were taken on a powder diffractometer type ARL X'TRA (Thermo Scientific) equipped with a Cu Kα (λ = 1.5405 Å) tube, goniometer, and Peltier cooled Si(Li) solid state detector in the 2θ region 5−50°.

Figure 7-2: Powder diffractometer

For luminescence experiments, steady state emission and excitation measurements were performed on an Edinburgh Instruments FLSP920 UV−VIS−NIR spectrometer, using a 450 W Xenon lamp as the steady state excitation source, a Hamamatsu R928P PMT detector for the visible range, and a Hamamatsu R5509-72 NIR PMT detector for the near-infrared (NIR) range. The emission spectra have been corrected for the detector response and the excitation spectra for the lamp spectrum. Solid powdered samples were put inbetween quartz plates (Starna cuvettes for powdered samples, type 20/C/Q/0.2). Lifetime measurements were done with a 60 W Xenon microsecond flash lamp, operating at a pulse frequency of 100 Hz, or with a Continuum Surelite I-10 Nd:YAG laser (450 mJ @ 1064 nm), using the third harmonic (355 nm), operating at a

pulse frequency of 10 Hz. Typically, a small amount of crystalline powder was clasped between the quartz plates and then brought into the sample chamber. After aligning the sample with the emission monochromator, the data were recorded.

Figure 7-3: Setup for Luminescence with double sample chamber: one for VIS and NIR detectors (left) and the other for IR detectors (right)

Figure 7-4: Nd:YAG laser (left), harmonics selection (middle), optically pumped parameter oscillator (OPO, right)

For IR analysis, FTIR measurements were done with a Bruker Equinox 55 FTIR spectrometer equipped with a DRIFTS-cell. All samples were recorded with a 2 cm^{-1} step size in the 4000−650 cm^{-1} range. Typically, a measurement was preceded by a KBr

powder background spectrum measurement as reference, after which the powdered sample was layered on top of the KBr background layer.

For porosity and internal surface determination, a Micromeritics Tristar 300 surface area and porosity analyzer was employed. Typically, 5 mg of powder was used.

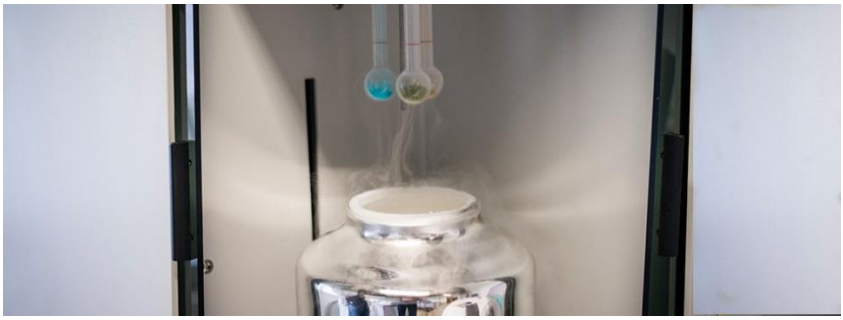

Figure 7-5: Sorption equipment:

For elemental analysis, a Thermo Scientific Interscience Flash 2000 organic elemental analyzer was available. Typically 2.5 mg of sample was placed into an Ag cup mixed together with a V_2O_5 catalyst.

Figure 7-6: Elemental Analyzer

7.2 Experimental

7.2.1 Compounds with BDC

$Pr(NO_3)_3 \cdot 6H_2O$ (130.5 mg, 0.30 mmol) and 1,4-H_2BDC (48 mg, 0.30 mmol) were dissolved in a solvent mixture of DMF (30 mL), H_2O (6 mL), and EtOH (6 mL) at room temperature. Six drops (about 0.15 mL) of TETA were added to this mixture. HNO_3 (6 mol·L^{-1}) was then added (about 0.5 mL) until the mixture became clear (the solution pH was then about 8). The resulting mixture was left undisturbed at 60 °C for 7 days, after which it was filtered and washed with DMF (10 mL) and THF (10 mL) to yield a green crystalline powder. The yield was 37.4% based on Pr. Anal. Calcd for $C_{33}H_{33}N_3O_{16}Pr_2 \cdot H_2O$: C, 38.58; H, 3.43; N, 4.09%. Found: C, 38.64; H, 3.36; N, 4.63%. The syntheses for the Nd, Sm and Eu homologues follow the same procedure except that the corresponding lanthanide nitrate salt was used: $Nd(NO_3)_3 \cdot 6H_2O$ (131.5 mg, 0.30 mmol), $Sm(NO_3)_3 \cdot 6H_2O$ (133 mg, 0.30 mmol) and $Eu(NO_3)_3 \cdot 5H_2O$ (128 mg, 0.30 mmol). For $C_{33}H_{33}N_3O_{16}Nd_2 \cdot H_2O$ the yield of violet crystalline powder was 39.1% based on Nd. Anal. Calcd: C, 38.33; H, 3.41; N, 4.06%. Found: C, 38.42; H, 3.42; N, 4.65%. For $C_{33}H_{33}N_3O_{16}Sm_2 \cdot 2.5H_2O$ the yield was 27.6% based on Sm. Anal. Calcd: C, 36.92; H, 3.57; N, 3.91%. Found: C, 36.33; H, 2.99; N, 4.10%. For $C_{33}H_{33}N_3O_{16}Eu_2 \cdot H_2O$ the yield of white crystalline powder, from which crystals suitable for single crystal X-ray diffraction were harvested, was 42.6% based on Eu. Anal. Calcd: C, 37.76; H, 3.36; N, 4.00%. Found: C, 37.33; H, 2.96; N, 3.52%.

The Lu-BDC compound was obtained in slightly different manner: 1,4-H_2BDC (0,1 mmol, 16 mg) and $Lu(NO_3)_3 \cdot 5H_2O$ (0.1 mmol, 43 mg) were dissolved into a mixture of 10 mL

DMF and 4 mL H_2O. Two drops of triethylamine were added. The solution was stirred, a white flaky solution was obtained. Drops of 6 $mol \cdot L^{-1}$ nitric acid were added until the solution became clear. This clear solution was kept at 55°C for seven days, upon which white crystalline powders precipitated. The precipitate was washed with DMF and filtered off. For $LuC_{19}H_{21}NO_{12}$ the yield was 50% based on Lu. Anal. Calc.: C, 36.17; H, 1.75; N, 2.38%. Found: C, 35.47; H, 2.61; N, 2.64%.

7.2.2 Compounds with PDC

To synthesize the Nd-PDC compounds, $Nd(NO_3)_3 \cdot 6H_2O$ (131 mg, 0.30 mmol) and 2,5-H_2PDC (75 mg, 0.45 mmol) were mixed within 5 mL of H_2O. After stirring for 30 min, the mixture was placed in a 100 mL Teflon lined reactor and heated at 160°C in an oven for 3 days. Afterward the resulting solution was slowly cooled to room temperature at 0.1 °C min^{-1}. Filtration and washing with H_2O provided the brown crystals suitable for single-crystal X-ray diffraction analysis. The yield was 43.3% based on Nd. Anal. Calcd for $C_{14}H_7N_2O_8Nd \cdot H_2O$: C, 34.08; H, 1.84; N, 5.68%. Found: C, 34.50; H, 1.45; N, 5.85%.

For the Lu-PDC network, H_2PDC (0,1 mmol, 17 mg) and $Lu(NO_3)_3 \cdot 5H_2O$ (0.05 mmol, 22 mg) were mixed in H_2O (5 mL) in a pyrex test tube of 15 mL and kept at 160°C during three days. Afterwards the solution was allowed to cool to room temperature at 10°C $hour^{-1}$.

7.2.3 TAE

The synthesis route followed was practically identical to the one describes by Charles *et al.*[3] First, Na(acac) is made. Afterwards, two Na(acac) entities are coupled by iodine reduction.

NaOH (40 g, 1 mole) is dissolved in 50 mL H_2O. To this solution is added 200 mL MeOH. This solution is added dropwise, with stirring, to pure acetylacetone (100 g, 1 mole). White precipitation occurs immediately. The flask is cooled overnight, after which the sodium salt is filtered off and washed with cold methanol. The product is dried in the vacuum oven.

Na(acac) (24.4 g, 0.2 mol) is ground to a fine powder and brought into 300mL diethylether. A solution of iodine (25.4 g, 0.1 mole) in 300 mL of diethylether is added dropwise to the Na(acac) solution with vigorous stirring. The ether is allowed to evaporate overnight. The NaI is extracted by addition of 500 mL H_2O. This solution is filtered and recrystallized with MeOH.

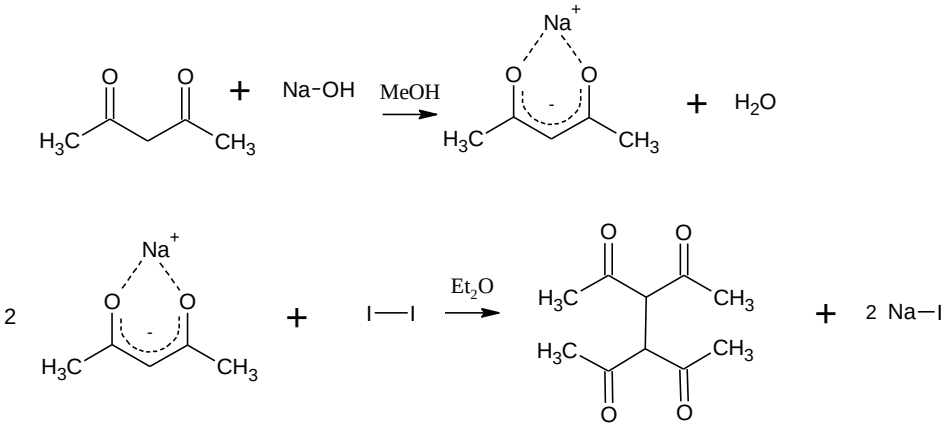

Figure 7-7: Reaction scheme for the synthesis of TAE

7.2.4 BAB

Under nitrogen, butanedione (biacetyl, 8.7 mL, 0.1 mol) and trimethylphosphite (14.85 g, 0.126 mol) are mixed to obtain 2,2,2-trimethoxy-4,5-dimethyl-1,3-dioxaphospholene[4,5,6,7]. The solution is transferred to a dichloromethane solution (20 mL) of terephthaldehyde (6.7 g, 0.05 mol) and stirred for 10 hours. Additional dichloromethane (20 mL) is added, and the solution is again stirred for 16 hours. The solvent is rotary evaporated and the residu dried in the vacuum oven. The solid is brought in MeOH (50 mL), stirred at reflux for 3 hours and filtered off after cooling. The product is then recrystallized from a fresh batch of MeOH.

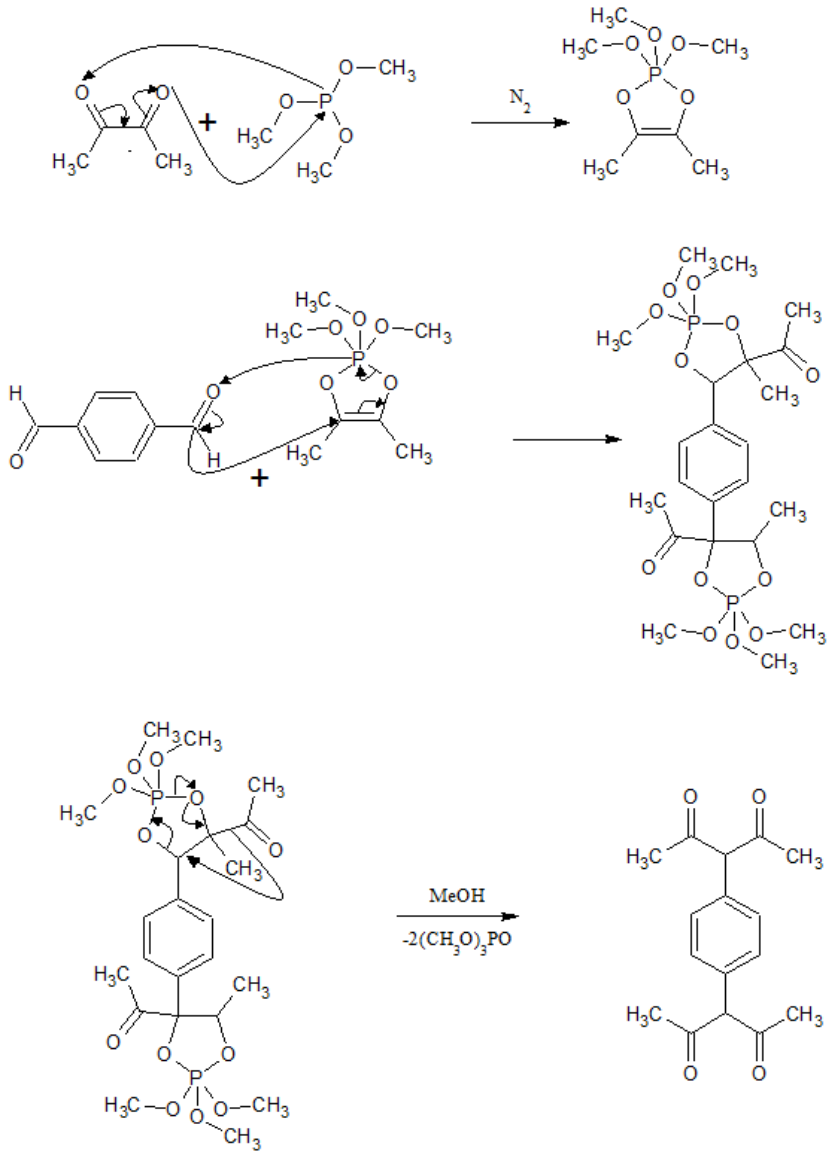

Figure 7-8: Reaction scheme and suggested mechanism for the synthesis of BAB

7.2.5 Synthesis of the HCNDBM ligand

Anhydrous THF (32 mL) was added under nitrogen to NaH (60% dispersion in mineral oil, 1.383 g, 34.58 mmol). After cooling to 0°C, 4-acetylbenzonitrile (1.652 g, 11.38 mmol) was added to the slurry. After addition, a solution of methyl 4-cyanobenzoate (2.013 g,

12.49 mmol) in anhydrous THF (8 mL) was slowly added. The solution was refluxed for 16 hours and quenched with ice. After this, 0.1 mol·L^{-1} HCl was added, upon which the ligand precipitated as a pale yellow solid, which was recovered by filtration.

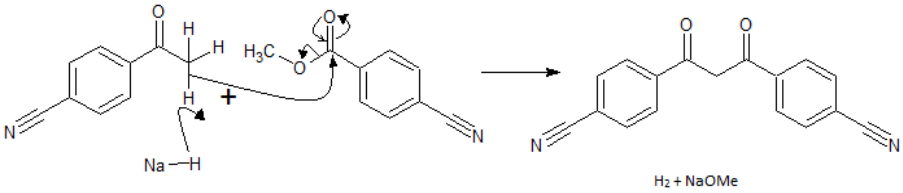

Figure 7-9: Synthesis and mechanism thereof of the CNDBM ligand

7.2.6 Synthesis of the CNDBM complexes

7.2.6.1 [Ln(CNDMB)$_3$(phen)]·solv

In a typical synthesis, the HCNBDM ligand (0.45 mmol, 125 mg) was dissolved in 15 mL warm MeOH. 1,10-phenanthroline (0.15 mmol, 27 mg) was added to this solution. A methanolic solution of NaOH (0.5 mL, 1 mol·L^{-1}) was added, the solution turned dark red. Dropwise and with stirring, a methanolic solution of hydrated Ln(NO$_3$)$_3$ was added (5 mL, 0.03 mol·L^{-1}). Pale yellow precipitation occurred during addition. When addition was complete, the solution was left to stir for 1 more hour. Afterwards, the pale yellow powder was filtered off and washed with MeOH and THF. For crystallization, the powder was dissolved in DMF, and the vial with this solution was placed in a larger vial that contained H_2O. Yellow crystals suitable for X-ray single crystal diffraction analysis formed within a week.

7.2.6.2 [Ln(CNDMB)$_3$(DMF)$_2$]·solv

In a typical synthesis, the CNBDM ligand (0.45 mmol, 125 mg) was dissolved in 15 mL warm MeOH. A methanolic solution of NaOH (0.5 mL, 1 mol·L^{-1}) was added, the solution turned dark red. Dropwise and with stirring, a methanolic solution of hydrated Ln$(NO_3)_3$ (5 mL, 0.03 mol·L^{-1}) was added. Pale yellow precipitation occurred during addition. When addition was complete, the solution was left to stir for 1 more hour. Afterwards, the pale yellow powder was filtered off and washed with H_2O, MeOH and THF. For crystallization, the powder was dissolved in DMF, and the vial with this solution was placed in a larger vial that contained H_2O. Yellow crystals suitable for X-ray single crystal diffraction analysis formed within a week.

7.2.6.3 [Ln(CNDBM)$_4$](Et$_3$NH)$_2$Cl

For this synthesis, we modified the reported synthesis of the triboluminescent [Eu(DBM)$_4$]Et$_3$NH complex[8]. The CNDBM ligand (0.60 mmol, 165 mg) was dissolved in a 60°C solution of 25 mL EtOH. Dropwisely, an ethanolic solution of hydrated $LnCl_3$ was added (5 mL, 0.03 mol L^{-1}). Then Et_3N (0.5 mL) was added to the mixture. The precipitates that formed were filtered off and recrystallized from EtOH.

7.3 References

[1] CrysAlis PRO, Version 1.171.36.32; Agilent Technologies UK Ltd: Yanton, U.K

[2] SHELXS, Sheldrick, G. Acta Cryst. **2008**, A64, 112-122

[3] Tetraacetylethane, R.G. Charles, Org. Synth. **1959**, 39, 61

[4] A Cyclic Saturated Pentaalkoxyphosphorane, Diketols via Oxyphosphoranes, F. Ramirez, N. Ramanathan, N.B. Desai, J. Am. Chem. Soc., **1962**, Vol. 84, Issue 7, p. 1317

[5] Flavoring Ingredients, U.S. Patent, no. US 7,794,767 B2, R. Naef, A. Jaquier, **2010**

[6] Molecular Rearrangements during Solvolyses of Pentaoxyphosphoranes. Polyketones Derived from Phthalaldehyde and Terephthaldehyde, F. Ramirez, S.B. Bathia, A.V. Patwardhan, C.P. Smith, J. Org. Chem., **1967**, Vol. 32, Issue 11, p. 3547

[7] Dinuclear Cu(II) Complexes of Isomeric Bis-(3-acetylacetonate)benzene Ligands: Synthesis, Structure, and Magnetic Properties, M. Rancan, A. Dolmella, R. Seraglia, S. Orlandi, S. Quici, L. Sorace, D. Gatteschi, L. Armelao, Inorg. Chem. **2012**, Vol. 51, p. 5409, supporting information

[8] Luminescent properties of lanthanide dibenzoylmethide triethylammonium compounds, R. S. Fontenot, W.A. Hollerman, K.N. Bhat, S.W. Allison, M.D. Aggarwal, J. Theor. Appl. Phys., **2013,** Vol. 7, Issue 30

8 Acronyms, abbreviations, figures and tables

8.1 List of abbreviations

1,4-PDA	1,4-phenylenediacetic acid
acac	acetylacetone
ADP	adipic acid
BABP	3,3'-(biphenyl-4,4'-diyl)-dipentane-2,4-dione
BET-analysis	internal surface determination technique based on Brunauer-Emmett-Teller-theory
bipy	bipyridine
BPPD	1,3-bis(pyridine-4-yl)propane-1,3-dione
BTEC	1,2,4,5-benzenetetracarboxylic acid
CNDBM	1,3-bis(4'-cyanophenyl)-1,3-propanedione
CTAB	cetyltrimethylammoniumbromide
dbm	dibenzoylmethane
DEF	N,N-diethylformamide
DMA	N,N-dimethylacetamide
DPA	dipyridylamine
$EMIM^+$	1-ethyl-3-methylimidazolium ion
H_2BDC	benzenedicarboxylic acid (terephthalic acid)
H_2CDC	1,2-cyclohexanedicarboxylic acid
H_2NDC	2,6-naphthalenedicarboxylic acid
H_2PDC	2,5-pyridinedicarboxylic acid
H_3BTC	benzenetricarboxylic acid
HBC	benzenecarboxylic acid
HKUST-1	the MOF with Cu^{2+} and benzenetricarboxylic acid, made in Hong Kong University of Science and Technology

HMT	hexamethylenetetramine
HSAB	hard-soft acid base
Ln	any lanthanide (usually specified in text)
MAUD	Material Analysis Using Diffraction, name of the Rietveld refinement program
MIL	Materials of Institut Lavoisier
MOF	metal-organic framework
MOF-5	the MOF with Zn_4O clusters and terephthalic acid
MWAS	microwave assisted synthesis
NIC	nicotinic acid
phen	1,10-phenanthroline
phpa	dipivaloylmethanate
S_0, S_1	ground singlet state, first excited singlet state
salen	the condensate of salicylaldehyde and ethylenediamine
SUC	succinic acid
T_0, T_1	ground triplet state, first excited triplet state
TAE	1,1,2,2-tetraacetylethane
TAE	1,4-bis-(3-acetylacetone)-benzene
TMED	N,N,N',N'-tetrametylethylenediamine

8.2 List of Figures

8.3 List of Tables

9 List of articles

Redetermination of $[Pr(NO_3)_3(H_2O)_4]\cdot 2H_2O$
R. Decadt, P. Van Der Voort, I. Van Driessche, R. Van Deun, K. Van Hecke, Acta Cryst., **2012**, E68, i59-i60.

Synthesis, crystal structures, and luminescence properties of carboxylate based rare-earth coordination polymers
R. Decadt, K. Van Hecke, D. Depla, K. Leus, D. Weinberger, I. Van Driessche, P. Van Der Voort, R. Van Deun, Inorg. Chem., **2012**, 51, 11623-11634.

Bipyridine based nanosized Metal-Organic Framework with tuneable luminescence by a postmodification with Eu(III): an experimental and theoretical study
Y.-Y. Liu, **R. Decadt**, T. Bogaerts, K. Hemelsoet, A. M. Kaczmarek, D. Poelman, M. Waroquier, V. Van Speybroeck, R. Van Deun, P. Van Der Voort, J. Phys. Chem. C, **2013**, 117, 11302-11310.

Syntheses, structures, properties and DFT study of hybrid inorganic–organic architectures constructed from trinuclear lanthanide frameworks and Keggin-type polyoxometalates
M. Mirzaei, H. Eshtiagh-Hosseini, N. Lotfian, A. Salimi, A. Bauzá, R. Van Deun, **R. Decadt**, M. Barceló-Oliver, A. Frontera, Dalton Trans., **2014**, 43, 1906-1916.

10 Nederlandse samenvatting

10.1 Inleiding en doelen

Coördinatiepolymeren zijn, ruw omschreven, materialen waarin discrete metaalionen of metalloclusters aan elkaar gekoppeld worden door organische liganden. Dit kan aanleiding geven tot een geordende structuur in 1, 2 of 3 dimensies, waarbij de anorganische ionen en de organische linkermoleculen resp. een keten, een vlak of een raamwerk vormen.[1]

De virtueel oneindige mogelijkheden van deze groep materialen komt uit de mogelijkheid tot variatie van de identiteit van de metalen, de geometrie waarin ze gecoördineerd worden, en de identiteit van de organische groepen.

Deze thesis had als doel het synthetiseren van nieuwe materialen in deze klasse met lanthanide-ionen als keuze voor de metalen. Lanthaniden zijn, zonder veel in detail te gaan, in vele opzichten verschillend van transitiemetaalionen.[2] Door hun elektronische structuur vertonen zij een onvoorspelbare coördinatiechemie die gebaseerd is op elektrostatische aantrekking en sterische hinder, niet zozeer op interactie van donor-acceptor orbitalen. De reden daarvoor is dat de elektronen binnenin de 4f-schil afgeschermd van de omgeving, wat bovendien aanleiding geeft tot scherp gedefinieerde pieken in de excitatie- en emissie-spectra. De energieën die gepaard gaan met deze transities zijn afhankelijk van het type lanthanide en kunnen in het NIR, UV of zichtbare gebied van het elektromagnetisch spectrum liggen. Lanthaniden verwerken in

coordinatiepolymeren zou, in sommige gevallen, de luminescentie ten goede moeten komen omwille van de rigiditeit van de matrix.[3]

In een eerste fase trachtten we nieuwe structuren gebaseerd op bestaand werk te verkrijgen door als organische linker te kiezen voor 1,4-benzeendicarboxylaat (BDC^{2-}) en 2,5-pyridinedicarboxylaat (PDC^{2-}), beide commercieel verkrijgbaar en goed bestudeerd. Het voornaamste doel was het achterhalen van nieuwe kristalstructuren.[4]

In een volgende stap werd de luminescentie van dergelijke structuren gemeten en gepoogd om deze terug te koppelen aan hun structurele eigenschappen.

Het voornaamste doel was het synthetiseren en karakteriseren van lanthanide-gebaseerde coordinatiepolymeren waarbij de β-diketonaat-functionaliteit dienst deed als ligand, voor zowel binaire netwerken waarin het lanthanide-ion gecombineerd werd met een bifunctionele linker, als ternaire netwerken die volgens een bouwsteen-benadering samengesteld zijn.

10.2 Bespreking

Vijf nieuwe structuren met BDC^{2-} werden gesynthetiseerd. Daarvan waren er twee die éénkristallen vormden van voldoende kwaliteit om via éénkristal-X-straaldiffractie hun structuur te achterhalen. Van deze twee zijn de formules $Eu_2(BDC)_3(DMF)_2(H_2O)\cdot DMF$ (**1**) en $Lu_2(BDC)_3(DMF)_3(H_2O)_2$ (**2**).

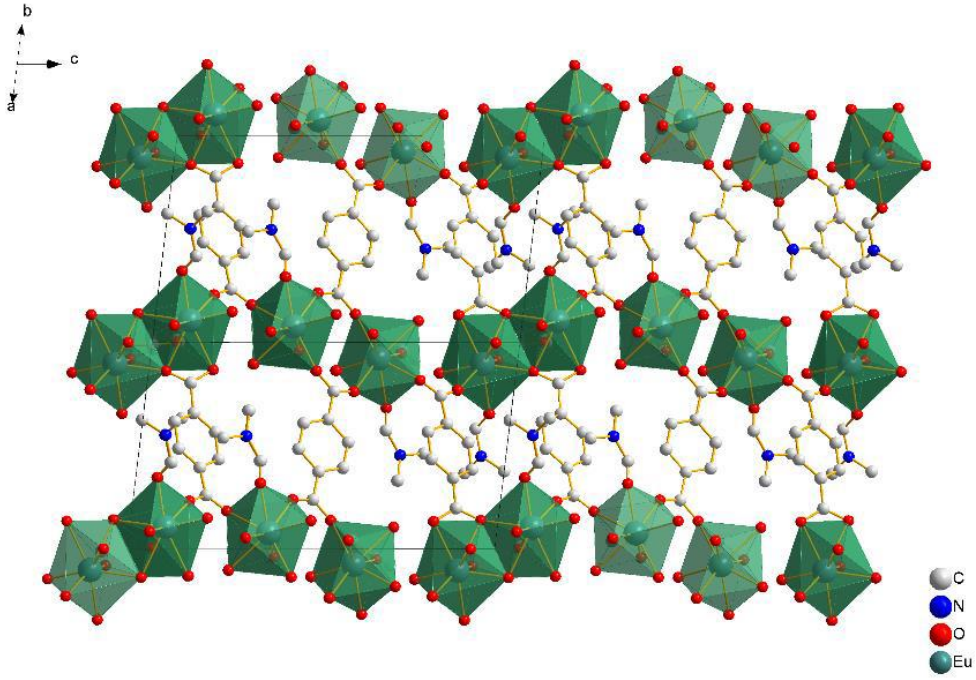

Kristalstructuur van $Eu_2(BDC)_3(DMF)_2(H_2O)\cdot DMF$

Drie structuren analoog aan **1** werden gesynthetiseerd op dezelfde manier behalve dat in plaats van europium(III)nitraat the nitraatzouten van praseodymium(III), neodymium(III), en samarium(III) gebruikt werden om structuren met formules resp. $Pr_2(BDC)_3(DMF)_2(H_2O)\cdot DMF$ (**3**) $Nd_2(BDC)_3(DMF)_2(H_2O)\cdot DMF$ (**4**) en $Sm_2(BDC)_3(DMF)_2(H_2O)\cdot DMF$ (**5**) te bekomen. Hun kristalstructuur werd niet achterhaald maar door middel van Rietveldverfijning werd aangetoond dat zij een gelijkaardige eenheidscel bezitten en dus een gelijkaardige kristalstructuur.

Van **1**,**3**, **4** en **5** werd vervolgens de luminescentie opgemeten. De resultaten daarvan liggen in de verwachtingen en vergelijken positief met literatuurwaarden.

label	λ (nm)	ῡ (cm^{-1})	transitie
a	362.1	27620	$^5D_4 \leftarrow {}^7F_0$
b	367.0	27250	$^5D_4 \leftarrow {}^7F_1$
c	375.4	26640	$^5G_4 \leftarrow {}^7F_0$
d	380.6	26275	$^5G_2 \leftarrow {}^7F_0$
e	385.4	25950	$^5G_2 \leftarrow {}^7F_1$
f	394.4	25355	$^5L_6 \leftarrow {}^7F_0$
g	416.4	24015	$^5D_3 \leftarrow {}^7F_1$

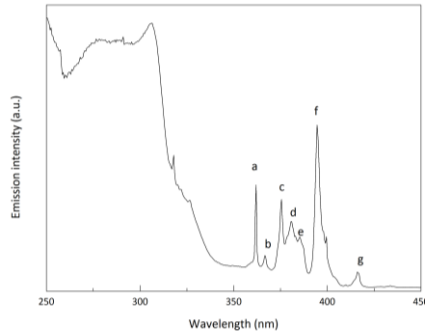

label	λ (nm)	ῡ (cm^{-1})	transition
De transitie gelabeld met * is te wijten aan Tb contaminatie van de kuvet.			
a	579.0	17270	$^5D_0 \rightarrow {}^7F_0$
b	592.5	16880	$^5D_0 \rightarrow {}^7F_1$
c	616.0	16235	$^5D_0 \rightarrow {}^7F_2$
d	652.3	15330	$^5D_0 \rightarrow {}^7F_3$
e	700.0	14285	$^5D_0 \rightarrow {}^7F_4$

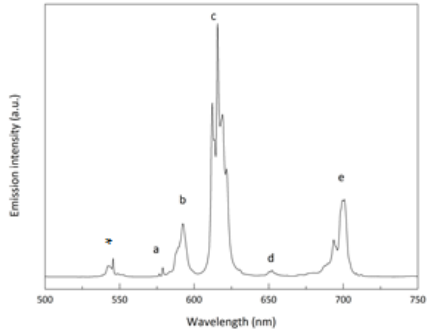

Excitatie- (bovenaan) en emissiespectra (onderaan) van $Eu_2(BDC)_3(DMF)_2(H_2O)\cdot DMF$

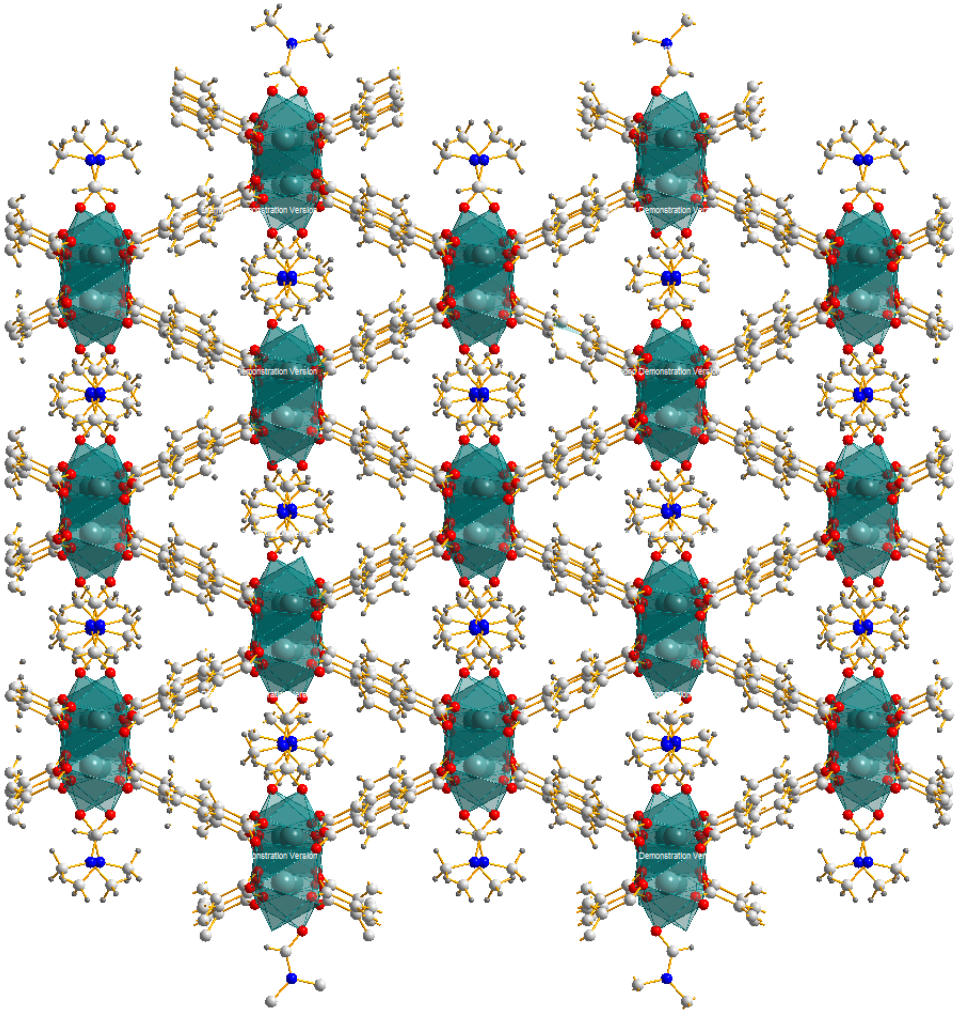

Kristalstructuur van $Lu_2(BDC)_3(DMF)_3(H_2O)_2$

Vervolgens werden twee andere coördinatiepolymeren gemaakt met PDC^{2-} met de formules Nd(PDC)(HPDC) (**6**) en Lu(PDC)(HPDC)$(H_2O)_2 \cdot 4H_2O$ (**7**). In beide structuren moet om de landingsbalans te behouden elke andere H_2PDC slechts éénmaal gedeprotoneerd zijn. Dit zorgt in beide gevallen voor waterstofbruggen die een belangrijke rol spelen in het creëren van de driedimensionale structuur.

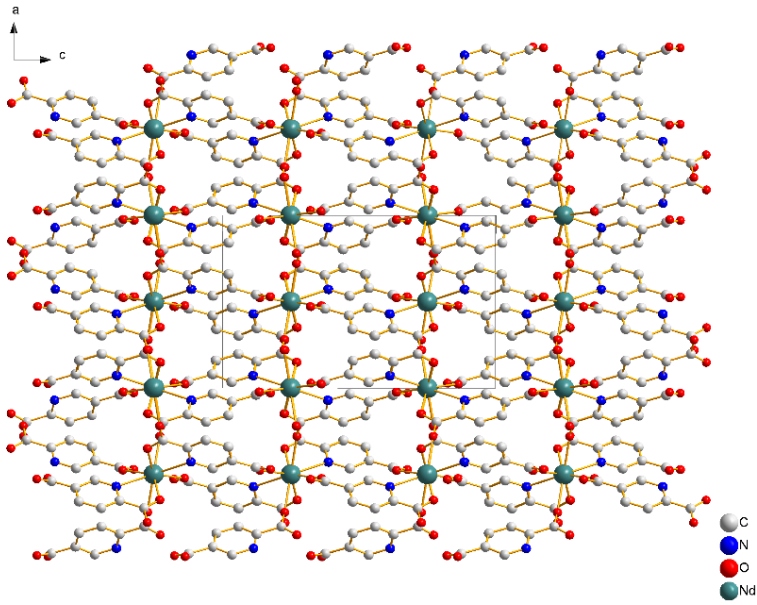

Kristalstructuur van Nd(PDC)(HPDC)

Van **6** werd de karakteristieke Nd^{3+} luminescentie gemeten in het nabije IR-gebied.

label	λ (nm)	ῡ (cm^{-1})	transitie
a	356.5	27360	$^4D_{3/2}$, $^4D_{5/2}$, $^2I_{11/2}$, $^4D_{1/2} \leftarrow {}^4I_{9/2}$
b	419.5	23838	$^2D_{5/2} \leftarrow {}^4I_{9/2}$
c	429	23310	$^2P_{1/2} \leftarrow {}^4I_{9/2}$
d	467	21413	$^4G_{11/2}$, $^2D_{3/2}$, $^2P_{3/2}$, $^2G_{9/2}$, $^2K_{15/2} \leftarrow {}^4I_{9/2}$

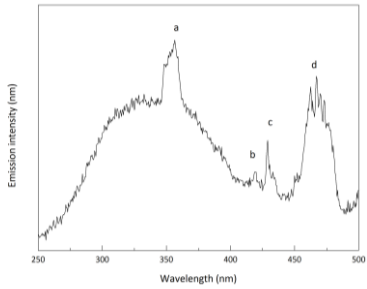

label	λ (nm)	ῡ (cm^{-1})	transitie
a	885	11300	$^4F_{3/2} \rightarrow {}^4I_{9/2}$
b	1055	9478	$^4F_{3/2} \rightarrow {}^4I_{11/2}$
c	1330	7519	$^4F_{3/2} \rightarrow {}^4I_{13/2}$

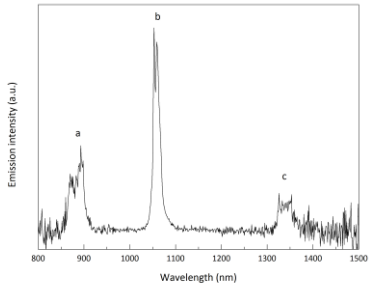

Excitatie- (bovenaan) en emissiespectra (onderaan) van Nd(PDC)(HPDC)

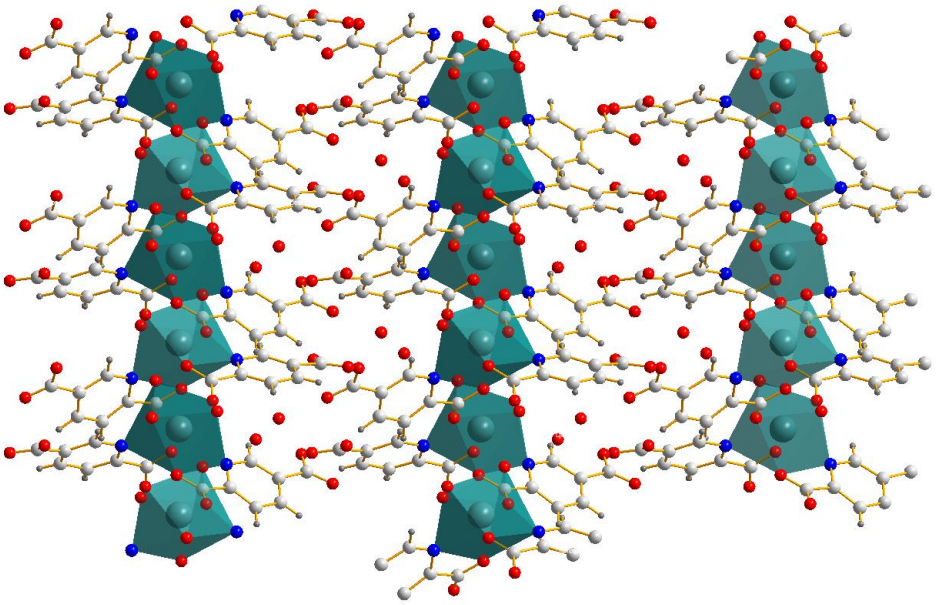

Kristalstructuur van $Lu(PDC)(HPDC)(H_2O)_2 \cdot 4H_2O$

Vervolgens werd de luminescentie opgemeten van twee reeksen materialen, gesynthetiseerd door een verwante onderzoeksgroep gevestigd in Lille. Het gaat om de materialen met formules LnCl(NDC)(DMF) met Ln = Ce^{3+}, Nd^{3+}, Tb^{3+} en Eu^{3+} en NDC = 2,6 naftaleendicarboxylaat, en Ln(CDC)(form)(H_2O) met Ln = Ce^{3+}, Pr^{3+}, Nd^{3+}, Sm^{3+}, Eu^{3+}, Gd^{3+}, Tb^{3+} en Dy^{3+}, CDC = *trans*-1,2-cyclohexaandicarboxylaat en form = formiaat. De verwachte transfer van energie van NDC^{2-} naar het lanthanide-ion werd waargenomen, net zoals het verwachte uitblijven van deze transfer bij CDC^{2-}. Dit komt doordat het aromatisch geconjugeerd system van NDC^{2-} een hogere absorptiviteit heeft, waardoor er dus meer energie beschikbaar is voor transfer. CDC^{2-} bezit dit geconjugeerd systeem niet, enkel rechtstreekse excitatie van het lanthanide-ion levert de karakteristieke luminescentie.

In een ander deel van de thesis werden uitgebreide pogingen gedaan om een nieuwe insteek te geven aan lanthanide-houdende coördinatiepolymeren. Het is namelijk zo dat mononucleaire lanthanidecomplexen met β-diketonaten als ligand uitgebreid bestudeerd zijn.[5] Als het mogelijk zou zijn om moleculen te gebruiken als linker waarbij twee van deze functionaliteiten gebruikt worden, dan kan de stap gemaakt worden naar coördinatiepolymeren.[6] Daarvoor werden twee linkers gekozen: 1,1,2,2-tetra-acetylethaan (H_2TAE) en 1,4-bis-(3-acetylaceton)-benzeen (H_2BAB). Deze moleculen zijn analoog aan de dicarbonzuren oxaalzuur en tereftaalzuur, respectievelijk, in die zin dat hun functionele groepen rechtstreeks aan elkaar gekoppeld zijn dan wel op de 1,4-posities gesubstitueerd zijn van een benzeenring.

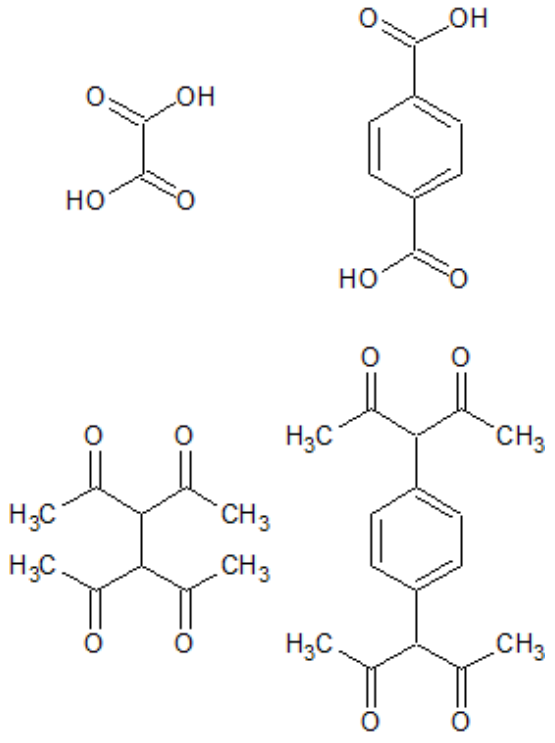

Boven: oxaalzuur en tereftaalzuur, onder: H_2TAE en H_2BAB

Er is een matige hoeveelheid aan literatuur beschikbaar waarin TAE^{2-} en BAB^{2-} weliswaar gebruikt worden als ligand maar steeds in di, tri of tetranucleaire complexen van transitiemetalen. Er is hoegenaamd geen informative over vorming van geordende coordinatiepolymeren met lanthaniden gebaseerd op deze linkers.

Een groot aantal experimenten later werd duidelijk dat dit niet toevallig was. Hoewel het idee intuïtief haalbaar lijkt, zijn er toch enkele belangrijke chemische verklaringen voor het mislukken van deze netwerkvorming, zijnde: een te hoge affiniteit van β-diketonaten voor lanthaniden en andere metalen, sterische hinder in de linkers, karakteristiek gebrek aan symmetrie in de coordinatie van lanthaniden en degradatie van de linker in oplossing. Een andere reden kan zijn dat, hoewel de structuren niet onmogelijk zijn om te bekomen, de toegestane foutenmarge voor de precieze reactieparameters bijzonder klein is. Dat wil zeggen dat, als het al mogelijk is, de voorwaarden voor succes zeer specifiek zijn, en het dus nagenoeg onhaalbaar is zonder een portie geluk of zonder *high-throughput* methoden om tot de beste *design of experiment* te komen. Het is namelijk mogelijk om de ionen en de linkers te laten reageren, maar de uitkomst moet finaal éénkristallen opleveren, anders wordt opheldering van de absolute structuur onmogelijk.

Met deze pogingen indachtig werd getracht om op onrechtstreekse manier tot een network te komen waarin lanthaniden door β-diketonaatliganden gekoppeld werden. Daarvoor werd een gesubstitueerde vorm van dibenzoylmethaan aangewend, namelijk 1,3-bis(4-cyanofenyl)-1,3-propaandion (HCNDBM).[7] Deze molecule bevat twee cyano-groepen, die volgens de Pearson HSAB-theorie “zachte” liganden zijn, terwijl de zuurstofatomen “hard” zijn. Lanthanide-ionen zijn ook “hard”. In een eerste stap

werden mononucleaire complexen gevormd met formules [Ln(CNDBM)$_3$phen] waar Ln = Nd^{3+}, Tb^{3+}, Ho^{3+}, Er^{3+}, Y^{3+} en phen = 1,10-phenanthroline, [Ln(CNDBM)(DMF)$_2$]·H_2O met Ln = Nd^{3+} en Er^{3+} en [Sm(CNDBM)$_4$]Et_3N. Hierin worden de lanthaniden gecoordineerd door de diketonaatgroepen.

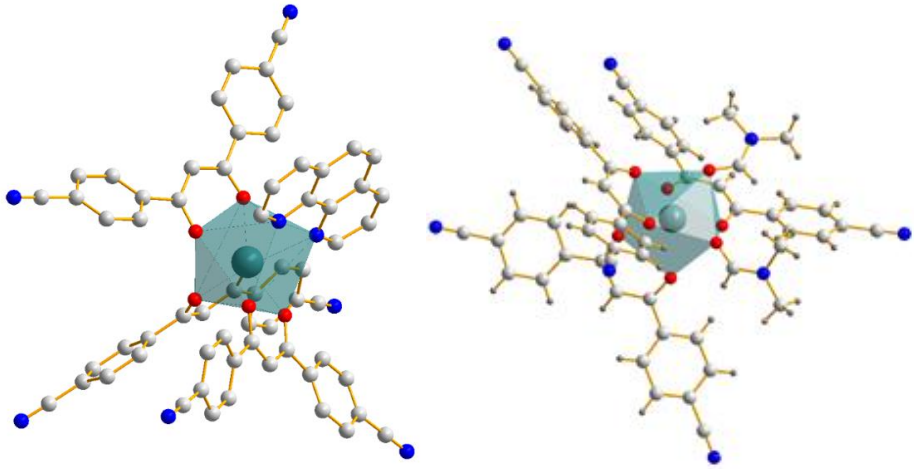

Kristalstructuur van [Nd(CNDBM)$_3$phen] en [Nd(CNDBM)$_3$(DMF)$_2$]·H_2O

In een tweede fase werd gepoogd om deze complexen te gebruiken als bouwstenen door ze aan elkaar te koppelen in een geordend network via “zachte” zilver(I) ionen die interageerden met de vrije cyanogroepen. Ook hier leverden deze pogingen geen succes op. De reden hiervoor kan gevonden worden in de symmetrie. Als bijvoorbeeld drie CNDBM groepen coördineren, dan zijn er 6 cyanogroepen aanwezig in exo-oriëntatie. In het geval van transitiemetaalcomplexen met CNDBM dan vormen die cyanogroepen, indien verbonden met elkaar met imaginaire lijnen, een licht vervormde octaëder. Voor de gesynthetiseerde lanthanidecomplexen is het duidelijk dat die octaëder sterk vervormd is. Als bouwsteen zijn ze daarom minder geschikt.

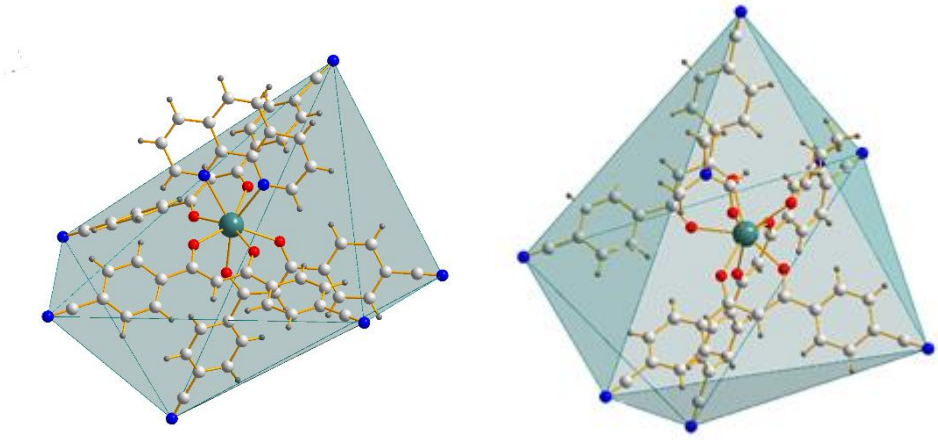

Kristalstructuur van $[Nd(CNDBM)_3phen]$ en $[Nd(CNDBM)_3(DMF)_2]\cdot H_2O$ waarin de cyano-stikstofatomen verbonden worden met vorming van sterk vervormde octaeders

10.3 Conclusie

De pogingen tot het vormen van lanthanide-gebaseerde coördinatiepolymeren als geordende netwerken legde doorheen het onderzoek een aantal pijnpunten bloot. Niet alleen is de symmetrie van elke bouwsteen van belang, ook de ideale reactiecondities moeten achterhaald worden. Verder is het zo dat de grootste moeilijkheid het bekomen van éénkristallen is. Zonder deze is het niet mogelijk om nieuwe materialen in deze klasse op een absolute manier te karakteriseren. Dit zou in principe kunnen via *high-throughput*-methoden.

10.4 Referenties

1. Reticular synthesis and the design of new materials, O.M. Yaghi, M. O'Keeffe, N.W. Ockwig, H.K. Chae, M. Eddaoudi, J. Kim, Nature, **2003**, Vol. 423, p. 705
2. Lanthanide and actinide chemistry, S. Cotton, ISBN: 978-0-470-01005-1, **2006**
3. Lanthanide-Based Luminescent Hybrid Materials, K. Binnemans, Chem. Rev., **2009**, Vol. 109, No. 9
4. Synthesis, crystal structures, and luminescence properties of carboxylate based rare-earth coordination polymers, R. Decadt, K. Van Hecke, D. Depla, K. Leus, D. Weinberger, I. Van Driessche, P. Van Der Voort, R. Van Deun, Inorg. Chem., **2012**, 51, 11623-11634.
5. RARE-EARTH BETA-DIKETONATES, chapter 225 in the Handbook on the Physics and Chemistry of Rare Earths, K. Binnemans, Vol. 35, **2005**, Elsevier, and all references contained therein
6. Self-assembled Metallo-supramolecular Systems Incorporating β-diketone motifs as Structural Elements, D.J. Bray, J.K. Clegg, L.F. Lindoy, D. Schilter, Adv. Inorg. Chem, **2007**, vol. 59, ISSN 0898-8838
7. Heterometallic Modular Metal–Organic 3D Frameworks Assembled via New Tris-β-Diketonate Metalloligands: Nanoporous Materials for Anion Exchange and Scaffolding of Selected Anionic Guests, L. Carlucci, G. Ciani, S. Maggini, D.M. Proserpio, M. Visconti, Chemistry Eur. J., **2010**, Vol. 16, Issue 41, p. 12328